THESIS FOR THE DEGREE OF DOCTOR OF PHILOSOPHY

Pair production, vacuum birefringence and radiation reaction in strong field QED

GREGER TORGRIMSSON

Department of Physics
CHALMERS UNIVERSITY OF TECHNOLOGY
Göteborg, Sweden 2016

Pair production, vacuum birefringence and radiation reaction in strong field QED

GREGER TORGRIMSSON
ISBN 978-91-7597-319-7

Doktorsavhandlingar vid Chalmers tekniska högskola
Ny serie nr 4000
ISSN 0346-718X

Department of Physics
Chalmers University of Technology
SE-412 96 Gothenburg
Sweden
Telephone + 46 (0)31-772 1000

Chalmers Reproservice
Gothenburg, Sweden 2016

Pair production, vacuum birefringence and radiation reaction in strong field QED

GREGER TORGRIMSSON
Department of Physics
Chalmers University of Technology

ABSTRACT

In this thesis we consider three QED phenomena in strong electromagnetic fields: Schwinger pair production, vacuum birefringence and radiation reaction. We study electron-positron pair production in a variety of field configurations and, using complex worldline instantons, reveal new insights into the case of fields with lightlike inhomogeneities. We also find universal scaling for the pair production probability near critical points.

Vacuum birefringence is the change in polarisation of a probe laser beam induced by interaction with a second electromagnetic field. We relate this macroscopic phenomena to the microscopic physics of individual photons in the probe flipping polarisation or helicity in a strong background field, and use this to make predictions for upcoming birefringence experiments, by considering the impact of realistic field geometry.

Radiation reaction is the recoil effect on the motion of a radiating particle as it is accelerated by a background field. Due to the existence of unphysical solutions to the equation of motion derived in classical electrodynamics, several alternative classical equations have been proposed. We derive radiation reaction from QED and take the classical limit to test the validity of a number of these classical equations. Choosing a plane wave background allows us to treat the background field exactly and also to make general predictions about the form of a classical equation. We treat both vacuum birefringence and radiation reaction in a field theory formalism that naturally lends itself to systems with plane wave backgrounds - namely lightfront quantisation.

Keywords: nonperturbative pair production, worldline instantons, vacuum birefringence, radiation reaction, lightfront quantisation

List of Appended Papers

This following list contains the papers upon which this thesis is based and my contribution to each.

I "Quantum radiation reaction: from interference to incoherence."
V. Dinu, C. Harvey, A. Ilderton, M. Marklund and G. Torgrimsson.
arXiv:1512.04096 [hep-ph]. *To appear in Phys. Rev. Lett.*
I performed calculations for the electron momentum expectation value in scalar and spinor QED, and contributed in discussions.

II "Critical Schwinger pair production."
H. Gies and G. Torgrimsson.
arXiv:1507.07802 [hep-ph].
I performed calculations for the critical scaling of the pair production probability and contributed to the writing of the paper.

III "Nonperturbative pair production in interpolating fields."
A. Ilderton, G. Torgrimsson and J. Wårdh.
Phys. Rev. D **92** (2015) 6, 065001
It was my idea to use interpolating coordinates, and I performed the bulk of the calculations. I contributed to the writing of the paper.

IV "Pair production from residues of complex worldline instantons."
A. Ilderton, G. Torgrimsson and J. Wårdh.
Phys. Rev. D **92** (2015) 2, 025009
I took an active role in the many discussions which lead to the solution, and together with AI and JW I performed calculations for the pair production probability.

V "Photon polarization in light-by-light scattering: Finite size effects."
V. Dinu, T. Heinzl, A. Ilderton, M. Marklund and G. Torgrimsson.
Phys. Rev. D **90** (2014) 4, 045025
I contributed in discussions and with calculations for vacuum birefringence signals.

VI "Vacuum refractive indices and helicity flip in strong-field QED."
V. Dinu, T. Heinzl, A. Ilderton, M. Marklund and G. Torgrimsson.
Phys. Rev. D **89** (2014) 12, 125003
It was my idea to use the expectation value of the electromagnetic field operator in lightfront quantisation to study vacuum birefringence. I performed analytical calculations for the vacuum birefringence signals and contributed in discussions and to the writing of the paper.

VII "Radiation reaction from QED: lightfront perturbation theory in a plane wave background."
A. Ilderton and G. Torgrimsson.
Phys. Rev. D **88** (2013) 2, 025021

Together with AI I worked out how to obtain the electron momentum expectation value at finite times, in particular to compare a number of different classical equations with the classical limit of QED. It was my idea to use the position and velocity operators.

VIII "Radiation reaction in strong field QED."
A. Ilderton and G. Torgrimsson.
Phys. Lett. B **725** (2013) 481
I contributed in discussions and with calculations that lead to the results for radiation reaction at asymptotic times.

IX "Scattering in plane-wave backgrounds: infra-red effects and pole structure."
A. Ilderton and G. Torgrimsson.
Phys. Rev. D **87** (2013) 085040
I performed calculations for the part of the paper on infrared divergences and contributed to the writing of the paper.

Acknowledgements

I thank my supervisor Anton Ilderton for many interesting discussions and for all the time and effort he has put into helping and supporting me during my PhD. I also thank my other collaborators V. Dinu, H. Gies, C. Harvey, T. Heinzl, M. Marklund and J. Wårdh. I would like to give special thanks to J. Wårdh for many interesting discussions during his master's project, to V. Dinu for a fruitful and enjoyable collaboration, and to M. Marklund for an amazing chocolate cake. I thank TPI, FSU Jena, and HI Jena for hospitality during a research visit. I am grateful to ILCAC for a "Gary McCartor Travel Award" to attend LC2014. I acknowledge support from the Swedish Research Council, contract 2011-4221. Feynman diagrams have been created using JaxoDraw [239, 240]. Finally, I thank my family for support.

Contents

1 Physics at high intensity

Physics in electromagnetic fields with extremely high intensities is an active research area [1–4]. The presence of external fields provides new means of probing fundamental physics; a perfect example is the Schwinger effect [5–7], where electron-positron pairs are spontaneously produced by the field itself, which could offer a means to test nonperturbative QED. Strong field QED saw a lot of theoretical development in the 60's, following the invention of lasers, but at that time the laser fields available were much too weak to use for strong field QED experiments. This though will soon change. A worldwide interest in laser physics is driving the upgrade of existing, and construction of a new generation of, laser facilities; a few examples are the Extreme Light Infrastructure Nuclear Physics (ELI-NP) in Romania [8] (one of the four pillars of ELI [9]), the Helmholtz International Beamline for Extreme Fields (HIBEF) [10] at the European XFEL in Germany [11], the Exawatt Center for Extreme Light Studies (XCELS) in Russia [12], and the updgrade of Vulcan at the Central Laser Facility (CLF) in the UK [13], see [3] for more. Several of these new facilities will go online in just a few years' time and will open the door to unexplored intensity regimes, which will allow us to observe for the first time processes such as vacuum birefringence and light-by-light scattering with real photons [14–16]. In fact, experiments with intensities of the same order of magnitude as those already available will allow us study radiation reaction and gain insights into this nontrivial problem. Extremely high intensities are envisaged at e.g. ELI and XCELS, which, in light of several recent studies, may take us to the brink of the nonperturbative Schwinger pair production regime.

These developments in many ways parallel the drive to reach higher energies in particle-particle collisions, e.g. at the Large Hadron Collider (LHC), to search for physics beyond the Standard Model. In fact, in addition to detecting unobserved Standard Model processes, strong external fields can also be used to search for new beyond-the-Standard-Model particles, e.g. axion-like and minicharged particles, in vacuum birefringence and light-shining-through-walls experiments [17–19].

The QED critical field strength is $E_c := m_e^2/e \sim 10^{18}\text{V/m}$ or $m_e^2/e \sim 4.4 \times 10^{13}\text{G}$. This is much higher than what is currently available in laser experiments (see below). So, it is worth noting at this point that, though we here mainly focus on strong laser fields, there are other sources of strong fields. For example, very strong magnetic fields are produced on the surface of magnetars $B \sim 10^{15}\text{G}$ and in heavy ion collisions, e.g. at the Relativistic Heavy Ion Collider (RHIC) and LHC, with $B \sim m_\pi^2/e \sim 10^{18}\text{G}$ (where m_π is the pion mass) or even higher [20]. It is also believed that very strong magnetic fields were present in the early universe. Despite these high field strengths, magnetic fields alone cannot produce pairs. However, strong magnetic fields can affect properties of QCD [21], and can be used to study e.g. the QCD phase diagram. One example is the transition to a superconducting QCD vacuum for magnetic fields strengths above a certain critical point $B_c \sim 10^{20}\text{G}$ [22]. It has also been pointed out [23, 24] that strong electromagnetic field effects can become important in future linear colliders because of increasing luminosity and energy, e.g. at the International Linear Collider (ILC) and the Compact Linear Collider (CLIC).

Reaching intensities high enough to see Schwinger pair production is an ultimate goal in strong field physics. One can picture Schwinger pair production as a virtual electron-positron pair being pulled apart into a real pair by a sufficiently strong electric field. In the case of a constant electric field E, the probability scales as $\mathbb{P} \sim V_4(eE)^2 e^{-\pi E_c/E}$ for field strengths smaller than the critical, which can be thought of as the field strength required to give a virtual electron an energy equal to the (real) electron mass over a distance of the Compton wavelength, $eE_c/m = m$. An interesting aspect of the Schwinger effect is its nonperturbative dependence on the field, which necessitates nonperturbative methods going beyond the usual perturbative Feynman diagrams. On the other hand, this nonperturbative dependence means that the Schwinger effect is exponentially suppressed for fields below the critical field and very difficult to observe in experiments. Indeed, the critical field corresponds to an intensity $I_c \sim E_c^2 \sim 10^{29}\mathrm{W/cm}^2$ several orders of magnitude larger than the highest intensity recorded so far $\sim 2 \times 10^{22}\mathrm{W/cm}^2$ [25]. This constant field estimate might seem discouraging, but several recent studies suggest that Schwinger pair production could be observed at intensities well below critical, which raises hopes that this effect could actually be detected in laser facilities in the not too distant future. One reason for this is simply the large (in comparison to the Compton scale) space-time volumes (V_4) of lasers, which partly compensates for the exponential suppression [26, 27] reducing the required intensity down to $\sim 10^{27}\mathrm{W/cm}^2$. The probability can also be significantly enhanced by well-designed field configurations. One way to increase the probability is to collide several laser pulses [28]. In [29] it was shown that by superimposing an X-ray beam with a high-intensity optical laser, the required intensity can be reduced to $9 \times 10^{25}\mathrm{W/cm}^2$. This set-up might be possible with ELI's fourth pillar [9], which is envisaged to reach intensities of up to $10^{26}\mathrm{W/cm}^2$. Other set-ups to enhance nonperturbative pair production have been considered in [30, 31]. Pair production has also been studied in strong electromagnetic fields in pulsars [32–34]. One could also gain insights into the Schwinger mechanism by studying analogue systems such as (quasi-) particle production in graphene [35, 36] and semiconductors [37, 38] and with ultracold atoms in optical lattices [39–43]. Though experiments to directly test Schwinger pair production are probably still quite some time away, any progress in understanding Schwinger pair production in the meantime will likely also lead to new insights and ideas into general nonperturbative effects and techniques, which could be useful e.g. for atomic ionisation [44], cosmological particle production [45] (and references therein), Hawking radiation [46] (and references therein), and production of quark-antiquark pairs and gluons by chromo-electric fields [47–49], see also [50]. Conversely, the Schwinger effect could offer a testing ground for new theoretical ideas such as Lefschetz thimbles [51, 52] and resurgence [53, 54].

In any case, there are many other unobserved processes that take place already at intensities that are or will soon become available, e.g. at ELI-NP which is aiming for intensities as high as $10^{23} - 10^{24}\mathrm{W/cm}^2$ [8]. One process that may soon be observed in experiments is vacuum birefringence, which was first studied by Toll more than half a century ago [55]. In classical electrodynamics the field equations are linear, implying that two laser beams would pass through each other without being affected. In QED, on the other hand, there are nonlinear effects. An initially linearly polarised beam will emerge with an elliptical polarisation after interacting with a second beam. This is reminiscent of a beam that passes through a birefringent medium, and hence the name vacuum birefringence. Phrased in optics terms, a probe passing through a background effectively experiences a refractive index n that depends on the polarisation of the probe. For instance, consider a low energy probe with propagation vector $\mathbf{k}$ passing through a weak magnetic background field $\mathbf{B}$. The difference between the refractive indices for probe polarisation parallel and perpendicular to the plane containing $\mathbf{k}$ and $\mathbf{B}$ scales as $n_{\parallel} - n_{\perp} \sim \alpha B^2/B_c^2$ (see e.g. [56–58]). In the PVLAS experiment [59] one hopes to find vacuum birefringence by sending a laser through a static magnetic field. To make up for the relatively weak field, the laser is reflected back and forth several times through the field. Another experiment to detect vacuum birefringence using, instead, two colliding lasers has been proposed in [14], which is the focus of our studies. Such an experiment will soon be performed at HIBEF, European XFEL with one optical laser with an intensity on the order of $10^{22}\mathrm{W/cm^2}$ colliding with an XFEL beam with photon energy ~ 13 keV [15]. Detecting the small induced ellipticity is an experimental challenge [60]. The higher optical intensities and probe energies that will soon be reached with ELI-NP [8] could help in detecting vacuum birefringence. There is also hope to detect vacuum birefringence with state of the art technology by exploiting the diffraction spreading of the birefringent signal with respect to the incident probe beam [16]. Although vacuum birefringence can be studied with classical methods applied to effective actions [61, 62], the effect is essentially due to photon-photon scattering, and, as explained in Paper VI (reference [63]), Paper V (reference [64]), and [65], the ellipticity induced on the probe field is closely related to the probability for a single probe photon to flip between two orthogonal polarisations. Since photon-photon scattering has so far only been observed in processes involving virtual photons, observing vacuum birefringence in upcoming experiments would hence also give the first detection of photon-photon scattering with only real photons; this is one reason why vacuum birefringence attracts so much interest. As mentioned, vacuum birefringence can also be used to search for new beyond-the-Standard-Model particles that could couple to photons via a virtual fermion loop as in Fig. 1 (see [17]). Vacuum birefringence has also been studied in superstrong magnetic fields in [61], which could be relevant for e.g. magnetars. In addition to vacuum birefringence, the nonlinearity in QED also leads to processes such as photon reflection [66, 67], matterless double slit interference [68], and vacuum high harmonic generation [69, 70]. In [71] an experiment was proposed to observe photon-photon scattering by colliding three lasers to produce a fourth wave. Another process is photon splitting [56, 72–74], which seems difficult to test with lasers [75], but might be relevant in strong fields in pulsars. For a recent review of vacuum birefringence and other photon-photon scattering effects see [76].

Another strong field example is the possibility of using high-intensity lasers to study the dynamics of radiating particles in electromagnetic fields. An electron in a background field will obviously accelerate due to the Lorentz force, and because of this acceleration the electron will radiate energy; in a quantum description this is described by the emission of photons as in Fig. 2. It is also clear that due to this radiation the electron must recoil, but how to modify the Lorentz force equation to include this radiation reaction (RR) is a somewhat controversial problem with a long history (see [77] for a recent review of RR). There is obviously a strong motivation from a purely theoretical point of view to understand

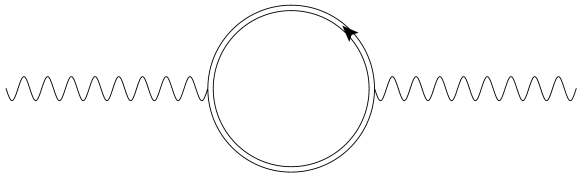

Figure 1. A probe photon interacting via a dressed fermion loop with the background field. The real part of this diagram is related to birefringence and the imaginary part gives via the optical theorem the probability for a photon decaying into a electron-positron pair.

this basic effect. In addition, understanding RR is also important in a wider context as there are many potential applications for accelerating electrons to generate high energy photons [11, 78] (see also [3]). It has been shown that RR can trap electrons around electric field maxima [79–81], but RR can also make high-intensity regions of lasers impenetrable for colliding electrons [81]. RR can therefore have a large impact on the emitted radiation. RR also affects the distribution of accelerating electron-bunches and can lead to both focusing as well as spreading [82–84], which could be important for particle accelerators. Since RR becomes significant already for intensities of the same order of magnitude as those available today [82, 83, 86–88] e.g. at the Berkley Lab Laser Accelerator BELLA [89] or Gemini at CLF [13], see Paper I (reference [90]), high-intensity laser experiments could very soon offer insights into these RR effects.

So, lasers will soon reach intensities high enough to observe processes like vacuum birefringence and RR. At the moment though, very few high-intensity experiments have been performed. There is a famous experiment performed at the Standford Linear Accelerator Center (SLAC) [91, 92], where electrons with energies $\sim 46.6\text{GeV}$ collided with a laser with an intensity $\sim 10^{18}\text{W/cm}^2$ (a fairly modest intensity by today's standards). Two processes were observed in these collisions: the emission of a photon by a single electron (nonlinear Compton scattering), $e^- \to e^- + \gamma$, and stimulated electron-positron pair production by a single photon, $\gamma \to e^- + e^+$. See [93–98] and [99–102], respectively, for recent studies of these two processes. An arbitrary number of background field photons can contribute in these processes, neither of which can occur in vacuum without a background field. Fig. 2 shows the corresponding Feynman diagrams, where double lines indicate electrons and positrons moving through the background field. Probabilities for higher order processes can often be approximated by simply gluing together probabilities for low order processes, e.g. those shown in Fig. 2. In general, though, there are additional contributions. For example, part of the trident process $e^- \to 2e^- + e^+$ is obtained by gluing together the probabilities for nonlinear Compton scattering and photon stimulated pair production. The question of when this two-step process gives a good approximation for the total trident process is investigated in [103]. Double nonlinear Compton scattering $e^- \to e^- + 2\gamma$ has been studied in [104, 105].

The strength of a laser with field strength E and frequency ω is often characterised by the classical nonlinearity parameter $a_0 = eE/m\omega$, which is roughly the ratio of the work done by the field on an electron over one wavelength and the electron mass (see [106] for

Figure 2. Feynman diagrams for nonlinear Compton scattering and photon stimulated pair production.

an invariant definition of a_0). In SLAC-E144 [91, 92], the relatively low intensity meant that $a_0 < 1$. Modern lasers though can easily have $a_0 > 1$. Electrons in such lasers become relativistic within a single laser period, and, importantly, since $a_0 > 1$ the background field cannot be treated perturbatively.

With the next generation of high-intensity laser facilities we will soon be in a position where we can test predictions dating back to the very beginning of quantum field theory: In the 30's, Heisenberg and Euler [6] calculated the one-loop effective action for QED in a constant electromagnetic field (see [107] for more on the effective action and its history). The Euler-Heisenberg effective action, as it became known, has both a real and an imaginary part; the real part describe e.g. vacuum birefringence, and the imaginary part leads to pair production. In the 50's, Schwinger derived [7] the probability for pair production by a constant field in the QED formalism. He also showed that the effective action vanishes for a single plane wave background (i.e. a transverse field depending on $t + z$), which in particular means that such a field cannot (spontaneously) produce pairs. In addition to constant fields and plane waves, different types of Sauter pulses also allow for exact solutions; see [108, 109] for the time-dependent electric field $E\text{sech}^2\omega t$, [110] for the spatially inhomogeneous electric $E\text{sech}^2 kz$, and [111] for the spatially inhomogeneous magnetic field $B\text{sech}^2 kz$ (see also [107]).

In the 60's, after the invention of lasers, much progress was made [112–115] for processes in plane waves, which are used as models of single, unfocused lasers. One reason to use plane waves is that they allow for an exact treatment of the background field strength, which, as mentioned, is necessary for lasers with $a_0 > 1$. Early investigations used either monochromatic or constant plane waves. These are good approximations for laser pulses containing many cycles, e.g. those used in SLAC-E144 [92]. However, reaching higher intensities is achieved by tightly focusing and compressing the laser. Recent years have therefore seen an increased effort to study pulsed plane waves (i.e. fields that vanishes as $|t + z| \to \infty$), e.g. in nonlinear Compton scattering [93, 94, 96–98], in stimulated pair production [99–102], and for the mass shift [116]. Pulsed plane waves still allow for exact solutions, but for e.g. narrow beams or combinations of several beams, it is necessary to go beyond plane waves, which is theoretically challenging. Simple field models give us a starting point, but they might miss important features. In fact, several recent studies on Schwinger pair production have shown that even small differences in the fields can have a large impact on observables [117–124]. For example, in dynamical assistance [117–122] the pair production probability is significantly enhanced by superimposing a strong, slowly varying field with a weak, rapidly varying field. It is important to understand more about field configuration dependences, both for accurate descriptions of upcoming experiments and also to find optimal field configurations [125] to lower the required field strengths and to guide experimental field designs. This is urgent for experiments designed to detect RR and vacuum birefringence, which are only a couple of years away or even less.

It is thus important to find methods that can both treat the background field strength nonperturbatively and also deal with various field inhomogeneities. The standard approach to QED is to use a quantum field formalism. To study pair production it has become popular lately to use instead the worldline formalism, where field path integrals are replaced with path integrals over particle worldlines [126–128]. See [129] for different applications of the worldline formalism and its history. In the 80's, Affleck et al. [127] studied Schwinger pair production by a constant field in the semiclassical regime by performing the worldline integral with a saddle point approximation; the saddle point equation resembles the Lorentz force equation for a particle in an electromagnetic field and its solutions are referred to as worldline instantons. Two decades later, this instanton approach was generalized in a series of papers by Dunne et al. [130–133], first to fields depending on either time or one spatial coordinate, and then to fields depending on up to three spatial coordinates. Time dependent fields with up to three nonzero components were considered in [134]. In Paper IV (reference [135]) worldline instantons were used for fields depending on lightfront time $t+z$, and in Paper III (reference [136]) to study fields depending on a coordinate that interpolates between time t, lightfront time $t+z$ and position z. In a recent paper [118] the worldline instanton formalism was used to study the probability for pair production by a superposition of a strong spatially inhomogeneous electric field and a weak time-dependent field, see also [137]. For fields that depend on only time or one spatial coordinate the results obtained with worldline instantons can also be obtained with ordinary WKB methods. An advantage of the worldline formalism is that it naturally extends to more complicated fields with multi-dimensional inhomogeneities [118, 132, 137], and thus provides a powerful tool to study field configuration dependences. Moreover, the worldline formalism is not only useful in the semiclassical regime. In [138] the worldline formalism was used to derive the exact probability for pair production by a longitudinal field with lightlike inhomogeneities $E(t+z)$ [139, 140]; this derivation is simpler than previous ones based on canonical quantisation. Further, H. Gies et al. have developed a numerical technique to evaluate worldline integrals [141–144]. Another numerical method that can be used to study multi-dimensional inhomogeneities is the Dirac-Heisenberg-Wigner formalism [145–148].

We have noted that there is increased interest in going beyond plane waves. With that said, plane waves can nevertheless be useful and convenient. The Lorentz force equation is analytically solvable in an arbitrary plane wave and the solution is simple. A plane wave background can also be treated exactly in a quantum description as both the Klein-Gordon and the Dirac equation are analytically solvable [149]. These, so called, Volkov solutions are then employed in the Furry picture [150], which is a separation of the total Hamiltonian into a "free" and an interacting part where, unlike the usual interaction picture, the "free" part contains the background field. As a consequence, the electrons and positrons become dressed by the background field, which in Feynman diagrams is indicated by double lines as in Fig. 2. The solutions to these equations depend only (non-trivially) on lightfront time $x^+ = t + z$. According to Dirac [151] there exist different "forms" of dynamics characterised by different "time"-parameters. Using ordinary time t to parameterise the dynamics corresponds to the instant form. Using lightfront time instead corresponds to the front form, which has applications in e.g. QCD [152, 153]. For processes in plane waves it is natural to use the front form instead of the instant form. This was first noted by Neville and Rohrlich [154] in the 70's, but despite the perfect match between laser plane waves and the front form, this idea has received scant attention compared to the approach used in [113–115]. The front form was used in Papers I, VI, VII (reference [155]) to study RR and vacuum birefringence in plane waves.

Treating realistic laser pulses is theoretical challenging. It becomes even more challenging as we enter regimes where the background can no longer be treated as a non-dynamical classical field, but where it becomes necessary to take into account the back-reaction of the produced particles on the background. This is a very difficult problem. Despite progress [156–160] many problems remain. At sufficiently high intensities, sequences of nonlinear Compton scattering and stimulated pair production could lead to a cascade of prolific particle production [161, 162]. Recent results suggest that cascades could be triggered already at intensities of around $10^{24}\mathrm{W/cm}^2$ [161, 163–165], which means that cascades might soon be observed e.g. at ELI. It has been suggested [166] that the back-reaction of cascades on the background could prevent us from ever reaching the Schwinger limit. Also for this the field structure can have a large impact [167].

1.1 Aims, summary of papers and outline

In this thesis we will consider three different problems in strong field QED: pair production, vacuum birefringence and RR. We begin in Sect. 2 with Schwinger pair production in the worldline formalism and provide background for Papers II (reference [169]), III, IV. The aim is to better understand how different space-time inhomogeneities affect the pair production probability. In Paper II we showed that close to critical points, the pair production probability vanishes with a scaling that is independent on the local details of the electric fields - this is similar to universality in critical phase transitions in statistical physics. In Paper IV we used the worldline instanton formalism to study pair production by fields depending on lightfront time, and in Paper III we studied pair production by fields depending on a coordinate that interpolates between time, lightfront time and a spatial coordinate.

Sect. 3 gives a short motivation for using plane waves and lightfront quantisation. In Sect. 4 and Sect. 5 we consider in some detail the combination of lightfront quantisation and plane wave backgrounds in both scalar and spinor QED. In Sect. 6 and Sect. 7 we explain how to use this formalism to study vacuum birefringence and RR, respectively. This provides background to Papers I, VII, VIII (reference [168]) (RR) and to Papers V, VI, [65] (vacuum birefringence).

The aim of Papers V, VI, [65] is to better understand vacuum birefringence and to provide predictions for upcoming experiments. We consider high-energy effects, and use a scattering formalism to explain the macroscopic phenomenon of vacuum birefringence in terms of photon helicity/polarisation flip.

The aim of Papers VII, VIII is to better understand how to obtain RR from QED, and to determine which of several different proposed classical equations agree with the classical limit of QED. In Paper VII we derived dynamical radiation reaction for an electron in a plane wave background field and compared to predictions from a number of classical equations. In Paper VII we used scalar QED instead of spinor QED, which is justified since in the classical limit they give the same predictions, as we will show explicitly in this thesis. In Paper VIII we derived asymptotic RR from spinor QED using ordinary scattering methods and discussed which processes contribute to RR. In Paper I we compared results obtained with the method developed in Paper VII with predictions from numerical simulations.

In this thesis we will also look at the infrared divergences in the probabilities for nonlinear Compton scattering and scattering without emission. We note that the cancelation of the soft divergences when summing probabilities for degenerate processes is essentially due to unitarity. Since the expectation values used for RR automatically include such sums they are infrared finite. In Paper IX (reference [227]) we studied IR divergences in plane wave backgrounds using ordinary scattering methods and showed that divergences cancel to higher orders as well.

We conclude in Sect. 8 with some unresolved puzzles.

2 Schwinger pair production

As mentioned in the introduction, exponential suppression makes Schwinger pair production much harder to detect in experiments than RR and vacuum birefringence. Nevertheless, several studies [117–122] have shown that taking into account the electric field shape can significantly enhance the probability with respect to Schwinger's constant field estimate. In order to find the optimal field shape it is important to understand more about how different spacetime inhomogeneities and pulse shapes affect the probability. In this chapter we will investigate such effects. In particular, we investigate why the expression for the probability for pair production by a longitudinal electric field with lightlike inhomogeneities is so simple compared to fields with temporal or spatial inhomogeneities. We use the worldline instanton formalism together with interpolating coordinates to study the transition between temporal, lightfront and spatial inhomogeneities. This allows us to clearly explain why the lightlike case is so simple and why performing the calculations precisely on the lightfront can be subtle. We will also consider pair production near critical points for electric fields with spacelike inhomogeneities. The critical point corresponds to the minimum electrostatic energy required to produce pairs. We show that as one approaches the critical point, the scaling of the probability only depends on the asymptotic form of the electric field, but is independent on the local structure of the field. This universality is similar to universality in critical phase transitions in statistical physics.

2.1 Introduction

There are many ways to study Schwinger pair production. Here we will obtain the pair production probability by a background $A_\mu^{\rm ext}$ from the imaginary part of the QED effective action $\Gamma[A_\mu^{\rm ext}]$. We consider for simplicity scalar QED, which will be justified below. Our starting point is the field-path-integral representation of the vacuum persistence amplitude which is directly related to the effective action via

$$e^{i\Gamma} := \langle 0_{\rm out}|0_{\rm in}\rangle = \langle 0_{\rm in}|U|0_{\rm in}\rangle = \int \mathcal{D}\phi\mathcal{D}\bar{\phi}\; e^{i\int {\rm d}^4x - \bar{\phi}(\mathcal{D}^2+m^2)\phi} \;, \tag{2.1}$$

where $|0_{\rm in}\rangle$ is the initial vacuum state, the background covariant derivative is given by $\mathcal{D}_\mu = \partial_\mu + ieA_\mu^{\rm ext}$ and the $i\epsilon$ in $m^2 - i\epsilon$ is left implicit. In (2.1) we have neglected the interaction with the quantised photon field, which would lead to terms of order $\alpha = e^2/4\pi$; this approximation is almost always used when studying the Schwinger effect. Since the background field is always multiplied by e, we will absorb e into the field, $eA_\mu^{\rm ext} \to A_\mu$. The probability for pair production is given by

$$\mathbb{P}_{\rm pairs} = 1 - e^{-2{\rm Im}\,\Gamma} \;, \tag{2.2}$$

which is illustrated in Fig. 3. The real part of the effective action describes e.g. vacuum birefringence, which we will consider in Sect. 6.

The Gaussian path integral in (2.1) leads to the functional determinant Det $(\mathcal{D}^2+m^2)$, so the effective action can be expressed as (subtraction of $A \to 0$ terms are implicit)

$$i\Gamma = -\ln {\rm Det}\;(\mathcal{D}^2+m^2) = -{\rm Tr}\;\ln(\mathcal{D}^2+m^2) \;. \tag{2.3}$$

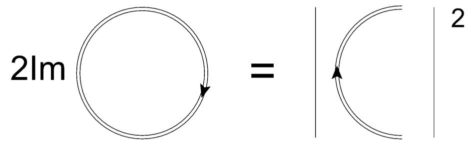

Figure 3. The diagram on the left-hand-side represents the one-loop effective action, and the diagram on the right-hand-side gives the probability for production of one pair.

We express the logarithm in terms of an ordinary one-dimensional integral, referred to as a proper time integral [7], and the (functional) trace is evaluated by summing over a position basis,

$$i\Gamma = \int\limits_0^\infty \frac{\mathrm{d}T}{T} \int \mathrm{d}^4x \, \langle \, x \, | e^{-i\frac{T}{2}(\mathcal{D}^2+m^2)} | \, x \, \rangle \; , \tag{2.4}$$

where the factor of 2 in the exponent is merely convention. Schwinger evaluated (2.4) by interpreting the exponent as a Hamiltonian for a quantum mechanical problem and then solved for a constant field the equations of motion for x and p in the Heisenberg picture [7]. We will instead follow Affleck et al. [127] and rewrite (2.4) in terms of a path integral over position x. Following standard techniques (see e.g. [170]) one finds

$$\Gamma = \int\limits_0^\infty \frac{\mathrm{d}T}{T} \oint \mathcal{D}x \; \exp -i\left(\frac{Tm^2}{2} + \int\limits_0^T \mathrm{d}\tau \; \frac{\dot{x}^2}{2} + A\dot{x} \right) \; , \tag{2.5}$$

where the path integral is over closed worldlines $x^\mu(0) = x^\mu(T)$. We have written (2.5) in Minkowski space. Affleck et al. [127] rotated proper time $T \to -iT$ and time x^0 to Euclidean time x^4, which makes the exponent real for the constant field studied in [127]. The same rotations also work for the symmetric fields considered in [131]. However, as noted in [133], this rotation does not make the exponent real for more general fields. We will therefore not rotate to Euclidean time.

So, what is achieved by writing the effective action in the worldline representation (2.5)? For a constant field the path integral is Gaussian and yields the Euler-Heisenberg effective action [129]. However, the strength of (2.5) is that it allows us to study inhomogeneous fields. In the semiclassical regime, which is experimentally relevant, one can perform the path integral by saddle point methods. The saddle points for (2.5), referred to as worldline instantons, are complex, closed trajectories obeying a Lorentz type equation. Unlike many other pair production methods, e.g. WKB, the worldline instanton formalism naturally extends to multi-dimensional inhomogeneities [118, 132, 137]. The path integral can also be evaluated numerically [141–144]. The worldline formalism has also proven useful e.g. for N-photon amplitudes [128], photon splitting [74], and vacuum polarisation amplitudes [143, 171]. The worldline formalism has also been applied to amplitudes with external scalars [172, 173]. Worldline representations like (2.5) are also conceptually appealing as they allow us to think about quantum field theory (QFT) processes in terms of particle trajectories, which can be more intuitive than quantum fields.

As a first step from constant fields to more realistic fields, it is natural to start by considering fields with various one-dimensional inhomogeneities. Three special cases are fields depending on time t, on a spatial coordinate z, or on lightfront time $t+z$. For slowly varying fields one can estimate the probability by simply replacing the volume factors in Schwinger's constant field result with space-time integrals. This locally constant field approximation (LCA) was used in [26–28] to study pair production by focused laser pulses modelled by exact solutions to Maxwell's equations. However, this locally constant field approximation sometimes misses interesting features, such as criticality. It has been shown (see e.g. [130, 131]) that temporal inhomogeneities tend to enhance the pair production probability with respect to LCA, while spatial inhomogeneities tend to lower the probability. For longitudinal fields depending on lightfront time $E(z+t)$, the probability is exactly given by LCA [139, 140] (i.e. also outside the semiclassical regime); this result can be derived quickly and elegantly in the wordline formalism [138] and in Paper IV we studied this case using the worldline instanton approach.

For pair production by longitudinal fields depending on lightfront time $E(x^+)$ one encounters problems with so-called zero modes [139, 140]. In the original papers [139, 140], this zero mode problem was solved by quantising on two lightfront surfaces instead of only one. To better understand zero modes, Hornbostel [174] used coordinates that interpolate between ordinary time t and lightfront time $t+x$, and approached the lightfront as a limit (see also [175, 176]). Inspired by their work, we used in Paper III similar coordinates to interpolate between electric fields with temporal, lightfront and spatial inhomogeneities. This allowed to us to better understand the transition between the three cases $E(t)$, $E(z)$ and $E(t+z)$, and to give a clear explanation for why the pair production is simply given by LCA in the lightfront case.

2.2 Notation

In analogy with [174], we define interpolating coordinates with an angle θ such that the components of an arbitrary vector V are given by

$$\begin{pmatrix} V^q \\ V^d \end{pmatrix} = \begin{pmatrix} \cos\frac{\theta}{2} & \sin\frac{\theta}{2} \\ -\sin\frac{\theta}{2} & \cos\frac{\theta}{2} \end{pmatrix} \begin{pmatrix} V^0 \\ V^3 \end{pmatrix} \tag{2.6}$$

and for the particular case that V is the position vector we write $q = x^q$ and $d = x^d$. Note that this is not a Lorentz transformation. Important special cases are

$$\begin{pmatrix} q \\ d \end{pmatrix}\bigg|_{\theta=0} = \begin{pmatrix} x^0 \\ x^3 \end{pmatrix} \qquad \begin{pmatrix} q \\ d \end{pmatrix}\bigg|_{\theta=\frac{\pi}{2}} = \frac{1}{\sqrt{2}} \begin{pmatrix} x^0 + x^3 \\ -x^0 + x^3 \end{pmatrix} \qquad \begin{pmatrix} q \\ d \end{pmatrix}\bigg|_{\theta=\pi} = \begin{pmatrix} x^3 \\ -x^0 \end{pmatrix} . \tag{2.7}$$

Lower and upper indices are related by

$$\begin{pmatrix} x_q \\ x_d \end{pmatrix} = \begin{pmatrix} \cos\theta & -\sin\theta \\ -\sin\theta & -\cos\theta \end{pmatrix} \begin{pmatrix} V^q \\ V^d \end{pmatrix} \tag{2.8}$$

and for scalar products we have

$$V^0U^0 - V^3U^3 = \cos\theta(V^qU^q - V^dU^d) - \sin\theta(V^qU^d + V^dU^q) = V^qU_q + V^dU_d . \tag{2.9}$$

We will also use the shorthand $c = \cos\theta$ and $s = \sin\theta$.

We consider electric fields depending on the interpolating coordinate q and for simplicity we restrict to purely longitudinal fields,

$$E(q) = A'(q) \qquad A(q) = \frac{1}{\gamma} f(kq) \;, \tag{2.10}$$

where $\gamma = k/E_0$ is the adiabaticity or the Keldysh parameter, where k is the inverse of some characteristic length and E_0 is the field strength, and we use units with $m = 1$. We will show how the pair production probability for fields with the same strength E_0, shape f and direction, depends on the interpolating angle θ or equivalently c. Our results interpolate continuously between fields depending on time $\{c = 1, q = x^0\}$, lightfront time $\{c = 0, q = (x^0 + x^3)/\sqrt{2}\}$ and a spatial coordinate $\{c = -1, q = x^3\}$. In Paper III we considered q-dependent fields with up to three nonzero components.

2.3 Wordline Instantons

We will follow essentially the same steps as presented in [131]. The starting point is (2.5), which for our interpolating fields becomes

$$\Gamma = \int_0^\infty \frac{\mathrm{d}T}{T} \oint \mathcal{D}x \exp -i\left(\frac{T}{2} + \int_0^1 \frac{\dot{x}^2}{2T} + A(q)\dot{d}\right) . \tag{2.11}$$

We generalise the fields studied in [131] in two ways: 1) we have an arbitrary interpolating coordinate q, and 2) we allow for less symmetric field shapes, with details below. However, as long as we are not precisely on the lightfront $c \neq 0$, we can still follow the steps in [131] mutatis mutandis.

We first write the path integral with Dirichlet boundary condition,

$$\oint \mathcal{D}x = \int \mathrm{d}x_0 \int_{\delta x(0)=\delta x(1)=0} \mathcal{D}\delta x \;, \tag{2.12}$$

where $x \to x + \delta x$, $x(0) = x(1) = x_0$, and x is chosen such that the action in (2.11) contains no term linear in the fluctuation δx. x is the instanton, which is a complex periodic solution to a Lorentz force type equation. Next we expand the action to second order in δx and perform the Gaussian integration. This gives a prefactor with a relatively simple dependence on x_0, which allows us to perform the x_0 integral. Lastly we perform the proper time integral with a saddle point approximation.

The saddle point equations for the path integral are

$$\begin{aligned} c\ddot{q} - s\ddot{d} &= TA'(q)\dot{d} \\ c\ddot{d} + s\ddot{q} &= TA'(q)\dot{q} \;. \end{aligned} \tag{2.13}$$

The second equation is integrated directly and gives

$$\dot{d} = \frac{1}{c}\left(T(A(q) - \bar{A}) - s\dot{q}\right) \;, \tag{2.14}$$

where the average of the potential

$$\bar{A} := \int_0^1 \mathrm{d}\tau A(q(\tau)) \tag{2.15}$$

is needed for d to be periodic. For the class of fields considered in [131], $\bar{A}$ is zero with an appropriate choice of gauge. In general though, $\bar{A}$ depends non-trivially on the other parameters e.g. c. We also have

$$\dot{x}^2 = c(\dot{q}^2 - \dot{d}^2) - 2s\dot{q}\dot{d} = \text{const} =: T^2 a^2 \ , \tag{2.16}$$

which defines a second constant of motion a. In the lightfront limit $c \to 0$, (2.14) becomes a constraint equation for $q \propto x^+$, which we recognise from Paper IV, and d is then obtained from (2.16). Using (2.16) and (2.14) gives an equation involving only q,

$$\dot{q} = \pm T\sqrt{ca^2 + (A(q) - \bar{A})^2} \ . \tag{2.17}$$

The two constants of motion a and $\bar{A}$ can be determined from the two implicit conditions

$$1 = \int_0^1 \mathrm{d}\tau = \oint \frac{\mathrm{d}q}{\dot{q}} = \oint \mathrm{d}q \frac{1}{T\sqrt{ca^2 + (A - \bar{A})^2}} \tag{2.18}$$

and

$$\bar{A} = \int_0^1 \mathrm{d}\tau A \implies 0 = \oint \mathrm{d}q \frac{A - \bar{A}}{\sqrt{ca^2 + (A - \bar{A})^2}} \ , \tag{2.19}$$

where the integration contours circulate the branch cut between the turning points where the square root in (2.18) and (2.19) vanishes, which correspond to the points where $\dot{q} = 0$. The contours can be chosen along the complex instanton loop, but we are free to deform them to other contours circulating the branch. In the lightfront limit the branch shrinks to a pole and integrals can be performed with the Cauchy residue theorem - this localisation is the reason for the simplicity on the lightfront (Paper IV). The residue for (2.19) is proportional to the derivative of the electric field[1], implying (Paper IV)

$$c \to 0 : \qquad \bar{A} = A(\bar{q}) \qquad E'(\bar{q}) = 0 \ , \tag{2.20}$$

which says that the instanton has to circle the maximum/minimum of the electric field.

All nontrivial terms in the effective action as well as (2.18) and (2.19) can be written in terms of the function

$$G(a^2, \bar{A}) = \frac{1}{c} \oint \mathrm{d}q \sqrt{ca^2 + (A(q) - \bar{A})^2} \tag{2.21}$$

and its derivatives $G_0 := \partial_{a^2} G$, $G_1 := \partial_{\bar{A}} G$. This function is closely related to g in [131] (see below), but has one more argument corresponding to the potential average. Essentially

[1] One has to expand (2.19) to first order in c as the zeroth order term is identically zero.

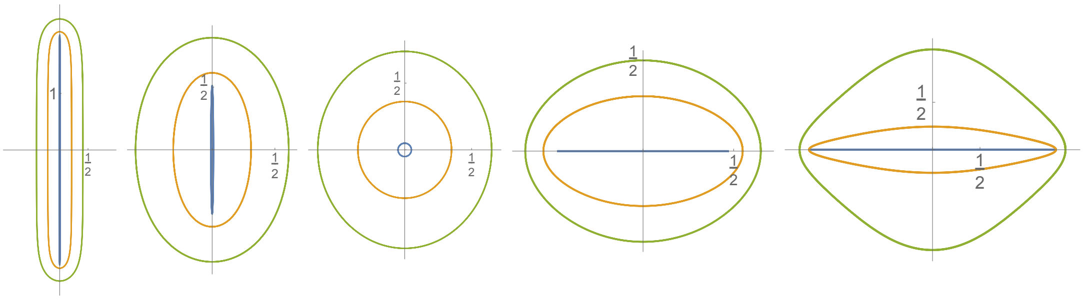

Figure 4. Instantons with different initial position. The plots show the q component in the complex q plane, for $c\gamma^2 = 100, 0.3, 0, -0.2, -0.8$.

the same G also appears in the WKB treatment in [134], where the momentum p takes the place of the potential average $\bar{A} \leftrightarrow p$. See also [178]. The two conditions (2.18) and (2.19) for a and $\bar{A}$ can be expressed in terms of G as

$$G_0(ca^2, \bar{A}) = \frac{T}{2} \qquad G_1(ca^2, \bar{A}) = 0 \,. \tag{2.22}$$

We observe for later reference that G satisfies

$$(4a^2\partial^2_{a^2} + c\partial^2_{\bar{A}})G = 0 \,. \tag{2.23}$$

2.3.1 Instanton examples

It is common to study electric fields with pulse shape given by sech^2. Here we will instead consider a Gaussian pulse

$$E(q) = E_0 e^{-\pi(kq)^2/4} \tag{2.24}$$

where the numerical factor in the exponent is chosen such that the potential

$$A(q) = \frac{1}{\gamma}\text{erf}\,\frac{\sqrt{\pi}kq}{2} \tag{2.25}$$

is normalised as

$$-\frac{1}{\gamma} = A(-\infty) < A(q) < A(\infty) = \frac{1}{\gamma} \,. \tag{2.26}$$

Because of the symmetry of this field we can take $\bar{A} = 0$ independently of c and other parameters (at least for the instanton circulating the field maximum). Some instanton examples are shown in Fig. 4, which are obtained by solving (2.13) with initial conditions consistent with (2.14) and (2.17). As was shown in Paper III, the length of the branch depends on the interpolating parameter c, and for $c \to 0$ the branch collapses into a pole. The length of the branch diverges as $c\gamma^2 \to -1$, which is the critical point for interpolating fields. In Paper III we plotted similar instantons but for $E = E_0\text{sech}^2 kq$, which has poles on the imaginary axis that restrict the length of the branch for timelike fields. For the Gaussian pulse that we consider here (2.24), the field is entire without such poles. This difference can have a large impact on the probability [119].

It turns out, though, that for the class of fields we consider here one actually does not need to obtain the instantons to evaluate the final result for the pair production probability.

However, fields with one-dimensional inhomogeneities is only a first step to more realistic fields with multi-dimensional inhomogeneities. Instantons for fields depending on time and one spatial coordinate separately were considered in [118, 137].

2.4 Prefactor

One can often obtain a reasonable approximation by evaluating the exponent in (2.11) at the saddle point (for both the path integral and the proper time integral) and neglecting the prefactor. However, the prefactor is important e.g. close to the critical point. The prefactor is much harder to calculate than the exponent, but for the class of fields we consider here this is possible with the method developed in [131].

2.4.1 Path integral

The second variation of the action in (2.11) around the instanton is

$$S_2 = \frac{1}{2T}\delta x \Lambda \delta x \; , \tag{2.27}$$

where

$$\Lambda = \begin{pmatrix} -c\partial^2 + \frac{\dot{d}}{\dot{q}}\partial\left(\frac{c\ddot{d}+s\ddot{q}}{\dot{q}}\right) & s\partial^2 + \frac{c\ddot{d}+s\ddot{q}}{\dot{q}}\partial \\ s\partial^2 - \partial\frac{c\ddot{d}+s\ddot{q}}{\dot{q}} & c\partial^2 \end{pmatrix} . \tag{2.28}$$

The δx integral is Gaussian and gives the (functional) determinant of Λ, which can be computed with the Gelfand-Yaglom method as in [131]. For Dirichlet boundary condition $\delta x(0) = \delta x(1) = 0$ the determinant is given by

$$\det \Lambda = \det \phi^3 \phi^4(1) \; , \tag{2.29}$$

where ϕ^3 and ϕ^4 are the two solutions of the Jacobi equation

$$\Lambda \phi = 0 \; , \tag{2.30}$$

which satisfy the initial conditions

$$\phi^3(0) = \phi^4(0) = 0 \qquad \dot{\phi}^3(0) = \begin{pmatrix} 1 \\ 0 \end{pmatrix} \qquad \dot{\phi}^4(0) = \begin{pmatrix} 0 \\ 1 \end{pmatrix} . \tag{2.31}$$

Formula (2.29) applies to ratios of two determinants, in particular to the ratio of the field dependent and the free determinant. With our conventions, the right-hand side of (2.29) equals one for the free determinant. To find ϕ^3 and ϕ^4, we begin by expressing a general solution of (2.30) as a linear combination of the two trivial solutions

$$\phi = H \begin{pmatrix} \dot{q} \\ \dot{d} \end{pmatrix} + D \begin{pmatrix} 0 \\ 1 \end{pmatrix} . \tag{2.32}$$

Constant H and D corresponds to reparameterisation and translation invariance. By multiplying (2.30) with $\begin{pmatrix} \dot{p} & \dot{n} \end{pmatrix}$ and $\begin{pmatrix} 0 & 1 \end{pmatrix}$ we obtain two relatively simple equations for H and D with solutions depending on two constants k_1 and k_2,

$$\dot{H} = \frac{-k_1 c + k_2(s\dot{q} + c\dot{d})}{\dot{q}^2} \qquad \dot{D} = \frac{k_1(s\dot{q} + c\dot{d}) + k_2\dot{x}^2}{\dot{q}^2} . \tag{2.33}$$

It is easy to check that for $c = 1$ we recover the solutions in [131]. Imposing the boundary conditions (2.31) we find

$$H^3(\tau) = \int\limits_0^\tau \frac{s(s\dot{q}+c\dot{d})+c(c\dot{q}_0-s\dot{d}_0)}{\dot{q}^2} \qquad D^3 = \int\limits_0^\tau \frac{s\dot{x}^2-(c\dot{q}_0-s\dot{d}_0)(s\dot{q}+c\dot{d})}{\dot{q}^2} \tag{2.34}$$

and

$$H^4 = \int\limits_0^\tau \frac{c(s\dot{q}+c\dot{d})-c(s\dot{q}_0+c\dot{d}_0)}{\dot{q}^2} \qquad D^4 = \int\limits_0^\tau \frac{c\dot{x}^2+(s\dot{q}_0+c\dot{d}_0)(s\dot{q}+c\dot{d})}{\dot{q}^2} \,. \tag{2.35}$$

Substituting these solutions into (2.29) gives

$$\det\Lambda = \dot{q}_0^2\left[c\dot{x}^2\bigg(\int\limits_0^1 \frac{1}{\dot{q}^2}\bigg)^2 + \bigg(\int\limits_0^1 \frac{s\dot{q}+c\dot{d}}{\dot{q}^2}\bigg)^2\right] \,. \tag{2.36}$$

Note that (2.36) is a simple generalisation of the determinant in [131], to which it reduces for $\{c = \pm 1, \bar{A} = 0\}$. Both terms in (2.36) are in general nonzero. The second term vanishes for field shapes considered in [131]. Both terms vanish[2] in the lightfront limit $c \to 0$, which signals the presence of zero modes and suggests that, although the result is simple on the lightfront, the calculation can be more subtle. In any case, everything in the square brackets in (2.36) will cancel against a term coming from the proper time integral, and the final result is finite for all c. The determinant can also be written in terms of G. For the first term in (2.36) we have

$$\int\limits_0^1 \frac{1}{\dot{q}^2} = -\frac{4G_{00}}{cT^3} \,. \tag{2.37}$$

At first sight the left-hand side of (2.37) looks divergent because of the turning points $\dot{q} = 0$. However, if we start with instantons circulating the branch cut so that $\dot{q} \neq 0$ along the whole contour, we can write the integral in terms of G and then deform the contour to the branch cut without encountering any divergences. For the second term in (2.36) we have

$$\int\limits_0^1 \frac{s\dot{q}+c\dot{d}}{\dot{q}^2} = \frac{1}{T^2}\oint \mathrm{d}q \frac{A-\bar{A}}{(ca^2+(A-\bar{A})^2)^{3/2}} = \frac{2G_{01}}{T^2} \,. \tag{2.38}$$

Putting (2.37) and (2.38) together we find a neat expression for the determinant

$$\det\Lambda = 4\frac{\dot{q}_0^2}{T^4}\left(\frac{a^2}{c}(2G_{00})^2 + (G_{01})^2\right) \,. \tag{2.39}$$

Taking the square root of the determinant (2.39) yields the following for the integral over initial position,

$$\int \mathrm{d}q_0 \frac{1}{\dot{q}(0)} \,, \tag{2.40}$$

[2] The second integral vanishes because $1/\dot{q} \propto \dot{d}$ when $c \to 0$.

where

$$\dot{q}(0) = \pm T\sqrt{ca^2 + (A(q_0) - \bar{A})^2} \; . \tag{2.41}$$

As described in Paper III, this integral gives a factor of 1/2 essentially because the integration is only over half of the integral in (2.18).

2.4.2 Proper time integral

Next we perform the proper time integral. The exponent is at this stage e^{-iS} with

$$S = \frac{T}{2}(1-a^2) + \frac{1}{c}\oint \mathrm{d}q\sqrt{ca^2 + (A-\bar{A})^2} = \frac{T}{2}(1-a^2) + G(ca^2, \bar{A}) \; . \tag{2.42}$$

The T integral can also be performed with a saddle point approximation. The two conditions (2.22) for a and $\bar{A}$ simplify the proper time derivative

$$\frac{\mathrm{d}S}{\mathrm{d}T} = \frac{\partial S}{\partial T} + \frac{\mathrm{d}a^2}{\mathrm{d}T}\Big(-\frac{T}{2} + G_0\Big) + \frac{\mathrm{d}\bar{A}}{\mathrm{d}T}G_2 = \frac{1}{2}(1-a^2) \tag{2.43}$$

so the saddle point is determined simply by setting $a^2 = 1$ and

$$S_s = G(c, \bar{A}) \qquad T_s = 2G_0(c, \bar{A}) \qquad G_1(c, \bar{A}) = 0 \; , \tag{2.44}$$

where the last equation determines the potential average $\bar{A}$ in terms of c. The second derivative is simplified by differentiating (2.22) and using (2.23) to replace G_{11} in favor of G_{00},

$$\frac{\mathrm{d}^2 S}{\mathrm{d}T} = -\frac{G_{00}}{c}\Big(\frac{1}{c}(2G_{00})^2 + (G_{01})^2\Big)^{-1} \; , \tag{2.45}$$

where $a^2 = 1$.

2.5 Final result

Collecting all terms from the path and proper time integrals we find

$$\mathrm{Im}\;\Gamma = \mathrm{Im}\;V_3\int \mathrm{d}p_0 \frac{\sqrt{2\pi}}{T\sqrt{i\mathrm{d}_T^2 S}}\frac{1}{(2\pi T)^2}\frac{e^{-iS}}{\sqrt{\det}} = \frac{\sqrt{2\pi}}{32\pi^2}V_3\frac{e^{-iG}}{iG_0\sqrt{-iG_{00}/c}} \; . \tag{2.46}$$

The big round brackets in (2.45) and (2.39) cancel along with the G_{01} terms. This simplification might not come as a surprise given Gutzwiller's trace formula [177]. Now everything is expressed in terms of $G(c, \bar{A})$ and the first two derivatives with respect to the first argument. Note that in general this is not the total derivative with respect to c, because the potential average $\bar{A}$ may depend on c. For the large class of fields studied in [131], though, one has $\bar{A} = 0$ for all c.

It might be useful to rewrite (2.46) in a WKB form by introducing an integral over the average,

$$\mathrm{Im}\;\Gamma = \frac{V}{2c}\int \frac{\mathrm{d}^3\bar{A}}{(2\pi)^3}e^{-iG} \; , \tag{2.47}$$

where G is now also a function of $\bar{A}_\perp$,

$$G = \frac{1}{c}\oint \mathrm{d}q\sqrt{c + (A(q) - \bar{A})^2 + \bar{A}_\perp^2} \; . \tag{2.48}$$

The integral expression (2.47) is equivalent to (2.46) in the semiclassical regime. This is shown by performing the integral with the saddle point method; the saddle point is determined by $\bar{A}_\perp = 0$ and $G_1 = 0$, the $\bar{A}_\perp$ integrals give the G_0 factor, and the $\bar{A}$ integral gives the G_{00} factor. In WKB [134, 178] one finds expressions like (2.47) with momentum instead of $\bar{A}$. Hence, the condition (2.19) for $\bar{A}$ simply corresponds to the saddle point for a momentum integral in a WKB approach.

So far we have discussed scalar QED. However, for the fields we consider here, the only difference between scalar and spinor QED in the semiclassical regime is a numerical factor in front of (2.46). This is shown in the same way as in [130, 133]. The spin factor that has to be included in the path integral involves a trace over Dirac matrices and path ordering. For the fields considered here though, it simply reduces to

$$-2\cos\frac{iT}{2}\int\limits_0^1 E(q) \; . \tag{2.49}$$

Since, unlike the exponent, (2.49) is not rapidly oscillating, it does not affect the saddle points. The integral can be written

$$\int\limits_0^1 E(q) = \frac{1}{T}\oint \mathrm{d}q\frac{A'}{\sqrt{ca^2+(A-\bar{A})^2}} \; . \tag{2.50}$$

Changing variables from q to A yields

$$\frac{1}{T}\oint \mathrm{d}A\frac{1}{\sqrt{ca^2+(A-\bar{A})^2}} = \frac{2i}{T}\int\limits_{-1}^1\frac{\mathrm{d}y}{\sqrt{1-y^2}} = \frac{2\pi i}{T} \; . \tag{2.51}$$

Substituting (2.51) into (2.49) gives a factor of 2. We note as an aside that (2.51) can be written

$$T = \frac{2\pi i}{\langle E\rangle} \; , \tag{2.52}$$

which is a relation we recognise from Paper IV.

As noted in Paper III, there is a simple argument for the final result (2.46), which is based on the fact that for $c > 0$ ($c < 0$) a Lorentz transformation will turn the field into a time (z) dependent field, with frequency scaling with c as

$$k' = \sqrt{c}k \; . \tag{2.53}$$

So for symmetric fields with $\bar{A} = 0$ we can simply use the results in [131] for a time-dependent field to confirm the semiclassical result (2.46). We see that $c \to 0$ is effectively a zero frequency limit (2.53), which explains why pair production on the lightfront is exactly given by the locally constant field approximation.

2.6 Universality near critical points

For fields with space-like inhomogeneities (this includes fields with additional temporal inhomogeneities) there is a critical point where the pair production probability vanishes, see [110, 132, 142, 146], Paper III. This critical point corresponds to the threshold where the electric field provides the minimum amount of electrostatic energy needed to pull apart a virtual pair into a real pair. In Paper II we studied the behaviour of the probability near the critical point. We found aspects of universality similar to continuous phase transitions in critical phenomena; the electric fields divide into universality classes with critical scaling that only depends on the asymptotic behaviour of the fields. It is interesting to contrast the universality near the critical point with the extreme sensitivity on the pulse shape in regimes with dynamical assistance [117–122]. To produce pairs the electrostatic energy needs to be larger than twice the electron mass (recall $m = 1$)

$$\frac{2}{\gamma} = \int_{-\infty}^{\infty} \mathrm{d}x\, E > 2 \implies \gamma < 1 \,, \tag{2.54}$$

One find quite generally that the probability scales as

$$\mathrm{Im}\,\Gamma \propto (1-\gamma)^{\beta} \qquad \gamma \to 1 \,, \tag{2.55}$$

where the critical exponent $\beta > 0$ is independent on the local structure of the electric field. In the semiclassical regime

$$E^2 \ll 1 - \gamma^2 \tag{2.56}$$

the critical exponent depends on the asymptotic form of the field; e.g. for fields vanishing as $|x|^{-d}$ one finds (Paper II)

$$\beta = \frac{5d+1}{4(d-1)} \,. \tag{2.57}$$

In the immediate vicinity of the critical point, where in particular

$$1 - \gamma^2 \ll E^2 \,, \tag{2.58}$$

one finds that β is even more universal. In fact, all fields vanishing sufficiently fast share the same universal scaling with critical exponent $\beta = 3$ [179]. On the other hand, fields that vanish slowly, e.g. as $|x|^{-2}$, exhibit essential scaling (Paper II, [179])

$$\mathrm{Im}\,\Gamma \propto \exp -.../(1-\gamma^2)^{\lambda} \,. \tag{2.59}$$

3 Plane waves - an invitation to lightfront quantisation

In the rest of this thesis we will consider processes in plane wave backgrounds. One reason to choose plane wave backgrounds is that the calculations can be performed with no approximations other than the usual coupling expansion. Another reason is the prospect of detecting RR in experiments with the next generation of high intensity lasers, for which plane waves provide a model. (However, in order to achieve higher intensities the laser is focused, which cannot be accommodated in a plane wave model. Using more physical backgrounds is of course a challenge and one might have to turn to numerical methods.)

The plane wave background field is given by $f_{\mu\nu}(nx) = k_\mu a'_\nu(nx) - k_\nu a'_\mu(nx)$, where $k_\mu = \omega n_\mu$ is a null vector, ω a characteristic frequency, and a an arbitrary function of nx. It is convenient to use lightfront coordinates, which are defined by

$$v^\pm = 2v_\pm = v^0 \pm v^3 \qquad \text{and} \qquad v^\perp = \{v^1, v^2\} \, . \tag{3.1}$$

In these coordinates the background only depend on x^+, which is referred to as lightfront time. We choose gauge such that $a_+ = a_- = 0$ and $a_\perp(-\infty) = 0$.

We are particularly interested in how an electron moves in a background field when RR is included. Without RR an electron moves according to the Lorentz force equation (recall that a factor of e has been absorbed into the background)

$$m\ddot{x}^\mu = f^{\mu\nu}\dot{x}_\nu \, , \tag{3.2}$$

which in a plane wave has a relatively simple solution,

$$m\dot{x}^\mu = \pi^\mu(x^+) := p^\mu - a^\mu + \frac{2ap - a^2}{2kp}k^\mu \, , \tag{3.3}$$

where $p = \pi(-\infty)$ is the initial momentum of the electron before it has entered the (pulsed) plane wave.

In QED we can treat a plane wave background exactly by solving the Klein-Gordon equation for a scalar electron and the Dirac equation for an electron with spin. The Klein-Gordon equation is given by

$$(\mathcal{D}^2 + m^2)\varphi = 0 \, , \tag{3.4}$$

where $\mathcal{D}_\mu = \partial_\mu + ia_\mu$ is the background covariant derivative. The solution to (3.4) that reduces to e^{-ipx} for $a \to 0$, is readily found using the ansatz $\varphi = e^{-ipx}\eta(x^+)$, with which (3.4) becomes

$$\partial_+\varphi = -i(p_+ + V_p k_+)\varphi \, , \tag{3.5}$$

where

$$V_p = \frac{2ap - a^2}{2kp} \, . \tag{3.6}$$

We immediately find

$$\varphi_p(x) = \exp -i\left(px + \int^{kx} V_p\right) \, , \tag{3.7}$$

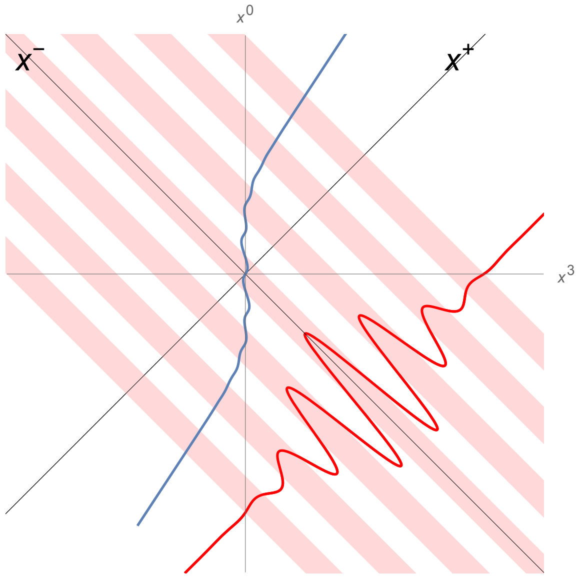

Figure 5. The red curve represents the plane wave background and the blue curve is the trajectory of an electron moving according to the Lorentz force.

which is the Volkov solution [149] for scalar QED. The Volkov solution for the Dirac equation is similar to (3.7) and is presented in Sect. 5. The (scalar) Volkov solution is an eigenfunction of the background covariant derivative

$$i\mathcal{D}_\mu \varphi = \pi_\mu \varphi \;, \tag{3.8}$$

and the eigenvalue is the Lorentz momentum. As we will see in Sect. 7, this means the Volkov solution describes an electron moving according to the Lorentz force.

Thus, plane waves allow for simple exact solutions both classically and in QED. The fact that everything non-trivial happens along the lightfront time direction makes it natural to use lightfront time instead of ordinary time to parameterise the dynamics. This brings us to the lightfront quantisation formalism, which is presented in Sect. 4 and Sect. 5. Then in Sect. 6 and Sect. 7 we apply this formalism to vacuum birefringence and RR, respectively.

4 Lightfront quantisation of scalar QED in a background field

To study RR and vacuum birefringence in Papers VI, VII, we used a formalism that combines plane wave backgrounds with lightfront quantisation [154]. In this section and in Sect. 5 we will introduce this formalism, and in Sect. 6 and Sect. 7 we will show how to apply it to the problems of RR and vacuum birefringence, respectively. We will start with scalar QED in this section and treat spinor QED in Sect. 5. Scalar QED is simpler, but is still relevant e.g. for classical RR.

The action for scalar QED is given by

$$S = \int \mathrm{d}^4x\sqrt{-g}\left(-\frac{1}{4}g^{\mu\rho}g^{\nu\sigma}\mathsf{F}_{\rho\sigma}\mathsf{F}_{\mu\nu} + g^{\mu\nu}(\mathsf{D}_\mu\phi)^\dagger\mathsf{D}_\nu\phi - m^2\phi^\dagger\phi\right) . \tag{4.1}$$

where $\mathsf{D}_\mu = \partial_\mu + ie\mathsf{A}_\mu$ is the covariant derivative. The reason for the unusual font is to distinguish A from a simpler field A that is introduced below. We have written out $g^{\mu\nu}$ explicitly in (4.1) only in order to obtain the energy-momentum tensor from a variation $\delta g^{\mu\nu}$. Varying the action with respect to the fields gives the Klein-Gordon equation

$$(\mathsf{D}^2 + m^2)\phi = 0 \tag{4.2}$$

and the Maxwell equations

$$\partial_\mu\mathsf{F}^{\mu\nu} = eJ^\nu \ , \tag{4.3}$$

with current given by

$$J_\mu = i\phi^\dagger\mathsf{D}_\mu\phi + \text{c.c.} = \phi^\dagger(i\overleftrightarrow{\partial}_\mu - 2e\mathsf{A}_\mu)\phi \ , \qquad \overleftrightarrow{\partial}_\mu = \overrightarrow{\partial}_\mu - \overleftarrow{\partial}_\mu \ . \tag{4.4}$$

4.1 Momentum

Of central importance here is the momentum operator, as we will use it to obtain RR from QED. Both the momentum operator and the Hamiltonian (the generator of lightfront time evolution) can be obtained from the energy-momentum tensor; we will therefore look at this tensor in some detail. The energy-momentum tensor can be obtained either by varying the action with respect to the metric or from the canonical definition. We use the former method here and the canonical method later in the spinor case.

The energy-momentum is obtained by varying the metric and is defined by [180]

$$\delta_{g_{\mu\nu}}S = -\int \mathrm{d}^4x\sqrt{-g}\frac{1}{2}T^{\mu\nu}\delta g_{\mu\nu} \ . \tag{4.5}$$

Using the standard results

$$\delta g^{\mu\nu} = -g^{\mu\rho}g^{\nu\sigma}\delta g_{\rho\sigma} \ , \qquad \delta\sqrt{-g} = \frac{1}{2}\sqrt{-g}g^{\mu\nu}\delta g_{\mu\nu} \ , \tag{4.6}$$

one finds

$$T_{\mu\nu} = \mathsf{F}_{\mu\tau}\mathsf{F}^\tau{}_\nu + (\mathsf{D}_\mu\phi)^\dagger\mathsf{D}_\nu\phi + (\mathsf{D}_\nu\phi)^\dagger\mathsf{D}_\mu\phi - g_{\mu\nu}\mathcal{L} \ . \tag{4.7}$$

This tensor is symmetric, gauge invariant and satisfies $\partial_\mu T^{\mu\nu} = 0$. The same tensor is also obtained with standard canonical methods (see e.g. [181]).

From the energy-momentum tensor (4.7) we obtain the momentum by integrating over a hypersurface Σ with a surface element given by [152]

$$d\sigma^\mu = d^4x\,\delta(s(x))\partial^\mu s \ . \tag{4.8}$$

The momentum is defined by

$$P_\mu = \int\limits_\Sigma d\sigma^\nu T_{\nu\mu} \ . \tag{4.9}$$

If the surface is a plane then $s(x) = nx - c$, where n_μ and c are constants. The most common choice for the surface is one of equal time, i.e. $n^\mu = \delta_0^\mu$,

$$P_\mu = \int d^3x T_{0\mu} \ . \tag{4.10}$$

Other surfaces are also possible. In [151] Dirac introduced three different "forms of relativistic dynamics". Different forms have different "time" parameters. Choosing x^0 to be the time parameter gives what is called the instant form. We will instead use the front form where the time parameter is lightfront time $x^+ = x^0 + x^3$. The corresponding surface is characterised by $nx = x^+$. The main reason for this choice here is that we will study plane wave backgrounds which only depend on lightfront time x^+ as emphasised in Sect. 3. Combining plane wave backgrounds with lightfront quantisation was first done in [154].

For coordinates we use superscripts while for the momenta we use subscripts, and

$$\bar{x} = \{x^-, x^\perp\} \qquad \bar{p} = \{p_-, p_\perp\} \ . \tag{4.11}$$

The measure for Lorentz invariant on-shell momentum integrals is

$$d\tilde{p} := \frac{d^4p}{(2\pi)^4} 2\pi\delta(p^2 - m^2)\theta(p_0) = \frac{dp_\perp dp_-}{(2\pi)^3 2p_-}\theta(p_-) \ . \tag{4.12}$$

A delta function corresponding to this measure is

$$\int d\tilde{q}\ \tilde{\delta}(q,p)F(q) = F(p) \ , \tag{4.13}$$

which in lightfront coordinates implies

$$\tilde{\delta}(q,p) = 2p_-(2\pi)^3\bar{\delta}(q-p) \ . \tag{4.14}$$

The surface element (4.8) becomes

$$d\sigma_\mu = d^4x\,\delta(x^+ - c)n_\mu = \frac{1}{2}d\bar{x}n_\mu \ , \tag{4.15}$$

and hence the momentum is given by

$$P_\mu = \int \frac{d\bar{x}}{2} T^+{}_\mu = \int d\bar{x}\ T_{-\mu} \ . \tag{4.16}$$

In the front form the states are specified and the operators quantised on the initial lightfront surface $x^+ =$ const. The lightfront Hamiltonian $H = P_+$ evolves the states and operators in lightfront time. This is variously called lightfront, light cone or null plane quantisation in the literature. For reviews of this formalism see [152, 153].

4.2 Lightfront gauge

In lightfront QED it is convenient to use the lightfront gauge $\mathsf{A}_- = 0$. The equation of motion

$$\partial_\mu \mathsf{F}^\mu{}_- = -2\partial_-^2 \mathsf{A}_+ + \partial_- \partial_\perp \mathsf{A}_\perp = J_- = \phi^\dagger i \overleftrightarrow{\partial}_- \phi \tag{4.17}$$

has no time derivatives ∂_+, which makes it a constraint equation. It is used to solve for A_+ in terms of the transverse components $\mathsf{A}_\perp$ and the current

$$\mathsf{A}_+ = \frac{\partial_\perp \mathsf{A}_\perp}{2\partial_-} - \frac{eJ_-}{2\partial_-^2} \ . \tag{4.18}$$

One is immediately confronted with the zero mode issue; how should the inverse of ∂_- be defined? In Fourier space the inverse becomes $1/p_-$ and the problem translates into how to treat $p_- \to 0$, hence the name zero mode. A principal-value prescription for defining $1/p_-$ is common, but we will not write out a zero mode regularisation explicitly, because for RR and vacuum birefringence we will have sufficiently many factors of p_- in numerators to cancel those in denominators. However, in other cases one must be careful in dealing with the zero modes in order to not miss important physics. As mentioned in Sect. 2, one encounters zero mode problems in Schwinger pair production by a longitudinal electric field that depends on lightfront time [140]. In the original papers [140] this problem was solved by quantising on two lightfront surfaces, i.e. effectively abandoning ordinary lightfront quantisation.

In the lightfront gauge the lightfront Hamiltonian becomes

$$H = P_+ = \frac{1}{2}\int \mathrm{d}\bar{x} |\partial_\perp \phi|^2 + m^2|\phi|^2 + \frac{1}{2}A_j(i\partial_\perp)^2 A_j + ejA - e^2A^2|\phi|^2 + \frac{e^2}{2} j_- \frac{1}{(i\partial_-)^2} j_- \ , \tag{4.19}$$

where the new field is given by $A_\perp = \mathsf{A}_\perp$ and (c.f. (4.18))

$$A_+ = \frac{\partial_\perp A_\perp}{2\partial_-} \ , \tag{4.20}$$

and the new current is

$$j_\mu = \phi^\dagger i \overleftrightarrow{\partial}_\mu \phi \ . \tag{4.21}$$

The spatial components of the momentum operator are given by

$$P_- = \int \mathrm{d}\bar{x} (\partial_- A_\perp)^2 + 2|\partial_-\phi|^2 \tag{4.22}$$

and

$$P_\perp = \int \mathrm{d}\bar{x} \partial_- A_j \partial_\perp A_j + \partial_{(-}\phi^\dagger \partial_{\perp)}\phi \ . \tag{4.23}$$

These are interaction independent (there are no factors of e), or in other words kinematical rather than dynamical [152].

4.3 Quantisation

The presence of constraints complicates the usual canonical quantisation procedure. One way to proceed would be to use the Dirac-Bergmann method for quantisation of constrained systems (see [182] for general systems and [183, 184] for lightfront quantisation). In [152] it is explained how to use either Schwinger's action principle or a method due to Faddeev and Jackiw to quantise on the lightfront. Here we will instead obtain the commutation relations by demanding that the momentum operator should give us translations (see also [181, 185] for more on this method), so that an operator transforms according to

$$\mathcal{O}(x) = e^{ixP}\mathcal{O}(0)e^{-ixP} \tag{4.24}$$

implying the Heisenberg equation

$$i\partial_\mu \mathcal{O}(x) = [\mathcal{O}(x), P_\mu] \ . \tag{4.25}$$

In particular, we should have

$$i\partial_- \phi = [\phi, P_-] \ , \tag{4.26}$$

which, together with (4.22) and $[\phi(x), \phi(y)] = 0$, leads to

$$i\partial_- \phi(x) = \int \mathrm{d}\bar{y}[\phi(x), 2\partial_- \phi^\dagger(y)]\partial_- \phi(y) \ , \tag{4.27}$$

with $x^+ = y^+$. This implies that the equal lightfront time commutator for the scalar field is

$$[\phi(x), 2\partial_- \phi^\dagger(y)]_{x^+=y^+} = i\bar{\delta}(x-y) \ . \tag{4.28}$$

In this case the ambiguity of the inverse of ∂_- is removed by the antisymmetry of the commutator, so

$$[\phi(x), \phi(y)^\dagger]_{x^+=y^+} = -\frac{i}{4}\epsilon(x-y)^- \delta(x-y)^\perp \ . \tag{4.29}$$

Similarly, the commutator for the photon field is found to be

$$[A_i(x), 2\partial_- A_j(y)]_{x^+=y^+} = i\bar{\delta}(x-y)\delta_{ij} \ . \tag{4.30}$$

Using the energy component of (4.25) we recover the Euler-Lagrange equations (4.2) and (4.3). These commutation relations agree with those obtained using other quantisation methods.

4.4 Expectation values

To obtain RR and vacuum birefringence we are interested in expectation values of observables O such as the momentum or the position operator for RR and the electromagnetic field operator for vacuum birefringence. We will begin in the interaction picture to define initial states $|\,\text{in}\,\rangle$ comprising photons in the background and either an electron (for RR) or photons in a probe (for vacuum birefringence). We will show in detail how the background photon state can be transformed into a classical field in the operators. After this we switch to the Furry picture, where the background field is included in the "free" part of the Hamiltonian, which allows in principle for an exact treatment of the background field. All calculations for the expectation values are then performed in the Furry picture.

4.4.1 Interaction picture

In the interaction picture the total Hamiltonian is split into V and H^0, which correspond to the terms in (4.19) with and without factors of e, respectively. Expectation values evolve in (lightfront) time according to

$$\langle O\rangle(x^+) = \langle\, \text{in}\,|U^{i\dagger}(x^+)O_I(x^+)U^i(x^+)|\,\text{in}\,\rangle\ , \tag{4.31}$$

where operators evolve according to the free Hamiltonian

$$O_I(x^+) = U^{0\dagger}(x^+)O_I(0)U^0(x^+)\ , \qquad U^0(x^+) = e^{-ix^+H_I^0(0)}\ , \tag{4.32}$$

and the initial state evolve according to the interaction Hamiltonian

$$U^i(x^+) = T_+ \exp -i\int^{x^+} V_I\ , \tag{4.33}$$

where T_+ means lightfront time ordering. The interaction picture fields obey

$$(\partial^2+m^2)\phi_I = 0\ , \qquad \partial^2 A_{I\perp} = 0\ , \tag{4.34}$$

and have mode expansions

$$\phi_I = \int \mathrm{d}\tilde{p}\ be^{-ipx} + d^\dagger e^{ipx} \tag{4.35}$$

and

$$A_{I\mu} = \int \mathrm{d}\tilde{l}\ a_\mu e^{-ipx} + a_\mu^\dagger e^{ipx}\ , \tag{4.36}$$

where for A_I the measure is (4.12) with $m \to 0$. The mode operators $b(p)$ and $d^\dagger(p)$ annihilate electrons and create positrons, respectively, with momentum p, and the equal lightfront time commutation relation (4.29) implies

$$[b(p), b^\dagger(q)] = [d(p), d^\dagger(q)] = \tilde{\delta}(p,q)\ . \tag{4.37}$$

For the photon mode operators we have $a_- = 0$ and $a_+ = l_\perp a_\perp/2l_-$ (c.f. (4.20)), and the commutation relation is

$$[a_\mu(l), a_\nu(l')] = -\tilde{\delta}(l',l)\Big(g_{\mu\nu} - \frac{1}{nl}n_{(\mu}l_{\nu)}\Big) =: -\tilde{\delta}(l',l)L_{\mu\nu}\ . \tag{4.38}$$

States are built as usual from the vacuum defined by $a|\,0\,\rangle = b|\,0\,\rangle = d|\,0\,\rangle = 0$, by multiplying it with the creation operators $a^\dagger$, $b^\dagger$ and $d^\dagger$.

We note that the photon field is often written with a sum over two orthogonal polarisation vectors ϵ^μ_λ

$$A_I^\mu = \int \mathrm{d}\tilde{l}\ \epsilon^\mu_\lambda(l)a_\lambda(l)e^{-ipx} + \text{c.c.} \tag{4.39}$$

where repeated λ indices are summed. The polarisation vectors can for example correspond to two linear or two circular polarisations. The two polarisation vectors are orthogonal $\bar{\epsilon}_{\lambda'}\epsilon_\lambda = -\delta_{\lambda'\lambda}$ and obey

$$\sum_\lambda \bar{\epsilon}^\mu_\lambda(l)\epsilon^\nu_\lambda(l) = -L^{\mu\nu}\ . \tag{4.40}$$

The photon operators are related by $a^\mu = \epsilon^\mu_\lambda a_\lambda$ and

$$[a_\lambda(l), a_{\lambda'}(l')] = \delta_{\lambda'\lambda}\tilde{\delta}(l', l) \; . \tag{4.41}$$

Since $a^\mu(l)$ is orthogonal to both the photon momentum l and the lightfront wave vector k, so are the polarisation vectors $l\epsilon(l) = k\epsilon(l) = 0$.

4.4.2 Coherent states

The background field and the probe beam (for vacuum birefringence) are described by coherent states, which are examples of states which are "the most classical" in that they have minimal uncertainty. We will transform the background coherent state into a classical field, so that only the electron (for RR) and the probe (for vacuum birefringence) are left in the initial state. See [186] for a similar discussion of coherent states.

The coherent states can be written

$$|\, C\,\rangle = N \exp\left(i \int \mathrm{d}\tilde{l} C^\mu(l) a^\dagger_\mu\right) |\, 0\,\rangle \; , \tag{4.42}$$

where N is a constant such that $\langle C|C\rangle = 1$. Coherent states are eigenstates of the annihilation operator

$$a_\mu(l)|\, C\,\rangle = -iL_{\mu\nu}C^\nu(l)|\, C\,\rangle \tag{4.43}$$

(but not of the electromagnetic field operator), and have a nonzero expectation value of the electromagnetic field, unlike states with a definite number of photons. To zeroth order in the interaction, the expectation value is given by

$$\langle\, C\,|A_{I\mu}(x)|\, C\,\rangle = 2\mathrm{Re}\int \mathrm{d}\tilde{l} - iL_{\mu\nu}C^\nu(l)e^{-ilx} =: C_\mu(x) \; , \tag{4.44}$$

which defines the classical field $C_\mu(x)$ corresponding to the coherent state $|\, C\,\rangle$. A coherent state (4.42) is obtained from the vacuum by multiplication of a unitary operator

$$|\, C\,\rangle = \mathcal{C}|\, 0\,\rangle \qquad \text{with} \qquad \mathcal{C} \propto \exp i\int \mathrm{d}\tilde{l}\; Ca^\dagger + C^* a \; . \tag{4.45}$$

$\mathcal{C}$ is called the translation or displacement operator and the coherent state is said to be obtained by translating or displacing the vacuum.

We are interested in expectation values (4.31) where the initial state consists of a background field and either an electron or a probe field,

$$|\, \mathrm{in}\,\rangle = \mathcal{C}|\, in\,\rangle \; , \tag{4.46}$$

where $\mathcal{C}$ is the displacement operator for the background and $|\, in\,\rangle$ describes an electron or a probe field. Now we use the following "shift" formula [187]

$$\mathcal{C}^\dagger O_I(A_\mu)\mathcal{C} = O_I(A_\mu + C_\mu) =: O^c_I(A_\mu) \tag{4.47}$$

to convert the background coherent state into a classical field in the operators. A shifted operator O^c has an explicit time dependence through the background field $C_\mu(x)$,

$$O^c_I(x^+) = U^{0\dagger}(x^+)O^c_S(x^+)U^0(x^+) \; , \tag{4.48}$$

where $O^c_S(x^+) := O(\phi(0), A(0) + C(x^+))$ (the subscript stands for Schrödinger).

4.4.3 Furry picture

In terms of shifted operators the expectation values become

$$(4.31) = \langle\, in\, | U^{ic\dagger}(x^+) O_I^c(x^+) U^{ic}(x^+) |\, in\,\rangle \ , \tag{4.49}$$

with the background coherent state converted into a classical field C_μ in the operators, so that the initial state $|\, in\,\rangle$ now only describes e.g. an electron or a probe but not the background. We are still in the interaction picture, but we have new terms in the interaction part of the Hamiltonian V_I^c as well as in the observables O_I^c. We could stop at this point and treat the new background field terms perturbatively. However, we want to treat the background exactly and for this we will use a separation of the Hamiltonian into different "free" and interacting parts. We begin by noting that the expectation values can be written

$$(4.49) = \langle\, in\, | \mathcal{U}^\dagger(x^+) O_S^c(x^+) \mathcal{U}(x^+) |\, in\,\rangle \ , \qquad \mathcal{U}(x^+) = T_+ \exp -i \int^{x^+} \mathcal{H}_S \ , \tag{4.50}$$

where the new, explicitly time dependent Hamiltonian $\mathcal{H}$ is obtained from H (4.19) by shifting $A \to A + C$ in the interaction part V. Since there is always a factor of e in front of the background field, we define $c_\mu = eC_\mu$, which also emphasises that the background is treated exactly. In order to treat the background field exactly, we split the new Hamiltonian into a "free" and an interacting term according to $\mathcal{H} = \mathcal{H}^0 + \mathcal{V}$ with

$$\mathcal{H}^0 = \frac{1}{2} \int \mathrm{d}\bar{x} |\mathcal{D}_\perp \phi|^2 + m^2 |\phi|^2 + 2c_+ j_- + \frac{1}{2} A_j (i\partial_\perp)^2 A_j \tag{4.51}$$

and

$$\mathcal{V} = \frac{1}{2} \int \mathrm{d}\bar{x} e\mathcal{J}A - e^2 A^2 |\phi|^2 + \frac{e^2}{2} j_- \frac{1}{(i\partial_-)^2} j_- \ , \tag{4.52}$$

where the new current and the background covariant derivative are given by

$$\mathcal{J}_\mu = i\phi^\dagger \mathcal{D}_\mu \phi + \text{c.c.} = \phi^\dagger (i \overleftrightarrow{\partial}_\mu - 2c_\mu)\phi \ , \qquad \mathcal{D}_\mu = \partial_\mu + ic_\mu \ . \tag{4.53}$$

This separation of the Hamiltonian is called the Furry picture [150] and is in many ways similar to the interaction picture, one only has to remember that the shifted Schrödinger operators are time dependent because of the background field. Furry picture operators evolve in time according to the "free" Hamiltonian

$$O_F^c(x^+) = \mathcal{U}^{0\dagger}(x^+) O_S^c(x^+) \mathcal{U}^0(x^+) \ , \qquad \mathcal{U}^0(x^+) = T_+ \exp -i \int^{x^+} \mathcal{H}_S^0 \ , \tag{4.54}$$

which implies

$$i\partial_+ O_F^c = [O_F^c, \mathcal{H}_F^0] + i(\partial_+ O^c)_F \ , \tag{4.55}$$

where

$$(\partial_+ O^c)_F = \mathcal{U}^{0\dagger} \partial_+ O_S^c \mathcal{U}^0 \tag{4.56}$$

takes into account the explicit time dependence coming from the background. Finally, the expectation values expressed in terms of Furry picture fields are given by

$$\langle O\rangle(x^+) = \langle\, in\,|\mathcal{U}^{i\dagger}(x^+)O^c_F(x^+)\mathcal{U}^i(x^+)|\, in\,\rangle \;, \qquad \mathcal{U}^i = T_+ \exp -i\int^{x^+} \mathcal{V}_F \;. \tag{4.57}$$

This is the form of the expectation values that we will use to obtain RR and vacuum birefringence.

To evaluate these expectation values we first need to find the Furry picture scalar field. From

$$i\partial_+\partial_-\phi_F = [\partial_-\phi_F, \mathcal{H}^0_F] \tag{4.58}$$

it follows that ϕ_F satisfies the Klein-Gordon equation with background covariant derivatives

$$(\mathcal{D}^2 + m^2)\phi_F = 0 \;. \tag{4.59}$$

The equation for the photon field is the same as in the interaction picture, $\partial^2 A_{F\perp} = 0$, and consequently A_F is given by (4.36). The Furry picture is most useful if we can solve (4.59) exactly (or in some non-perturbative approximation). We saw in Sect. 3 that the exact solution for plane waves is relatively simple.

From now on everything will be in the Furry picture and all observables are the ones obtained after making the shift $eA_\mu(x) \to eA_\mu(x)+c_\mu(x)$ in the interaction parts of operators, where A is the quantised photon field and $c_\mu(x)$ is the classical field corresponding to the background; we will therefore drop indices etc used above to denote this. The expectation values (4.57) are calculated using the mode expansions for the fields and the commutation relations for the mode operators. For the photon field we have (4.36) and (4.38). The scalar field satisfies the background field modified Klein-Gordon equation (4.59) and the solution in a plane wave is given by

$$\phi(x) = \int \mathrm{d}\tilde{p}\; b\varphi_p(x) + d^\dagger\varphi_{-p}(x) \;, \tag{4.60}$$

where the mode function $\varphi_p(x)$ is given by (3.7) and the mode commutation relations are given by (4.37).

5 Lightfront quantisation of spinor QED in a background field

We will now turn to spinor, or ordinary, QED, still using lightfront quantisation with a background field. We used this formalism in Paper V and I to study vacuum birefringence and RR, respectively. The first part of this section mirrors the scalar treatment, but this time with less detail. For more details on lightfront quantisation see [152, 153].

5.1 Equations of motion and constraints

The action for spinor QED is given by

$$S = \int \mathrm{d}^4x \, \frac{1}{2}\bar{\Psi}(i\not{\mathsf{D}} - m)\Psi + \text{c.c.} - \frac{1}{4}\mathsf{F}^2 \, . \tag{5.1}$$

We write it this way, with the c.c. term, because it will be helpful when we obtain the energy momentum tensor. We use Ψ and A to distinguish these fields from ψ and A that are introduced below. The equations of motion are the Maxwell equations

$$\partial_\mu \mathsf{F}^{\mu\nu} = eJ^\nu = e\bar{\Psi}\gamma^\nu\Psi \tag{5.2}$$

and the Dirac equation

$$(i\not{\mathsf{D}} - m)\Psi = 0 \, . \tag{5.3}$$

We continue to use the lightfront gauge $\mathsf{A}_- = 0$. Again, one of the components of (5.2) is a constraint equation implying

$$\mathsf{A}_+ = \frac{\partial_\perp \mathsf{A}_\perp}{2\partial_-} - e\frac{J_-}{2\partial_-^2} \, , \tag{5.4}$$

which has the same form as (4.18). In scalar QED this was the only constraint. Now we also have a constraint equation for the spinor field. To obtain this constraint, we use the two projection operators defined by

$$\Lambda_\pm = \frac{1}{4}\gamma^\mp\gamma^\pm \tag{5.5}$$

to separate the spinor field into two parts according to

$$\Psi = \Psi_+ + \Psi_- \qquad \Psi_\pm = \Lambda_\pm \Psi \, . \tag{5.6}$$

Multiplying the Dirac equation (5.3) by γ^+ leads to a constraint equation that allows us to express Ψ_- in terms of Ψ_+,

$$\Psi_- = \frac{1}{4i\partial_-}(m + i\gamma^\perp \mathsf{D}_\perp)\gamma^+\Psi_+ \, . \tag{5.7}$$

The equation of motion for the unconstrained part Ψ_+ is

$$i\mathsf{D}_+\Psi_+ = (m + i\gamma^\perp \mathsf{D}_\perp)\frac{1}{4i\partial_-}(m - i\gamma^\perp \mathsf{D}_\perp)\Psi_+ \, . \tag{5.8}$$

5.2 Momentum operators

Next we turn to the energy-momentum tensor. It is a little more complicated to obtain a tensor by varying with respect to the metric when one has spinors (see [188]). Instead we start with the canonical tensor and modify it to make it gauge invariant and symmetric. Using the definition of the canonical momentum tensor

$$T^c_{\mu\nu} = \frac{\partial \mathcal{L}}{\partial \partial^\mu \phi_r} \partial_\nu \phi_r - g_{\mu\nu} \mathcal{L} \ , \tag{5.9}$$

where ϕ_r denotes all the fields, one finds

$$T_c^{\mu\nu} = \bar{\Psi}\gamma^\mu \frac{i}{2} \overleftrightarrow{\partial}^\nu \Psi - \mathsf{F}^{\mu\rho}\partial^\nu \mathsf{A}_\rho + \frac{1}{4} g^{\mu\nu} \mathsf{F}^2 \ . \tag{5.10}$$

However, this is neither gauge invariant nor symmetric. We can make it gauge invariant by adding the term $\partial_\rho(\mathsf{F}^{\mu\rho}\mathsf{A}^\nu)$, which gives

$$\tilde{T}^{\mu\nu} = \frac{1}{2}\bar{\Psi}\gamma^\mu i\mathsf{D}^\nu \Psi + \text{c.c.} + \mathsf{F}^{\mu\rho}\mathsf{F}_\rho{}^\nu + \frac{1}{4} g^{\mu\nu}\mathsf{F}^2 \ . \tag{5.11}$$

To make it symmetric we have to add one more term. To find this term we write the tensor as a sum of a symmetric and an antisymmetric part

$$\tilde{T}^{\mu\nu} = \frac{1}{2}\tilde{T}^{(\mu\nu)} + \frac{1}{2}\tilde{T}^{[\mu\nu]} \ . \tag{5.12}$$

Using the Dirac equation one can show that the anti-symmetric part can be written as

$$\frac{1}{2}\tilde{T}^{[\mu\nu]} = \frac{i}{8}\partial_\rho \bar{\Psi}\gamma^{[\rho}\gamma^\nu\gamma^{\mu]}\Psi \ . \tag{5.13}$$

Due to the antisymmetry of the ρ and μ indices, it follows that $\partial_\mu \tilde{T}^{[\mu\nu]} = 0$. We can therefore drop this term from the tensor without violating $\partial_\mu T^{\mu\nu} = 0$. Thus, we have finally obtained a gauge invariant and symmetric tensor

$$T^{\mu\nu} = \frac{1}{4}\bar{\Psi}\gamma^{(\mu} i\mathsf{D}^{\nu)}\Psi + \text{c.c.} + \mathsf{F}^{\mu\rho}\mathsf{F}_\rho{}^\nu + \frac{1}{4} g^{\mu\nu}\mathsf{F}^2 \ . \tag{5.14}$$

Next we use definition (4.16) to obtain the momentum operator. The terms added to fix the canonical tensor actually give vanishing contributions to the momentum operator upon integration over the spatial volume. Hence, the fermionic part of the momentum operator becomes

$$P^\mu_f = \frac{1}{2}\int \mathrm{d}\bar{x} \frac{1}{4}\bar{\Psi}\gamma^{(+} i\mathsf{D}^{\mu)}\Psi + \text{c.c.} = \frac{1}{2}\int \mathrm{d}\bar{x}\frac{1}{2}\bar{\Psi}\gamma^+ i\mathsf{D}^\mu \Psi + \text{c.c.} \tag{5.15}$$

The next step is to eliminate the time derivatives and express the momentum operators in terms of the new fields $\psi_+ = \Psi_+$,

$$\psi_- = \frac{1}{4i\partial_-}(m + i\gamma^\perp\partial_\perp)\gamma^+\psi_+ \ , \tag{5.16}$$

$A_\perp = \mathsf{A}_\perp$ and $A_+ = \partial_\perp A_\perp / 2\partial_-$. We also write $j^\mu = \bar\psi\gamma^\mu\psi$. This step is straightforward for the the spatial components $a = {}_-, {}_\perp$. The fermion part becomes

$$P_a^f = \frac{1}{2}\int \mathrm{d}\bar x\ \bar\psi\gamma^+ iD_a\psi = \int \mathrm{d}\bar x\ \psi_+^\dagger iD_a\psi_+ \tag{5.17}$$

and the photon part

$$P_a^\gamma = \int \mathrm{d}\bar x\ eA_a j_- + \partial_- A_\perp \partial_a A_\perp = \int \mathrm{d}\bar x\ eA_a\psi_+^\dagger\psi_+ + \partial_- A_\perp\partial_a A_\perp \ . \tag{5.18}$$

Adding (5.17) and (5.18) gives the spatial components of the total momentum

$$P_a = \int \mathrm{d}\bar x\ \psi_+^\dagger i\partial_a\psi_+ + \partial_- A_\perp\partial_a A_\perp \ . \tag{5.19}$$

The terms proportional to e in P^f and P^γ cancel. It might be tempting to, instead of (5.17) and (5.18), use the first and the last term in (5.19) for the fermion and photon momentum operators respectively, but this is not a gauge invariant separation.

To produce the Hamiltonian we follow [153] and [189]. From the photon part of the momentum tensor we receive contributions analogous to scalar QED,

$$P_+^\gamma = \int \mathrm{d}\bar x\ \mathsf{F}_{-\mu}\mathsf{F}^\mu{}_+ + \frac{1}{8}\mathsf{F}^2 = \int \mathrm{d}\bar x\ -\frac{1}{4}A_i\partial_\perp^2 A_i + ej_-A_+ - \frac{e^2}{4}j_-\frac{1}{\partial_-^2}j_- \ , \tag{5.20}$$

while the fermion part contributes

$$P_+^f = \int \mathrm{d}\bar x\ \Psi_+^\dagger i\mathsf{D}_+\Psi_+ = \int \mathrm{d}\bar x\ \psi_+^\dagger(m + i\gamma^\perp D_\perp)\frac{1}{4i\partial_-}(m - i\gamma^\perp D_\perp)\psi_+ \ , \tag{5.21}$$

where in the last step the equation of motion for the unconstrained spinor field (5.8) was used. Expanding in the coupling yields

$$P_+^f = \int \mathrm{d}\bar x\ \psi_+^\dagger\frac{m^2 - \partial_\perp^2}{4i\partial_-}\psi_+ + \frac{e}{2}A_\perp j^\perp + \frac{e^2}{2}\bar\psi\not{A}\frac{\gamma^+}{4i\partial_-}\not{A}\psi \ . \tag{5.22}$$

Thus, the Hamiltonian is

$$\begin{aligned} H =& \frac{1}{2}\int \mathrm{d}\bar x\ \bar\psi\gamma^+\frac{m^2 + (i\partial_\perp)^2}{4i\partial_-}\psi + \frac{1}{2}A_i(i\partial_\perp)^2 A_i \\ &+ ejA + \frac{e^2}{2}j_-\frac{1}{(i\partial_-)^2}j_- + e^2\bar\psi\not{A}\frac{\gamma^+}{4i\partial_-}\not{A}\psi \ . \end{aligned} \tag{5.23}$$

We obtain the commutation relations with the same method as we used for scalar QED (see [181] for a similar quantisation of the Dirac field in the instant form). For the fermion field we demand that

$$i\partial_a\psi_+(x) = [\psi_+(x), P_a] \ . \tag{5.24}$$

Using (5.19) and the fact that ψ obeys anticommutation relations we find

$$i\partial_a\psi_+(x) = \int \mathrm{d}\bar y\ \{\psi_+(x), \psi_+(y)^\dagger\}_{y^+=x^+} i\partial_a\psi(y) \tag{5.25}$$

and thus

$$\{\psi_+(x), \psi_+(y)^\dagger\}_{y^+=x^+} = \Lambda_+\bar\delta(x - y) \ . \tag{5.26}$$

The commutation relations for the photon field are the same as for scalar QED.

5.3 Interaction picture

Before we introduce a background field and switch to the Furry picture we will briefly consider the interaction picture, mainly to introduce some notation. In the interaction picture the time evolution of the operators is governed by the first line in (5.23). The spinor field satisfies the free Dirac equation

$$(i\partial\!\!\!/ - m)\psi_I = 0 \tag{5.27}$$

and the mode expansion is given by

$$\psi_I(x) = \int \mathrm{d}\tilde{p}\; B(p)e^{-ipx} + D^\dagger(p)e^{ipx} \;, \tag{5.28}$$

where the mode operators obey

$$(p\!\!\!/ - m)B(p) = 0 \qquad (p\!\!\!/ + m)D^\dagger = 0 \;. \tag{5.29}$$

The mode operator B is a spinor that annihilates electrons and $D^\dagger$ is a spinor that creates positrons. Usually the spin structure and the annihilation/creation parts are separated with sums over spins

$$B_\alpha(p) = \sum_{s=1,2} b(p,s)u_\alpha(p,s) \qquad D^\dagger_\alpha(p) = \sum_{s=1,2} d^\dagger(p,s)v_\alpha(p,s) \;. \tag{5.30}$$

Since positrons do not contribute to the RR expectation values we are interested in we will focus on B. (This is related to the vanishing of vacuum creation graphs in lightfront field theory [153].) Using

$$B(p) = 2p_- \int \mathrm{d}\bar{x}\; e^{ipx}\psi_I(x) \tag{5.31}$$

the constraint (5.16) implies

$$B_- = \frac{1}{4p_-}(m + \gamma^\perp p_\perp)\gamma^+ B_+ \;. \tag{5.32}$$

Using (5.31) and the commutation relation (5.26) one finds that the unconstrained modes satisfies

$$\{B_+(p), B_+^\dagger(q)\} = 2p_-\Lambda_+\tilde{\delta}(p,q) \;. \tag{5.33}$$

From this and the constraint (5.32) it follows that

$$\{B(p), \bar{B}(q)\} = (p\!\!\!/ + m)\tilde{\delta}(p,q) \;. \tag{5.34}$$

In terms of b and u we have

$$\{b(p,s), b^\dagger(q,r)\} = \delta_{sr}\tilde{\delta}(p,q) \tag{5.35}$$

and

$$\sum_s u(p,s)\bar{u}(p,s) = p\!\!\!/ + m \qquad \bar{u}(p,s)u(p,r) = 2m\delta_{sr} \;. \tag{5.36}$$

A state with one electron is given by

$$|\, e\, \rangle = \int \mathrm{d}\tilde{p}\ \bar{B}F|\, 0\, \rangle\ , \tag{5.37}$$

where $F_\alpha(p)$ is a spinor which contains both the momentum and spin distribution of the electron. Because of (5.29) one can without loss of generality assume that

$$(\not{p} - m)F = 0\ . \tag{5.38}$$

The normalisation of the state implies

$$2m \int \mathrm{d}\tilde{p}\ \bar{F}F = 1\ . \tag{5.39}$$

For $F = f(p)u(p,s)/2m$ we have

$$\int \mathrm{d}\tilde{p}\ f(p)b^\dagger(p,s)|\, 0\, \rangle\ . \tag{5.40}$$

5.4 Plane waves and Furry picture

We know from our treatment of scalar QED how to transform a photon coherent state to a classical background field $c_\mu(x)$ in the operators; in the interacting terms, those with factors of e that is, one performs the shift $eA \to eA + c$. For simplicity we will assume from the start that the background field is a plane wave. Since from here on we will only work in the Furry picture and since all operators are the ones obtained after performing the shift we will drop all sub- and superscripts indicating this. Since the potential for a plane wave only depends on lightfront time and $a_+ = 0$ it is clear from (5.21) and (5.20) that the only effect on the Hamiltonian is to replace the derivatives in the free spinor part of (5.23) with background covariant derivatives

$$\begin{aligned} H =& \frac{1}{2} \int \mathrm{d}\bar{x}\ \bar{\psi}\gamma^+ \frac{m^2 + (i\mathcal{D}_\perp)^2}{4i\partial_-}\psi + \frac{1}{2}A_i(i\partial_\perp)^2 A_i \\ &+ ejA + \frac{e^2}{2} j_- \frac{1}{(i\partial_-)^2} j_- + e^2 \bar{\psi}\not{A}\frac{\gamma^+}{4i\partial_-}\not{A}\psi\ , \end{aligned} \tag{5.41}$$

with the constraint

$$\psi_- = \frac{1}{4i\partial_-}(m + i\gamma^\perp \mathcal{D}_\perp)\gamma^+\psi_+\ . \tag{5.42}$$

The first line in (5.41) is the "free" Hamiltonian H_0 and the second line is the interaction V. Just like for scalar QED only V_1, the term in V proportional to e, contributes to our expectation values to first order in e^2. Similarly, the spatial momentum for the fermions (5.17) becomes

$$P^f_a = \int \mathrm{d}\bar{x}\ \psi_+^\dagger (i\mathcal{D} - eA)_a \psi_+\ . \tag{5.43}$$

It follows immediately from H_0 that the unconstrained spinor field obeys the Klein-Gordon equation with background covariant derivatives

$$(\mathcal{D}^2 + m^2)\psi_+ = 0\ . \tag{5.44}$$

The solution which reduces to (5.28) when the background field vanishes is

$$\psi_+ = \int \mathrm{d}\tilde{p}\; B_+ \varphi_p + D_+^\dagger \varphi_{-p}\;, \tag{5.45}$$

where $\varphi_p(x)$ is the Volkov solution given in (3.7). From this and the constraint (5.42) it follows that

$$\psi(x) = \int \mathrm{d}\tilde{p}\; K_p B_p \varphi_p + K_{-p} D_p^\dagger \varphi_{-p}\;, \tag{5.46}$$

where the spin structure is given by

$$K_p(x^+) = 1 + \frac{\not{k}\not{a}}{2kp}\;. \tag{5.47}$$

The matrix K transforms the initial momentum p to the Lorentz momentum according to $K\not{p} = \not{\pi}K$, which ensures that the field satisfies the Dirac equation with a background covariant derivative

$$(i\not{D} - m)\psi = 0\;. \tag{5.48}$$

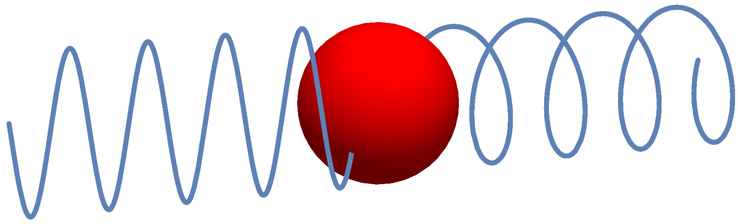

Figure 6. This figure illustrates vacuum birefringence. The blue curves represent the probe field and the red sphere represents the background field. The probe has initially linear polarisation and, after interaction with the background, emerges with elliptical polarisation.

6 Vacuum birefringence

Vacuum polarisation has a long history [55–58, 190–194] (see [61] for a review) and continues to be an active research area [195–198]. See [76] for a review of recent progress in vacuum birefringence and other related effects. Both vacuum birefringence and photon induced pair production are encoded in the polarisation tensor. In [56, 57, 61] the polarisation tensor for constant magnetic fields was obtained with Schwinger's proper time method [7]. The vacuum polarisation tensor in constant electromagnetic fields has also been studied with worldline methods in [171] and for spatially inhomogeneous magnetic fields with numerical worldline techniques in [143]. We saw in Sect. 2 that Schwinger pair production is obtained from the imaginary part of the effective action; the real part on the other hand can be used to obtain vacuum birefringence [61, 62, 73]. In QED one usually starts with the Euler-Heisenberg effective action, but other low-energy effective actions can be treated in the same way [62]. One obtains modified Maxwell's equations from a low-energy effective action $\mathcal{L}(\mathcal{F},\mathcal{G})$ with $\mathcal{F}=F_{\mu\nu}F^{\mu\nu}/4$ and $\mathcal{G}=F_{\mu\nu}\tilde{F}^{\mu\nu}/4$. One usually also assume weak fields so that

$$\mathcal{L}=-\mathcal{F}+c_1\mathcal{F}^2+c_2\mathcal{G}^2 \ . \tag{6.1}$$

These equations are then solved by splitting the total field into a background and a probe $F=F_{\rm ext}+F_{\rm probe}$ and linearising with respect to the probe field. A plane wave ansatz for the probe $A^\mu_{\rm probe}=\epsilon^\mu e^{-ilx}$ leads to two solutions with different polarisation $\epsilon^\mu_{1,2}$ and phase velocity $l^2_{1,2}$, which is often expressed in terms of the refractive index $n=|\mathbf{l}|/l_0$. Consider now a probe which initially has linear polarisation with nonzero components along both ϵ_1 and ϵ_2. The fact that the two components have different velocities inside the background leads to a phase shift, which means that the probe will emerge from the background with elliptical polarisation. This process is illustrated in Fig. 6. This induced ellipticity is directly related to the difference in the refractive indices and the path length.

In Paper VI we used a different method to study vacuum birefringence. Instead of first calculating two refractive indices and obtaining the ellipticity from them, we used a more direct approach, which makes the connection to the underlying photon-photon scattering process clear (Paper VI). In particular, we obtained the change in the probe polarisation directly from the expectation value of the electromagnetic field operator and related the induced ellipticity on the probe beam to the probability for a single probe photon to flip polarisation state. This allowed us to study high energy effects, such as anomalous dispersion and pair production, and to generalise high energy results in [62] from constant fields to pulsed plane waves. In the low energy limit our plane wave result for the induced ellipticity and polarisation flip amplitude reduces to a single lightfront time integral that can be written as a simple integral over a probe photon worldline. In Paper V we showed that the worldline expression actually gives the polarisation flip probability also for other low energy fields, and not just the plane waves considered in Paper VI. Further, in [65] it was shown that also the induced ellipticity is given by this photon worldline integral.

In this section we will briefly consider our method to study vacuum birefringence. Since we are thinking of macroscopic beams in the lab, both the background and the probe can be described by coherent states as in Sect. 4.4.2. We convert the background coherent state into a classical field as above, but keep the probe $\mathcal{P}$ as a coherent state,

$$|\,in\,\rangle = |\,\mathcal{P}\,\rangle = \mathcal{N}\exp\left(i\int\mathrm{d}\tilde{l}'\;\mathcal{P}\epsilon^\mu a^\dagger_\mu\right)|\,0\,\rangle\;. \tag{6.2}$$

The background is an arbitrary (pulsed) plane wave, but we assume here for simplicity that the probe is monochromatic[3] with wave vector l_μ, i.e. $\mathcal{P}(l')\propto\tilde{\delta}(l',l)$, and before interacting with the background the probe has polarisation $\epsilon_\mu(l)$. The change in probe polarisation is obtained from the expectation value of the electromagnetic field operator (note that we can use F instead of F to lowest order)

$$F_{\mu\nu}(x) = -\int\mathrm{d}\tilde{l}'\;l'_{[\mu}a_{\nu]} + \text{c.c.}\;. \tag{6.3}$$

Let $\epsilon'(l)$ be an orthogonal polarisation vector, $l\epsilon'=\epsilon'\epsilon=0$. Before interaction the expectation value of the probe electric field is

$$\epsilon^\mu\langle\,\mathcal{P}\,|F_{\mu0}|\,\mathcal{P}\,\rangle = E_p\cos lx \qquad \epsilon'^\mu\langle\,\mathcal{P}\,|F_{\mu0}|\,\mathcal{P}\,\rangle = 0\;. \tag{6.4}$$

Interaction with the background field induces a nonzero ϵ'-component which is obtained from

$$\epsilon'^\mu\langle\,\mathcal{P}\,|U^\dagger F_{\mu0}U|\,\mathcal{P}\,\rangle\;, \tag{6.5}$$

where the evolution operator U is given by (4.57) in which (in the spinor case) the interaction Hamiltonian is given by the second line (5.41). In Paper VI we calculated this (to first order in e^2) and found without assuming $\epsilon'\epsilon=0$,

$$\epsilon'^\mu\langle\,\mathcal{P}\,|U^\dagger F_{\mu0}U|\,\mathcal{P}\,\rangle = \text{Re}\;(-\epsilon'\epsilon + iT_{\epsilon'\epsilon})E_p e^{-ilx} \tag{6.6}$$

where $T_{\epsilon'\epsilon}$ is the amplitude for a single probe photon to change polarisation from ϵ to ϵ'. In Paper VI we presented a compact expression for $T_{\epsilon'\epsilon}$ valid for an arbitrary pulsed plane wave and for arbitrary energies. The probability for photon induced pair production is obtained from the non-flip amplitude via the optical theorem $\mathbb{P}_\epsilon(\text{pair}) = 2\text{Im}\;T_{\epsilon\epsilon}$. In the

[3] In Paper V we studied more physical field shapes by also taking into account the transverse shapes of the beams.

low energy limit $kl \ll 1$ (recall $m = 1$ and the background field is given by $a_\perp(kx)$), $T_{\epsilon'\epsilon}$ is real and reduces to a relatively simple integral over lightfront time, (Papers VI, V)

$$T_{\epsilon'\epsilon} = \frac{\alpha}{90\pi} kl \int \mathrm{d}(kx)(-7\epsilon'\epsilon\, a'^2 + 3\epsilon' a' \epsilon a') = \frac{\alpha}{90\pi} \frac{1}{E_S^2} \int \frac{\mathrm{d}(kx)}{kl} (7\epsilon'\epsilon\, l f^2 l + 3 l f \epsilon' l f \epsilon) \;, \quad (6.7)$$

where $f_{\mu\nu} = k_\mu a'_\nu - k_\nu a'_\mu$ is the background field. For polarisation flip $\epsilon'\epsilon = 0$ only the last term in the integral remains. The coefficients in front of the two terms in (6.7) allow us to deduce the two constants in the low-energy effective action (6.1), which agrees with the standard Euler-Heisenberg action - this is to the best of our knowledge the first lightfront derivation of the Euler-Heisenberg action (in the weak field limit). In the Sect. 7 we will use a similar matching to deduce an equation of motion for RR from plane wave results. In Paper V we interpreted the second integral in (6.7) as an integral over the worldline of a probe photon, and showed that it gives the correct polarisation amplitude for a probe passing through a more general low-energy background, which allowed us to study finite size effects. In [65] it was shown that the interpretation of (6.7) as a photon worldline integral also gives the correct ellipticity for probe fields that are narrow compared to the background (corrections to this assumption were also derived). Before finishing this section we note that taking into account the diffraction of the probe (which we have neglected) can be important for experimental observation of vacuum birefringence [16].

7 Radiation reaction

We will now turn to RR. As mentioned in the introduction, it is well known that an accelerating charged particle radiates energy, but how to describe the recoil on the particle motion, or RR, is a somewhat controversial subject with a long history. In classical electrodynamics one obtains the particle trajectory from the coupled system $m\ddot{x}^\mu = eF^{\mu\nu}_{\rm tot}\dot{x}_\nu$ and $\partial_\mu F^{\mu\nu}_{\rm tot} = j^\nu$. The total field $F_{\rm tot}$ in these equations includes not only external electromagnetic fields, but also the field generated by the particle. Integrating out this dynamical self-field gives rise to a divergence which is removed by a renormalisation of the electron mass. The result is the Abraham-Lorentz-Dirac (ALD) equation [199–201]. It says that the acceleration is equal to the Lorentz force of the external field plus a term that accounts for radiation reaction.

ALD has some unusual properties; it is a third order equation (it contains the time derivative of the acceleration), which means that the initial position and velocity are not enough to find a unique solution, and it admits unphysical solutions, where the particle accelerates outside the electromagnetic field. There are self-accelerating runaway solutions, where the particle accelerates to infinity in the absence of any external force. If one imposes a condition to remove runaways one is left with solutions with non-causal preacceleration, where the particle starts to accelerate before it enters the external field. However, the scale at which one runs into problems with causality is of the order of the classical electron radius $e^2/4\pi m$, which is smaller than the Compton wavelength $\hbar/m$ by a factor of the fine structure constant $e^2/4\pi\hbar \approx 1/137$. Since this is well within the quantum regime, one should use a quantum description at these scales anyway, which we will discuss later in this section. At larger time scales ALD might still give a correct description.

Nonetheless, the unusual properties of ALD have lead people to doubt its validity, and over the years several alternative equations have been proposed. The most common is the Landau Lifshitz (LL) equation [202], which is obtained from ALD as an approximation when RR is a small effect. We will also consider the equations proposed by Eliezer, Ford and O'Connell (EFO) [203, 204], Mo and Papas (MP) [205], Herrera (H) [206] and Sokolov (S) [207]. It is important to note that ALD has been derived using several different methods [201, 208, 209], and the alternative equations above have not been obtained by correcting some mistake in the derivation of ALD; proposing a different equation amounts to modifying the assumptions leading to ALD [210].

In Sect. 7.1 we recall how ALD arises in classical electrodynamics, and in Sect. 7.2 the problems associated with it. In Sect. 7.3 we consider some alternative equations proposed to avoid these problems. After this we turn to QED and discuss how to use it study RR.

7.1 Classical radiation reaction

The action for classical electrodynamics of a point particle $x^\mu(\tau)$ interacting with an electromagnetic field $F_{\mu\nu} = \partial_\mu A_\nu - \partial_\nu A_\mu$ is

$$S = -m_0 \int \mathrm{d}s - \int \mathrm{d}^4y \; \frac{1}{4} F_{\mu\nu}F^{\mu\nu} + j^\mu A_\mu \;, \tag{7.1}$$

where $\mathrm{d}s^2 = \mathrm{d}x_\mu \mathrm{d}x^\mu$ and the current is

$$j^\mu(y) = e \int \mathrm{d}\tau \, \dot{x}^\mu \delta^4(y - x(\tau)) \, . \tag{7.2}$$

The action is invariant under re-parameterisation of the particle's worldline, i.e. under $x(\tau) \to x(f(\tau))$ with $f'(\tau) > 0$. We will take τ to be proper time, defined by $\dot{x}^2 = 1$. Varying this action with respect to the field and the position of the particle gives Maxwell's equations

$$\partial_\mu F^{\mu\nu} = j^\nu \tag{7.3}$$

and

$$m_0 \ddot{x}^\mu = e F^{\mu\nu} \dot{x}_\nu \, . \tag{7.4}$$

We can divide the field into an external or background field F_e and the dynamical self-field F_s generated by the charge

$$F = F_e + F_s \, . \tag{7.5}$$

The external field satisfies the source free Maxwell's equations $\partial F_e = 0$. Now we want to obtain an explicit equation for $x(\tau)$ by using Maxwell's equations (7.3) to integrate out the self-field F_s. The problem is that in (7.4) the self-field is to be evaluated at the position of the charge where it diverges. These kinds of divergences, which come from short distances or large momenta, are ubiquitous in QFT. It is well known how to take care of them; first we regularise to make everything finite, and then we renormalise the parameters (and sometimes the operators) in the theory. In the present case it turns out that the mass parameter m_0 in (7.4) is not the physical mass and needs to be renormalised. See [209] for a lucid discussion of ALD in the language of renormalisation.

Let us first see how far we can come using only general arguments without actually solving the coupled equations (7.3) and (7.4). From (7.2), (7.3) and (7.4) it immediately follows that the force coming from the self-field will be proportional to e^2. If it is to be written as a polynomial in time derivatives of the position, then using dimensional analysis we see that it can only involve $\dot{x}$, $\ddot{x}$ and $\dddot{x}$. Since it must be orthogonal to the velocity it follows that

$$e F_s^{\mu\nu} \dot{x}_\nu \propto e^2 (\dddot{x}^\mu \dot{x}^\nu - \dot{x}^\mu \dddot{x}^\nu) \dot{x}_\nu = e^2 (\dddot{x}^\mu + \ddot{x}^2 \dot{x}^\mu) \, . \tag{7.6}$$

That the self force has the form (7.6) has been verified explicitly using a variety of methods [201, 208, 209].

We now proceed to solve the coupled equations to obtain the proportionality coefficient. (For a charge coupled to a scalar field there is a different coefficient [211].) We follow the treatment in [181]. For this problem it will be convenient to work in the Lorentz gauge $\partial_\mu A^\mu = 0$. In this gauge the field satisfies

$$\partial^2 A^\mu = j^\mu \, . \tag{7.7}$$

The solution for the dynamical self-field is

$$A_s^\mu(y) = \int \mathrm{d}^4 z \, G_{\mathrm{ret}}(y - z) j^\mu(z) \, , \tag{7.8}$$

where $G_{\rm ret}$ is the retarded Green's function, $\partial^2 G_{\rm ret}(z) = \delta(z)$, given by

$$G_{\rm ret}(z) = \frac{1}{2\pi}\theta(z^0)\delta(z^2)\ . \tag{7.9}$$

It is clear from (7.9) that $G_{\rm ret}$ has support only on the future lightcone. Substituting (7.9) into (7.8) yields

$$A_s^\mu(y) = \frac{e}{2\pi}\int \mathrm{d}\tau\ \theta(y^0 - x^0(\tau))\delta[(y-x)^2]\dot{x}^\mu\ . \tag{7.10}$$

The step function and the delta function select one point x on the particle worldline, called the retarded point, which satisfies

$$y^0 > x^0 \qquad \text{and} \qquad (y-x)^2 = 0\ . \tag{7.11}$$

Performing the proper time integral gives

$$A_s^\mu(y) = \frac{e}{4\pi}\frac{\dot{x}^\mu}{\dot{x}(y-x)}\ , \tag{7.12}$$

which is known as the Lienard-Wiechert potential. It is now clear that the self-field diverges on the world line, $y = x$, as expected.

One can derive Larmor's formula for the energy radiated by the particle from (7.12) without regularising, and from the Larmor's formula one can obtain the coefficient in ALD [181]. Instead, to see exactly how the renormalisation works out we will calculate the regularised self-field on the worldline. There are several ways to regulate, we will follow [209] and use "point splitting". We go back to (7.10) and introduce $\epsilon^2 \ll 1$ in the delta function,

$$A_s^\mu(y) = \frac{e}{2\pi}\int \mathrm{d}\tau\ \theta(y^0 - x^0(\tau))\delta((y-x)^2 - \epsilon^2)\dot{x}^\mu\ . \tag{7.13}$$

We take the derivative to obtain the field before performing the integral. Using

$$\frac{\partial}{\partial y}\delta(...) = -\frac{(y-x)^\mu}{\dot{x}(y-x)}\frac{\mathrm{d}}{\mathrm{d}\tau}\delta(...) \tag{7.14}$$

we find after integrating by parts

$$F_s^{\mu\nu}(x(\tau)) = \frac{e}{2\pi}\int \mathrm{d}\tau'\theta(x_0 - x_0')\delta((x-x')^2 - \epsilon^2)\frac{\mathrm{d}}{\mathrm{d}\tau'}\frac{(x-x')^{[\mu}\dot{x}'^{\nu]}}{(x-x')\dot{x}'}\ , \tag{7.15}$$

where $x' = x(\tau')$. Because of the delta function we only pick up contributions from small $s := \tau - \tau'$, making a Taylor expansion in s appropriate. Using

$$(x-x')^2 = s^2 + \mathcal{O}(s^4)\ , \tag{7.16}$$

$$\theta(x-x')^0\delta((x-x')^2 - \epsilon^2) = \frac{1}{2\epsilon}(1 + \mathcal{O}(\epsilon^2))\delta(s - \epsilon + \mathcal{O}(\epsilon^3)) \tag{7.17}$$

and

$$\frac{(x-x')^{[\mu}\dot{x}'^{\nu]}}{(x-x')\dot{x}'} = \frac{s}{2}\ddot{x}^{[\mu}\dot{x}^{\nu]} - \frac{s^2}{3}\dddot{x}^{[\mu}\dot{x}^{\nu]} + \mathcal{O}(s^3) \tag{7.18}$$

one finds the regularised self field

$$F_s^{\mu\nu} = \frac{e}{4\pi}\left(-\frac{1}{2\epsilon}\ddot{x}^{[\mu}\dot{x}^{\nu]} + \frac{2}{3}\dddot{x}^{[\mu}\dot{x}^{\nu]}\right) + \mathcal{O}(\epsilon)\ . \tag{7.19}$$

We can now write down the equation of motion for the charge by substituting the self-field (7.19) into (7.4)

$$m_0\ddot{x}^\mu = eF_e^{\mu\nu}\dot{x}_\nu + \frac{e^2}{4\pi}\left(-\frac{1}{2\epsilon}\ddot{x}^\mu + \frac{2}{3}[\dddot{x}^\mu + \ddot{x}^2\dot{x}^\mu]\right)\ . \tag{7.20}$$

The second term on the right hand side diverges when the regulator is removed, $\epsilon \to 0$. However, as the divergent term is proportional to the acceleration the divergence can be absorbed by renormalising the mass. Moving this term to the left and defining the physical mass m by

$$m = m_0 + \frac{e^2}{4\pi}\frac{1}{2\epsilon}\ , \tag{7.21}$$

we finally obtain ALD

$$m\ddot{x}^\mu = eF_e^{\mu\nu}\dot{x}_\nu + \frac{2}{3}\frac{e^2}{4\pi}[\dddot{x}^\mu + \ddot{x}^2\dot{x}^\mu]\ . \tag{7.22}$$

This equation is of course of the form expected on account of the general arguments in the beginning of this section. The first term is the Lorentz force. As the particle accelerates due to this term it radiates energy. This is accounted for by the second term. We will usually write ALD as

$$\ddot{x}^\mu = f^{\mu\nu}\dot{x}_\nu + r(\dddot{x}^\mu + \ddot{x}^2\dot{x}^\mu) \qquad f^{\mu\nu} = \frac{e}{m}F_e^{\mu\nu} \qquad r = \frac{2}{3}\frac{e^2}{4\pi m}\ . \tag{7.23}$$

Note the factor of e that is absorbed in the definition of f; this emphasises that, in the applications we are interested in where F_e represents intense lasers, the background is to be treated exactly without recourse to perturbation theory.

7.2 Unphysical solutions

As mentioned, ALD has some unusual properties. We illustrate this with two examples. Consider first a free particle. It should move in a straight line with constant velocity. It is however easy to show that ALD admits other solutions as well. Multiplying ALD by $\ddot{x}$ gives [208]

$$\ddot{x}^2 = r\ddot{x}\dddot{x} = \frac{r}{2}\frac{\mathrm{d}}{\mathrm{d}\tau}\ddot{x}^2 \qquad \Longrightarrow \qquad \ddot{x}^2 = Ce^{2\tau/r}\ . \tag{7.24}$$

For nonzero C we have a runaway solution, where the particle accelerates to the speed of light in the absence of any external force. Note that this is nonperturbative in $r \sim e^2$. Of course, in this free case we can simply take $C = 0$ to avoid runaways.

To see what happens when one imposes the no-runaway condition in a background field, let us assume that the field is sufficiently weak so that we can solve ALD perturbatively in the field strength, which allows us to treat RR effects exactly. To first order the solution is given by $x^\mu = x_0^\mu + \delta x^\mu$, where $\dot{x}_0^\mu = p^\mu$ is the (constant) initial momentum and the first order correction $\delta x = \mathcal{O}(f)$ obeys

$$\delta \ddot{x}^\mu = f(x_0(\tau))^{\mu\nu} p_\nu + r \delta \dddot{x}^\mu \, . \tag{7.25}$$

Although we only work to first order in the field strength, we can still see nonperturbative (in $r \sim e^2$) RR effects. (Compare this expansion with the common r-expansion below.) Since ALD has been reduced to a linear equation, it is now straightforward to solve,

$$e^{-\tau/r} \delta \ddot{x}^\mu \Big|_{\tau_1}^{\tau_2} = - \int_{\tau_1}^{\tau_2} \frac{\mathrm{d}\tau'}{r} e^{-\tau'/r} f^{\mu\nu} p_\nu \, . \tag{7.26}$$

We take $\tau_2 \to \infty$ and demand that the solution be finite asymptotically (we assume that the field vanishes asymptotically). This leads to

$$\delta \ddot{x}^\mu(\tau) = \int_0^\infty \mathrm{d}s \; e^{-s} f^{\mu\nu}(x_0(rs + \tau)) p_\nu \, . \tag{7.27}$$

The zeroth order solution is linear in τ, so we can without loss of generality assume that $x_0^\mu(\tau) = p^\mu \tau$. The correction δx is obtained from (7.27) with boundary condition $\delta \dot{x}(-\infty) = 0$ and $\delta x(-\infty) = 0$. In obtaining (7.27) we have discarded an unphysical solution that behaves asymptotically as (7.24). However, (7.27) might still not be completely satisfactory; the integral over $s > 0$ makes the solution noncausal.

To make this clear, assume that background field is a pulse (e.g. Gaussian) centered at $x^i = 0$ and with slow time-dependence. Now, send the electron with large momentum along, say, the z-axis. Then the electron sees a sharp pulse that can effectively be described as $f(x^\mu) = \tilde{f} \delta(z)$, where $\tilde{f}$ is constant tensor. The integral in (7.27) reduces to

$$\delta \ddot{x}(\tau) = \frac{\tilde{f} p}{|\bar{p}|} \theta(-\tau) \frac{e^{\tau/r}}{r} \, , \tag{7.28}$$

which, with the boundary conditions at $-\infty$, yields

$$\delta x(\tau) = \frac{\tilde{f} p}{|\bar{p}|} \Big(\theta(-\tau) r e^{\tau/r} + \theta(\tau) \tau \Big) \, . \tag{7.29}$$

According to (7.29), the electron starts to accelerate before it hits the background field. However, (7.29) also shows that this preacceleration is exponentially suppressed on scales on the order of the classical electron radius r which, although we did not need to assume it here, is very small; in fact, this is well within the quantum regime, so one should not trust classical predictions on these scales anyway. ALD might still give a correct description on larger scales.

7.3 Different equations

The fact that ALD admits unphysical solutions has led people to question its validity and to try to find a better equation. Several equations have been proposed. The most common is the Landau-Lifshitz equation (LL), which is obtained from ALD by reduction of order. Reduction of order means that ALD is substituted into itself to eliminate terms with two or more time derivatives. This leads to an infinite series in e^2 (which is studied in [212]). Under the assumption that RR is a small effect compared to the Lorentz force, one can truncate this series to some order in e^2, which leads to a second order equation. If one truncates at first order one finds LL

$$\ddot{x} = f\dot{x} + r(\dot{f}\dot{x} + ff\dot{x} + (f\dot{x})^2\dot{x}) \ . \tag{7.30}$$

This equation is free from the problems of ALD; it is second order in derivatives and does not admit any runaways or pre-acceleration. The exact solutions of ALD and LL in a rotating time-dependent field were compared in [88], it was shown that in a regime where quantum effects is expected to be negligible the two solutions agreed (see also [213]). However, the fact that LL was obtained from ALD has lead people to question the validity of LL too.

These equations can be tested by comparing with the classical limit of QED. Since we will only derive RR from QED to first order in e^2 (but exactly in the background field) we will only be able to test different equations to this order. For instance, to distinguish LL from ALD one needs to go to order e^4. It is therefore natural to ask what the most general equation of the form

$$\ddot{x} = f\dot{x} + rR \tag{7.31}$$

is. We do not have to consider terms in R with two or more time derivatives of the position, since such terms can be replaced with terms that only involve f and $\dot{x}$ by using reduction of order. Because of translation invariance x can only appear in the background field $f(x)$, and the orthogonality of the velocity and acceleration implies $\dot{x}R = 0$. Thus to first order in e^2 a general equation can be written as

$$\ddot{x} = f\dot{x} + r(c\dot{f}\dot{x} + d[ff\dot{x} + (f\dot{x})^2\dot{x}]) \ , \tag{7.32}$$

where c and d are coefficients to be determined. For ALD, LL and EFO $c = d = 1$ whereas for MP and H $c = 0$ and $d = 1$. Note the difference between the arguments leading to (7.6) and to (7.32); the argument leading to (7.6) starts with the coupled equations (7.3) and (7.4) and predicts that $c = d$, whereas the argument leading to (7.32) is more general and includes models which predict that $c \neq d$.

So, how do we determine which equation is correct? Given the excellent agreement between QED predictions and high energy scattering experiments [214], it is natural to look to QED for answers to the problems with RR. This brings us to the problem of how to obtain RR in QED, which is the topic of the next section. First though, let us briefly consider the results. One can deduce from the results in [215] that QED predicts $c = 1$, which rules out MP and H and any other equation with $c \neq 1$. The calculation in [215] is performed for an arbitrary background field, but only to first order in the field strength, so the second constant d is therefore not obtained. However, to determine the coefficients c and d it actually suffices to look at one suitable background field. In Paper VII we chose a plane wave background field as in Sect. 3, which allowed us to perform the calculation exactly in the field strength. In a plane wave the momentum predicted by (7.32) is given in terms of the Lorentz momentum π (3.3) by (we omit the P_+ component for simplicity)

$$\bar{P} = \bar{\pi} + kpr\Big(c\bar{\pi}' + d\int^{\phi} a'^2\bar{\pi}\Big) \, , \tag{7.33}$$

where $\bar{\pi} = \{\pi_-, \pi_\perp\}$. In Paper VII we compared (7.33) with the classical limit of QED, and found that QED predicts $c = d = 1$. This means that any RR equation, which can be written on the form (7.32) to first order in e^2, must to this order be equivalent to LL. Our calculation also shows that the d terms can be obtained from asymptotic times, that is from S-matrix elements, while the c term requires finite times. In other words, it is not possible to obtain c from S-matrix elements.

7.4 Quantum radiation reaction

One difficulty in obtaining an equation of motion with RR from QED is the need to consider dynamical objects at finite times, i.e. at non-asymptotic times when the particle is still inside the background field and its motion is nontrivial. In QFT, though, one usually focuses on objects defined for asymptotic times, such as scattering cross-sections and probabilities. There is of course a simple reason for this; to test QFT predictions one uses scattering experiments in which the measurements are performed far from the interaction region at very late (compared with relevant interaction scales) times, i.e. effectively asymptotic times. Asymptotic times would also be sufficient to test RR in an experiment. One can for example send an electron through a laser beam and measure the final momentum of the electron and compare it with the Lorentz force prediction, the difference would be a direct signal of RR. However, for the purpose of comparing different equations and to study preacceleration one needs dynamical objects at finite times. Looking at finite times brings new challenges, but also makes things more interesting. Not only are we curious to see which equations agree with the classical limit of QED, one might also hope to learn something about finite time QFT in the process.

So, how do we obtain the motion of an electron in QED? This is a nontrivial question. In general it is ambiguous to talk about the motion of a particle in QED since the number of particles is not conserved. For example, if one starts with one electron in a background field then that electron can emit a photon which can subsequently produce a positron and a second electron. In QFT even the interpretation of particles at finite times is non-trivial and in processes with pair production only the particle number at asymptotic times is considered physical. In fact, at finite times there exist different choices [45] of what might be thought of as particles; these choices exhibit very different behavior at finite times but all give the same asymptotic number of particles. For it to be meaningful to talk about the motion of an electron, one therefore has to restrict to a regime where the probability for pair production is negligible. The next step is to decide what to calculate. In a quantum theory the electron does not have a definite position, but one can calculate the expectation value of its position using a position operator. There are, however, some counterintuitive aspects about localisation in QED [216–218]. Another option, which might be more natural in QED, is to take the expectation value of the momentum operator. These expectation values are time-dependent functions which can be compared with classical predictions, as the expectation values reduce to classical trajectories in the low-energy limit. This is the approach that we have used. One could also look for signals of RR in the spectrum of the emitted photons, but this is a smaller effect [85] and one would have to go to higher orders to actually see RR (Paper VII). We note in passing that at higher orders, the problem of how to construct physical charges could become relevant [219]. In the next two sections we will compare our method to earlier work.

7.5 Different approaches to quantum RR

There have been several investigations of quantum RR. The most relevant for us here are [211, 215, 220–222]. In this section we will compare these approaches with the one that we used in Papers I, VII, VIII.

In [220] Moniz and Sharp compared the equations of motion for a nonrelativistic extended charge in classical and quantum theory. The classical equation only admits runaways and preacceleration if the radius of the charge is smaller than the classical electron radius, showing that there are problems with classical electrodynamics even for extended charges and not only for point charges. Starting with the Heisenberg equation for the position operator, a quantum equation of motion was obtained, which in the point charge limit resembles the classical equation for an extended charge with an effective size given by the Compton wavelength. It was shown that solutions to this quantum equation are free from runaways and noncausality, and in the classical limit one recovers the preacceleration solution to ALD (c.f. Sect. 7.2). Although [220] only considered nonrelativistic motion, it clearly illustrates the idea of how one expects quantum physics to solve the noncausality problems in classical physics.

In [215] Krivitsky and Tsytovich showed how one can obtain an equation of motion starting from ordinary QED by taking the classical limit of the expectation value of the momentum operator. The calculation was performed for an arbitrary background and to first order in the field strength, and the first order RR term in LL was obtained. As mentioned above, this term is in fact enough to rule out MP, H and S, but is not enough to confirm LL, as there are terms in LL that are quadratic in the field.

In [211, 221] Johnson and Hu derived semiclassical and stochastic equations using a worldline formalism. Equations of motion for the particles are obtained from in-in expectation values. In the semiclassical limit they obtained ALD from the saddle point equation for the worldline path-integral.

In [222] Higuchi and Martin considered the RR induced position shift for a particle that has passed through a background field. The position shift is obtained from the expectation value of the position operator in QED and it was shown that in the classical limit it agrees with the position shift predicted by ALD.

Our approach is similar to those used in [215] and [222]. We also obtain RR from expectation values that directly describe the particle trajectory (rather than looking at e.g. the emitted photons). The expectation values considered in [222] are effectively asymptotic. While asymptotic results will be sufficient for experiments, to first order in e^2 one needs dynamical results to distinguish between different equations. We therefore consider time dependent expectation values. In [215] the expectation value of the momentum operator was considered and [222] used the position operator. We consider both momentum and position in order to study classical equations like (S) [207] that predict that momentum and velocity are not proportional.

In [215] arbitrary background fields are considered, but only to first order in the field strength. We look at an explicit example but treat the background field exactly, which makes it easy to distinguish RR from Lorentz force effects and allows us to find all classical RR terms to first order in e^2. Choosing a particular background is not as restrictive as it might seem. As explained above, quite general arguments, such as dimensional analysis and relativistic invariance, limit the number of different terms that can appear in a classical equation to order e^2, and the problem becomes to find the constant coefficients (c and d above) in front of these terms. Although our results do not directly give us the trajectory in a general background, they do allow us to find these coefficients and thereby determine which equation one can use.

The charge e appears in two different places; the Lorentz force is linear in e and the RR term is quadratic. We treat the Lorentz force exactly and RR as a perturbation, which leads to an expansion in e^2 (see Paper VII for the corresponding dimensionless parameter). An exact treatment of the background in QED is achieved using the Furry picture. The coupling between the quantised fields is treated perturbatively as usual, giving a series in e^2 that we can compare to the classical expansion. We will only work to first order in e^2, as was done in [215, 222], but no other approximation is used.

Another difference from earlier works is that we use lightfront quantisation, where lightfront time $x^+ = t+z$ is used instead of the usual time t to parameterise time evolution. Lightfront quantisation has several appealing features and is particularly convenient in our case since our choice of background is a plane wave, which depends arbitrarily on lightfront time but not on the other coordinates. Combining lightfront quantisation and plane waves in the Furry picture was first done by Neville and Rohrlich in [154]. The backgrounds considered in [222] also depend on only one coordinate. There the WKB approximation was used to find the required solutions to the Klein-Gordon and Dirac equations in the classical limit. Our choice of plane waves allows us to solve the Lorentz, Klein-Gordon and Dirac equations exactly. Further, these solutions are very simple compared to those in other solvable backgrounds. Another reason to choose plane waves is that they are commonly used to describe (unfocused) lasers, which currently attract much interest and might in the near future provide us with the means to test RR in experiments.

7.6 RR from QED

In this section we will discuss which operators one can use to describe the motion of the electron. We will calculate the electron momentum expectation value in spinor QED and show that in the classical limit it is exactly the same as that obtained using scalar QED in Paper VII. That spin effects drops out in the classical limit is of course expected. However, the calculation presented here also gives background to Paper I where we compared our exact expressions for scalar and spinor QED with predictions from numerical codes based on a locally constant field approximation, for high energy electrons. We will also look at the individual probabilities for the two processes that contribute to (asymptotic) RR to first order, nonlinear Compton and scattering without emission. We focus in particular on the infrared divergences in these probabilities and explain why they cancel in expectation values.

One way to study the electron motion is to look at the momentum of the electron. For this we need an operator describing the momentum of only the electron. The energy momentum tensor and the momentum operator in (4.7) and (4.9) describe the total momentum of both the fermions and the photons. So the first thing to do is to separate out the part which describes the electron. Gauge invariance suggests that we separate the tensor into an electron (and positron) and a photon part according to

$$\begin{aligned} &\text{scalar:} \qquad T^e_{\mu\nu} = (\mathsf{D}_\mu\phi)^\dagger \mathsf{D}_\nu\phi + (\mathsf{D}_\nu\phi)^\dagger \mathsf{D}_\mu\phi - g_{\mu\nu}(|\mathsf{D}\phi|^2 - m^2|\phi|^2) \\ &\text{spinor:} \qquad T^e_{\mu\nu} = \bar{\Psi}\gamma_\mu i\mathsf{D}_\nu\Psi \end{aligned} \tag{7.34}$$

and

$$T^\gamma_{\mu\nu} = \mathsf{F}_{\mu\tau}\mathsf{F}^\tau{}_\nu + g_{\mu\nu}\frac{1}{4}\mathsf{F}^2 \; . \tag{7.35}$$

Recall the difference between Ψ, A and ψ, A. Note that these operators contain interacting terms (i.e. terms with factors of e), and

$$\mathsf{D}_\mu = \partial_\mu + ia_\mu + ie\mathsf{A}_\mu = \mathcal{D}_\mu + ie\mathsf{A}_\mu \; . \tag{7.36}$$

So, the electron momentum tensor $T^e_{\mu\nu}$ contains the quantised photon field A_μ and is not simply the free electron tensor. The electron momentum operator is given by

$$P^e_\mu = \int \mathrm{d}\bar{x}\; T^e_{-\mu} \; . \tag{7.37}$$

One can also use the current to obtain the velocity of the electron. In classical electrodynamics the current is related to the velocity through

$$J^\mu_{\text{cl}}(y) = \int \mathrm{d}x^\mu \; \delta^4(y-x) \; , \tag{7.38}$$

which, upon parameterising the trajectory x^μ with lightfront time, gives

$$J^\mu_{\text{cl}}(y) = 2\bar{\delta}(y-x)\, \frac{\mathrm{d}x^\mu}{\mathrm{d}x^+}\bigg|_{x^+=y^+} \; . \tag{7.39}$$

By integrating over $\bar{y}$ we find an expression for the lightfront velocity in terms of the current

$$\frac{\mathrm{d}x^\mu_{\text{cl}}}{\mathrm{d}x^+} = \int \frac{\mathrm{d}\bar{y}}{2} J^\mu_{\text{cl}} \; . \tag{7.40}$$

In order to compare this with QED, we calculate the expectation value of the current

$$\int \frac{\mathrm{d}\bar{y}}{2} \langle J^\mu \rangle \; , \tag{7.41}$$

where J is the total current,

$$\begin{aligned} \text{scalar:} \qquad & J^\mu = \phi^\dagger i \mathsf{D}^\mu \phi + \text{c.c.} = \phi^\dagger (i\overleftrightarrow{\partial} - 2a - 2e\mathsf{A})^\mu \phi \\ \text{spinor:} \qquad & J^\mu = \bar{\Psi}\gamma^\mu \Psi \end{aligned} \tag{7.42}$$

We refer to (7.41) as the expectation value of the lightfront velocity operator.

A third option is to use $j_- = J_-$ as the particle density and define a position operator by

$$\bar{X}(x^+) = \int \mathrm{d}\bar{x}\ \bar{x} j_-(x^+)\ . \tag{7.43}$$

In [222] the corresponding position operator in the instant form quantisation was used to derive RR from QED. We mention in passing that it is conceptually easier to work with momentum rather than position, since the concept of localisation in QED can be difficult and counterintuitive [216–218].

The motion of the electron is found from the expectation values (4.57) with initial state $|\, in \,\rangle = |\, e\,\rangle$ describing the electron. For an electron with spin s the initial state is given by

$$|\, e\,\rangle = \int \mathrm{d}\tilde{p}\ f(p) b^\dagger(s,p) |\, 0\,\rangle \qquad \int \mathrm{d}\tilde{p}\ |f|^2 = 1 \tag{7.44}$$

and similarly for a scalar electron. We will always take the wave packet f to be sharply peaked around the momentum p so that we can approximate

$$\int \mathrm{d}\tilde{p}\ |f(p)|^2 h(p) = h(p) \tag{7.45}$$

for a smooth function h. All observables, momentum (7.37), velocity (7.41) and position operator (7.43), have the form $O = O_0 + eO_1 + e^2 O_2$ and the interaction Hamiltonian $V = eV_1 + e^2 V_2$. To order e^2 the expectation values are given by

$$\begin{aligned} (4.57) = \langle\, e\,| O_0(x^+) |\, e\,\rangle + e^2 \Big\{ & \langle\, e\,| \int^{x^+} V_1 O_0 \int^{x^+} V_1 |\, e\,\rangle \\ & - 2\mathrm{Re}\langle\, e\,| O_0(x^+) \int^{x^+} \mathrm{d}y^+ \int^{y^+} \mathrm{d}z^+ V_1(y^+) V_1(z^+) |\, e\,\rangle + 2\mathrm{Im}\langle\, e\,| O_1(x^+) \int^{x^+} V_1 |\, e\,\rangle \Big\}\ , \end{aligned} \tag{7.46}$$

where the absence of terms with O_2 and V_2 is due to normal ordering. Hence for RR (and also for vacuum birefringence) to first order we only need V_1, which in both scalar and spinor QED is given by

$$V_1 = \frac{1}{2} \int \mathrm{d}\bar{x}\ e\mathcal{J}A\ , \tag{7.47}$$

where (c.f. 7.42)

$$\begin{aligned} \text{scalar:} \qquad & \mathcal{J}^\mu = \phi^\dagger i \mathcal{D}^\mu \phi + \text{c.c.} = \phi^\dagger (i\overleftrightarrow{\partial} - 2a)^\mu \phi \\ \text{spinor:} \qquad & \mathcal{J}^\mu = j^\mu = \bar{\psi}\gamma^\mu \psi\ . \end{aligned} \tag{7.48}$$

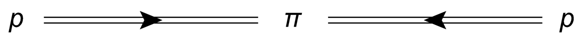

Figure 7. This diagram illustrates the first term in (7.50). The π_μ in the middle of the diagram comes from the zeroth order momentum operator P^0_μ.

Let us for example look at the expectation values of the momentum operator. To zeroth order in e^2 the expectation values of the momentum operator is

$$\langle\, e\,|P^e_\mu(x^+)|\, e\,\rangle = \langle\, e\,|\int \mathrm{d}\tilde{p}\;\pi_\mu(x^+)b^\dagger(p)b(p)|\, e\,\rangle = \pi_\mu(x^+)\;, \tag{7.49}$$

with π as in (3.3). So in the Furry picture the "free" evolution includes the effect of the background field and the electron moves according to the Lorentz force.

The $\mathcal{O}(e^2)$ terms in (7.46) describe RR and will in the classical limit tell us what the coefficients, c and d, in (7.32) should be for a classical equation to be consistent with QED to order e^2. The first steps in calculating these terms are to: use the mode expansions (4.60), (5.46) and (4.36) and the commutation relations (4.37), (5.34), (5.35) and (4.38) to commute away all the mode operators (i.e. $b(s,p)$ and $a_\mu(l)$); perform all the $\bar{x}$ integrals, which is possible since the background only depends on x^+; and use the resulting delta functions to perform some of the momentum integrals (for the position operator there is also a derivative on a delta function because of the factor of $\bar{x}$ in (7.43)). After these first steps one is left with nontrivial momentum- and x^+-integrals. The momentum integrals can also be performed; the transverse integrals are Gaussian and the longitudinal yields special functions (see [97], Paper I, VI). However, unless one chooses a specific plane wave, x^+-integrals will remain. In Paper VII we used all three operators: momentum (7.37), velocity (7.41) and position (7.43), and we showed that in the classical limit and to first order in e^2 one finds trajectories consistent with ALD, LL, EFO or any other classical equation that to this order reduces to (7.32) with $c = d = 1$.

7.7 Momentum expectation value in spinor QED

In Paper VII we considered scalar QED. Here we consider the momentum expectation value of a spinor electron, and for simplicity we focus on the spatial components. The formula for the expectation value is given by (7.46),

$$\begin{aligned}\langle P_\mu\rangle(x^+) =&\langle\, e\,|P^0_\mu(x^+)|\, e\,\rangle + e^2\bigg\{\langle\, e\,|\int^{x^+} V_1 P^0_\mu(x^+)\int^{x^+} V_1|\, e\,\rangle \\ &-2\mathrm{Re}\langle\, e\,|P^0_\mu(x^+)\int^{x^+}\mathrm{d}y^+\int^{y^+}\mathrm{d}z^+ V_1(y^+)V_1(z^+)|\, e\,\rangle + 2\mathrm{Im}\langle\, e\,|P^1_\mu(x^+)\int^{x^+} V_1|\, e\,\rangle\bigg\} \\ &=: L_\mu + C_\mu + W_\mu + O_\mu\;,\end{aligned} \tag{7.50}$$

with the electron state as in (5.37). The four terms in (7.50) are illustrated in Figs. 7, 8, 9 and 10. Using

$$P^0_\mu(x^+) = \int \mathrm{d}\tilde{p}\;\pi_\mu\frac{\bar{B}B}{2m} \tag{7.51}$$

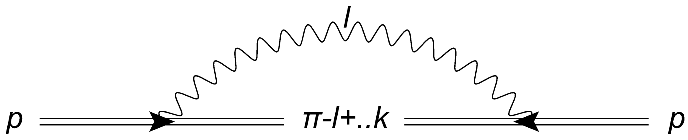

Figure 8. This diagram illustrates the second term in (7.50). The electron momentum in the middle of the diagram is $\pi_\mu - l_\mu + ...k_\mu$, where l_μ is the momentum of the emitted photon. This comes from the zeroth order momentum operator P^0_μ.

Figure 9. This diagram illustrates the third term in (7.50). The π_μ in the middle of the diagram comes from the zeroth order momentum operator P^0_μ.

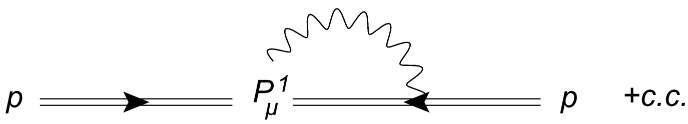

Figure 10. This diagram illustrates the last term in (7.50), which comes from the interaction part of the momentum operator, P^1_μ.

and (5.37), it follows immediately that the first term is simply the Lorentz momentum,

$$L_\mu = \int \mathrm{d}\tilde{p}\; \pi_\mu 2m\bar{F}F \to \pi_\mu \;, \tag{7.52}$$

where in the last step we used (5.39) and the assumption that the wave packet is sharply peaked around momentum p.

For the three RR terms in (7.50) we need

$$\int^{x^+} V_1|\,e\,\rangle = \frac{e}{2}2m\int^{\phi}\mathrm{d}\phi_1\int \mathrm{d}\tilde{p}\mathrm{d}\tilde{l}\;\frac{\theta(kp')}{kp'}a^\dagger_\mu(l)\bar{B}'\underset{1}{\bar{K}'}\gamma^\mu\underset{1}{K}F|\,0\,\rangle\exp i\int^{\phi_1}\frac{l\pi}{kp'}\;, \tag{7.53}$$

where p' corresponds to the momentum of the electron after emitting a photon with momentum l; the $\bar{x}$ integrals give $\delta_{-,\perp}(p'+l-p)$ and since all momentum vectors are on shell

$$p'_\mu = p_\mu - l_\mu + \frac{lp}{k(p-l)}k_\mu \;. \tag{7.54}$$

The second term in (7.50) corresponds to nonlinear Compton scattering (see Fig. 9), and with the help of (7.53) we find

$$C_\mu = -\frac{e^2}{kp}\int^{\phi}\mathrm{d}\phi_{12}\int\mathrm{d}\tilde{p}\mathrm{d}\tilde{l}\;\frac{\theta(kp')}{kp'}\underset{p'}{\pi_\mu}(\phi)S(\phi_2,\phi_1)\exp -i\int_{\phi_1}^{\phi_2}\frac{l\pi}{kp'}\;, \tag{7.55}$$

where $\mathrm{d}\phi_{12} = \mathrm{d}\phi_2\mathrm{d}\phi_1$ and the spin structure is given by

$$S(\phi_2,\phi_1) = \frac{(2m)^2}{4} L_{\nu\tau}\bar{F}\overbrace{\underset{p}{\bar{K}}\gamma^\nu \underset{p'}{K}}^{\phi_2}(\not{p}' + m)\overbrace{\underset{p'}{\bar{K}}\gamma^\tau \underset{p}{K}}^{\phi_1} F\,. \tag{7.56}$$

The third term in (7.50) corresponds to scattering without emission, and using again (7.53) we find

$$W_\mu = \frac{e^2}{kp}\int^{\phi}\mathrm{d}\phi_{12}\int\mathrm{d}\tilde{p}\mathrm{d}\tilde{l}\,\frac{\theta(kp')}{kp'}\underset{p}{\pi_\mu}(\phi)S(\phi_2,\phi_1)\exp -i\int_{\phi_1}^{\phi_2}\frac{l\pi}{kp'}\,, \tag{7.57}$$

where $S^\dagger(\phi_2,\phi_1) = S(\phi_1,\phi_2)$ has been used to eliminate the time ordering step function, $2\mathrm{Re}\,\theta_{21}\to 1$. Note the similarity between (7.55) and (7.57). As will be shown below, these two terms are both infrared divergent, but their sum is infrared finite (essentially because of unitarity),

$$C_\mu + W_\mu = \frac{e^2}{kp}\int^{\phi}\mathrm{d}\phi_{12}\int\mathrm{d}\tilde{p}\mathrm{d}\tilde{l}\,\frac{\theta(kp')}{kp'}(\underset{p}{\pi}-\underset{p'}{\pi})_\mu(\phi)S(\phi_2,\phi_1)\exp -i\int_{\phi_1}^{\phi_2}\frac{l\pi}{kp'}\,. \tag{7.58}$$

The difference $\pi(p)-\pi(p')$ measures the recoil due to photon emission. To make the sum (7.58) UV finite we have to renormalise. This is done in the same way as in Paper VII for the scalar case. We will discuss below compact renormalised expressions valid for arbitrary energies and field shapes. However, it is relatively straightforward at this point to show that (7.58) will agree in the classical limit with the scalar version found in Paper VII.

The classical limit is obtained by reinstating $\hbar$ and taking the limit $\hbar\to 0$. A physical expansion parameter is $\hbar kp/m^2 = \hbar\omega(p_0-p_3)/m^2$, where ω is the background field frequency. There is also a factor of $1/\hbar$ in front of (7.58) due to e^2, which is the reason why the probabilities (see below) for emitting a photon and scattering without emitting a photon have no classical limit. For the expectation values, on the other hand, these $1/\hbar$ terms cancel in the inclusive sum of the photon emission and the loop processes. We will see in the next section how this is related to the cancellation of infrared divergences. In the classical limit we can let the photon momentum go to zero, $l\to 0$, in the spin structure in (7.58)

$$\lim_{l\to 0} S(\phi_2,\phi_1)\to\frac{(2m)^2}{4}L_{\nu\tau}\bar{F}\underset{2}{\bar{K}}\gamma^\nu\underset{2}{K}(\not{p}+m)\underset{1}{\bar{K}}\gamma^\tau\underset{1}{K}F = 2m\bar{F}F\underset{2}{\pi}L\underset{1}{\pi} \tag{7.59}$$

and consequently

$$C_\mu + W_\mu \underset{\text{classical}}{\to}\frac{e^2}{kp}\int^{\phi}\mathrm{d}\bar{\phi}\int\mathrm{d}\tilde{l}\,\frac{\theta(kp')}{kp'}(\pi_\mu(p)-\pi_\mu(p'))\underset{2}{\pi}L\underset{1}{\pi}\exp -i\int_1^2\frac{l\pi}{kp'} = C_\mu^{\text{sc}} + W_\mu^{\text{sc}}\,. \tag{7.60}$$

This is exactly the same as the corresponding terms in scalar QED (Paper VII). The spin dependence in F has dropped out as expected.

At asymptotic times $C+W$ is the only contribution to RR (to this order). For finite time, though, we also need the the last term in (7.50), which comes from the term in the momentum operator linear in e,

$$P_a^1(x^+) = -\frac{e}{2}\int \mathrm{d}\bar{x}\; A_a\bar{\psi}\gamma^+\psi \;, \tag{7.61}$$

where $a = {}_-, {}_\perp$. This term is illustrated in Fig. 10, and for lack of a better name, we call it the operator term. Note that (7.61) has a structure similar to V_1, and analogous to (7.53) we find

$$P_a^1|\,e\,\rangle = -e\frac{2m}{2}\int \mathrm{d}\tilde{p}\mathrm{d}\tilde{l}\;\frac{\theta(kp')}{kp'}\underset{p'}{\bar{B}}\not{k}F\exp i\int^{\phi}\frac{l\pi}{kp'}\;, \tag{7.62}$$

which we use to obtain

$$O_a = \mathrm{Im}\; e^2\frac{(2m)^2}{2kp}\int \mathrm{d}\tilde{p}\mathrm{d}\tilde{l}\;\frac{\theta(kp')}{kp'}\int^{\phi}\mathrm{d}\phi_1 L_{a\mu}\bar{F}\not{k}(\not{p}'+m)\overbrace{\underset{p'}{\bar{K}}\gamma^{\mu}\underset{p}{K}}^{\phi_1}F\exp -i\int_{\phi_1}^{\phi}\frac{l\pi}{kp'}\;. \tag{7.63}$$

Again we find that the spin structure simplifies in the classical limit

$$\bar{F}\not{k}(\not{p}+m)\bar{K}\gamma^{\mu}KF = \frac{4kp}{2m}\pi^{\mu}\bar{F}F \tag{7.64}$$

and

$$O_a \underset{\text{classical}}{\rightarrow} 2\mathrm{Im}\; e^2\int \mathrm{d}\tilde{l}\;\frac{\theta(kp')}{kp'}\int^{\phi}\mathrm{d}\phi_1 L_{a\mu}\pi^{\mu}(\phi_1)\exp -i\int_{\phi_1}^{\phi}\frac{l\pi}{kp'} = O_a^{\mathrm{sc}}\;. \tag{7.65}$$

This is again precisely the same as the corresponding term in scalar QED. We have thus shown that in the classical limit the momentum expectation value in spinor QED agrees with the one in scalar QED. In Paper VII we show that in the classical limit this expectation value agrees with the solution to ALD.

It is of course no surprise that scalar and spinor QED agree in the classical limit, but we are also interested in quantum effects in RR. In fact, we can derive relatively compact expressions for the electron momentum without making any assumptions about the initial momentum or the shape of the plane wave. We begin with scalar QED. After renormalising as explained in Paper VII we find that the momentum expectation value can be expressed compactly in terms of trigonometric integrals,

$$S_n(x) = \int_0^{\infty}\mathrm{d}t\frac{1}{(1+t)^n}\sin xt \qquad C_n(x) = \int_0^{\infty}\mathrm{d}t\frac{1}{(1+t)^n}\cos xt\;, \tag{7.66}$$

which in turn can be expressed in terms of the standard $\mathrm{Si}(x)$ and $\mathrm{Ci}(x)$ [223]. These special functions come from the integrals over l_-, and the argument, x in (7.66), involves the effective mass M [116], which is related to the moving average of the Lorentz momentum according to

$$M^2 = \langle\pi\rangle^2 = 1 - \langle a^2\rangle + \langle a\rangle^2\;, \tag{7.67}$$

where the moving average is given by

$$\langle ...\rangle = \frac{1}{\phi_2-\phi_1}\int_{\phi_1}^{\phi_2} ...\;. \tag{7.68}$$

We change variable in the lightfront time integrals from ϕ_1 to $\theta = \phi_2 - \phi_1$. In the expressions with no integral over ϕ_2, we write $\phi_2 = \phi$. The terms that are removed by renormalisation can be separated out by performing partial integrations in θ.

The sum of the terms corresponding to Fig. 8 and Fig. 9 is given for scalar QED by (7.60). After renormalisation (7.60) becomes

$$C^{\rm sc} + W^{\rm sc} \underset{\rm renorm.}{\rightarrow} A^{\rm sc} + B^{\rm sc} \;, \tag{7.69}$$

where $A^{\rm sc}$ and $B^{\rm sc}$ come from $\pi\pi$ and $l\pi$ in $\pi L \pi$ in (7.60), respectively, and have the forms

$$A^{\rm sc} = \alpha kp \int^{\phi} \mathrm{d}\phi_2 \int_0^{\infty} \mathrm{d}\theta\; S_A\Big(\frac{\theta M^2}{2kp}\Big)... \tag{7.70}$$

and

$$B^{\rm sc} = \alpha kp \int_0^{\infty} \mathrm{d}\theta\; S_B\Big(\frac{\theta M^2}{2kp}\Big)... \tag{7.71}$$

where S_A and S_B (and S_O below) are linear combinations of S_n and C_n, and ellipses stand for terms that can be expressed in terms of $\pi(\phi_j)$, $\langle\pi\rangle$ and M^2. The operator term, which corresponds to Fig. 10 and is given by (7.65) in scalar QED, becomes

$$O^{\rm sc}(\phi) = \alpha kp \int_0^{\infty} \mathrm{d}\theta\; S_O\Big(\frac{\theta M^2}{2kp}\Big)... \tag{7.72}$$

Explicit expressions for A, B and O can be found in Paper I. Note that these expressions for A, B and O have been derived without assuming anything about energy scales or the shape of the plane wave. In the classical limit we find

$$A(\phi) = \alpha kp\Big(-\frac{1}{3}\bar{\pi}' + \frac{2}{3}\int^{\phi} a'^2 \bar{\pi}\Big) \tag{7.73}$$

and

$$B = O = \frac{\alpha kp}{2}\bar{\pi}' \;, \tag{7.74}$$

and if we add them all together

$$\langle \bar{P}\rangle = \bar{\pi} + \frac{2\alpha}{3}kp\Big(\bar{\pi}' + \int^{\phi} a'^2\bar{\pi}\Big) \;, \tag{7.75}$$

which agrees with the results in Paper VII. By comparing with (7.33) we thus find that QED predicts $c = d = 1$.

We can also find analogous expressions for spinor QED if we average over the electron spin. For an electron with spin s the spinor wave packet is

$$F = f(p)\frac{u(p,s)}{2m} \;. \tag{7.76}$$

Using the spin sum in (5.36) we find, assuming as usual that the wave packet is sharply peaked around p,

$$\frac{1}{2}\sum_s \int \mathrm{d}\tilde{p}\; S(\phi_2,\phi_1) = \frac{1}{8}L_{\nu\tau}\mathrm{Tr}(\not{p}+m)\overbrace{\underset{p}{\bar{K}}\gamma^\nu \underset{p'}{K}}^{\phi_2}(\not{p}'+m)\overbrace{\underset{p'}{\bar{K}}\gamma^\tau \underset{p}{K}}^{\phi_1}\;, \tag{7.77}$$

which after some calculation reduces to

$$(7.77) = \underset{2}{\pi}L\underset{1}{\pi} - \frac{kl^2}{4kpk(p-l)}(\underset{2}{\pi}-\underset{1}{\pi})^2 - \frac{1}{2}\frac{kl}{k(p-l)}l(\underset{2}{\pi}+\underset{1}{\pi})\;. \tag{7.78}$$

The first term, $\pi L\pi$, is the one we found in the classical limit (7.59) and in scalar QED (7.60). The terms with $l\pi$ give exact integrals which vanish for asymptotic times,

$$(7.77) \underset{\phi\to\infty}{\to} \underset{2}{\pi}\underset{1}{\pi} - \frac{kl^2}{4kpk(p-l)}(\underset{2}{\pi}-\underset{1}{\pi})^2 = m^2 - \frac{1}{2}\left(1+\frac{kl^2}{2kpk(p-l)}\right)(\underset{2}{a}-\underset{1}{a})^2\;, \tag{7.79}$$

which we recognise from Paper VIII where we calculated the momentum expectation value for asymptotic times using S-matrix methods instead of the Hamiltonian formalism used here (which is necessary for finite times). (Expression (7.79) can also be used for the probabilities.)

With (7.78) the calculation of the spinor version of A and B is very similar to the scalar case. We find expressions for A^{sp} and B^{sp} that are similar to A^{sc} and B^{sc}, see Paper I. Since the spin average of (7.63) is equal to the corresponding scalar term, the operator term remains unchanged, i.e. $O^{\mathrm{sp}} = O^{\mathrm{sc}}$.

Having these compact exact expressions (for A, B and O) allows us to study quantum RR. In Paper I we compared our exact scalar and spinor QED expressions with the classical predictions as well as results from numerical codes based on a locally constant field approximation. We showed, in particular, that for moderate intensity, $a_0 \sim 1$, and high electron energy, $\gamma \sim 10^5$, quantum interference effects are important and significantly reduce RR losses compared to both classical and code predictions.

7.8 Probabilities and infrared divergences

The two processes contributing to the RR expectation values to first order at asymptotic times, i.e. those shown in Fig. 8 and Fig. 9, are known to lead to infrared divergent probabilities. So, why then are all our expectation values infrared finite? To answer this and to relate our approach to some standard computations in QED, we will in this section consider the probabilities for photon emission and scattering without emission with focus on the infrared divergences coming from the low energy region of photon momentum integrals. In previous sections on RR and vacuum birefringence we have been working in the in-in formalism; for expectation values we only have to specify the initial states (the ends are justified by the means). For probabilities one has to specify also the outgoing state, which could be called the in-out formalism. To be able to transform the background into a classical field in the in-out formalism we have to assume that the background in the final state can be described by the same coherent state as in the initial state. This is a reasonable assumptions since in the processes we will consider the back-reaction on the background is a small effect. We will take the initial state to be the same as in the previous section, i.e. an electron in a plane wave background field. To first order in e^2 the final state is either just an electron or an electron and a photon. The process leading to the former state is scattering without emission, and that leading to the latter state is nonlinear Compton scattering. Additionally, one could keep track of the spins of the electron and the photon, but here we are content with summing over the final spins. Also, in this section we will only consider asymptotic times, which makes the connection with standard S-matrix and IR methods manifest.

To see the relation between the probabilities and the asymptotic momentum expectation value, we write the later

$$\langle\, e\,|S^\dagger P_\mu S|\, e\,\rangle = \sum_f p^f_\mu |\langle\, f\,|S|\, e\,\rangle|^2 \;, \tag{7.80}$$

where the sum is over a complete set of momentum eigenstates $P|\, f\,\rangle = p^f|\, f\,\rangle$ obeying

$$\sum_f |\, f\,\rangle\langle\, f\,| = 1 \;. \tag{7.81}$$

In Paper VIII we used (7.80) as a starting point to obtain asymptotic RR from S-matrix elements. Probabilities are obtained from (7.80) by removing the vectors p^f_μ and restricting the sum to the process of interest.

Let us start with the probability $\mathbb{P}(e \leftarrow e)$ for scattering without emission. In the one-electron sector we have

$$\int \mathrm{d}\tilde{p}\, \sum_s |\, p, s\,\rangle\langle\, p, s\,| = 1_{1e} \;, \tag{7.82}$$

where $|\, p, s\,\rangle = b^\dagger(p,s)|\,0\,\rangle$, so the probability is given by

$$\mathbb{P}(e \leftarrow e) = \int \mathrm{d}\tilde{p}' \sum_{s'} |\langle\, p', s'\,|S|\, e\,\rangle|^2 \;. \tag{7.83}$$

One has to keep in mind that, because of

$$P_\mu(x^+)|\, p, s\,\rangle = \pi_\mu(x^+)|\, p, s\,\rangle \;, \tag{7.84}$$

the state $|\, p, s\,\rangle$ describes an electron with final momentum $\hat{\pi}(p) = \pi(x^+ \to \infty, p)$, which is in general not equal to the initial momentum $p = \pi(x^+ \to -\infty, p)$. Since the initial state is sharply peaked around the initial momentum p, the integrand in (7.83) only has support for p' close to p, which means that the final momentum will be $\hat{\pi}(p)$. The calculation for $\mathbb{P}(e \leftarrow e)$ is very similar to the one in the previous section; in fact, we simply have to sum (7.52) and (7.57), remove the the vector π_μ and let $x^+ \to \infty$,

$$\mathbb{P}(e \leftarrow e) = 1 + \frac{e^2}{kp}\int \mathrm{d}\phi_{12} \int \mathrm{d}\tilde{p}\mathrm{d}\tilde{l}\; \frac{\theta(kp')}{kp'} S(\phi_2,\phi_1) \exp -i \int\limits_{\phi_1}^{\phi_2} \frac{l\pi}{kp'} \;. \tag{7.85}$$

The probability for nonlinear Compton scattering is

$$\mathbb{P}(e\gamma \leftarrow e) = \int \mathrm{d}\tilde{l}\ \mathrm{d}\tilde{p}' \sum_{\epsilon, s'} |\langle\, p', s'; l, \epsilon\, | \int\limits_{-\infty}^{\infty} V_1 |\, e\,\rangle|^2 \ , \tag{7.86}$$

where $|\, p', s'; l'\epsilon\,\rangle = b^\dagger(p', s')\epsilon(l)a^\dagger(l)|\,0\,\rangle$ describes an electron and an emitted photon with momentum l and polarisation $\epsilon_\mu(l)$. The momentum integrals for Compton scattering are implicitly restricted to a region of interest (e.g. to within a certain frequency or angular range appropriate to a given experiment), so the probability is a function of the final momenta; the total probability is obtained by integrating over all momenta. We can again use our previous results; the probability is obtained from the asymptotic limit of (7.55) by restricting the momentum integrals and removing the vector π'_μ,

$$\mathbb{P}(e\gamma \leftarrow e) = -\frac{e^2}{kp} \int \mathrm{d}\phi_{12} \int \mathrm{d}\tilde{p}\mathrm{d}\tilde{l}\ \frac{\theta(kp')}{kp'} S(\phi_2, \phi_1) \exp -i \int\limits_{\phi_1}^{\phi_2} \frac{l\pi}{kp'} \ . \tag{7.87}$$

It is immediately clear from (7.87) and (7.85) that the sum of the total probability for nonlinear Compton scattering and the probability for scattering without emission is 1 to order e^2. This follows from unitarity, since at this order these are the only two processes that can occur.

These probabilities diverge for small photon momenta, $l \to 0$. Using (7.59) to simplify the spin structure one finds that the infrared part of the probability for nonlinear Compton scattering is

$$\mathbb{P}_{\mathrm{IR}}(e\gamma \leftarrow e) = -\frac{e^2}{kp^2} \int \mathrm{d}\phi_{12} \int \mathrm{d}\tilde{l}\ \underset{2}{\pi} L \underset{1}{\pi} \exp -i \int\limits_{1}^{2} \frac{l\pi}{kp} \ . \tag{7.88}$$

To simplify this further we note that

$$\underset{2}{\pi} L \underset{1}{\pi} = \underset{2}{\pi}\underset{1}{\pi} - \frac{kp}{kl} l(\underset{2}{\pi} + \underset{1}{\pi}) \ , \tag{7.89}$$

where the last two terms are total derivatives with respect to ϕ_i and therefore vanish since we are considering asymptotic times in this section. Now the two ϕ integrals in (7.88) factorise, and after a partial integration in ϕ [224] we find

$$\mathbb{P}_{\mathrm{IR}}(e\gamma \leftarrow e) = -e^2 \int \mathrm{d}\tilde{l}\, \Big| \int\limits_{0}^{f} \mathrm{d}\phi \left(\frac{\pi}{l\pi}\right)' \exp i \int^{\phi} \frac{l\pi}{kp} \Big|^2 \ , \tag{7.90}$$

where we have assumed that the background field vanishes outside $0 < \phi < f$. To find the infrared divergence we can drop the exponent allowing the ϕ integral to be performed, giving

$$\mathbb{P}_{\mathrm{IR}}(e\gamma \leftarrow e) = -e^2 \int \mathrm{d}\tilde{l} \left(\frac{\pi}{l\pi} - \frac{p}{lp}\right)^2 \ . \tag{7.91}$$

From this we see that the probabilities diverge unless the final Lorentz momentum happens to be equal to the initial momentum. It is clear that since the sum of the two total probabilities is one, they contain the same divergence but with opposite signs. From a practical point of view the problem is solved by recognising that it is not possible to detect photons with arbitrarily low energy. Every physical detector has a resolution allowing photons with energies above a certain threshold to be detected, while photons with lower energies, called soft photons, will go undetected. Instead of considering only $\mathbb{P}(e \leftarrow e)$ one should therefore add to it the probability to emit a soft photon; the sum will be infrared finite. In the expectation values we considered in the previous section this sum was automatically included, which is why we did not encounter any infrared problems there.

This method can be generalised. States that cannot be distinguished in an experiment are called degenerate. Summing over degenerate final states to cancel infrared divergences is called the Bloch-Nordsieck method [225]. In [226] it was shown that soft infrared divergences cancel to all orders in QED. In Paper IX we showed that the Bloch-Nordsieck method also removes soft infrared divergences in QED with a plane wave background field.

The divergences that we have considered hitherto are soft infrared divergences. There is another type of divergence called collinear. For energies much higher than the electron mass, the momentum p of the electron effectively becomes a null vector. Collinear divergences arise from photon momenta l such that $lp \to 0$, which are not necessarily soft. There is, however, a general theorem due to Lee and Nauenberg [228] stating that if one sum over all degenerate states, both final and initial, all infrared divergences will cancel. However, as was shown in [229] there are still unresolved issues with this method.

8 Conclusions and outlook

We conclude this thesis with some interesting puzzles and problems. Throughout this thesis, and indeed in most of the literature on strong field QED, the background is treated as a fixed, non-dynamical classical field. This is justified if the background does not change significantly (due to e.g. depletion) during the process. Back-reaction for Schwinger pair production has been investigated in [156–160] by treating the background as a dynamical classical field, while neglecting the interaction with the quantised photon field (e.g. neglecting photon emission by the produced fermions). Back-reaction is in this approximation taken into account by including the expectation value of the current in Maxwell's equations,

$$(i\not{D}-m)\psi=0 \qquad \partial_\mu F^{\mu\nu}=\langle j^\mu\rangle \;, \tag{8.1}$$

where $F_{\mu\nu}=\partial_\mu A_\nu-\partial_\nu A_\mu$ and the covariant derivative is given by $D_\mu=\partial_\mu+ieA_\mu$. In [156] the time evolution of a spatially homogeneous background is studied, and the field and current is found to oscillate in time due to back-reaction. Similar oscillations have been found in [157–160]. In [159] back-reaction was studied in $1+1$ dimensions for a spatially (and temporally) inhomogeneous field. It was shown that close to the critical point, i.e. for small spatial extent, back-reaction can be neglected (for larger spatial extent the back-reaction was found to be important for the parameters considered). However, when back-reaction has to be taken into account one might expect formation of electron-positron-photon cascades [161–163, 166]. Indeed, even an initially slow fermion can in a strong field quickly accelerate to relativistic energies and emit hard photons that can subsequently decay into electron-positron pairs [162, 163, 166]. Back-reaction in a cascade process was considered in [163].

Even if back-reaction is neglected, including terms of higher order in e^2 can be a challenge. The one-loop effective action for an arbitrary constant electromagnetic field can be written in a relatively compact form with only one integral [6, 107]. The two-loop effective action for general constant fields was obtained by Ritus in the 70's [230] in terms of two integrals. To obtain the correct two-loop result [230] one has to be more careful with (mass) renormalisation [231] (see [107] for a review). The two-loop action is in general more complicated than the one-loop action, but for self-dual fields or in 2D the two-loop effective action is actually relatively simple [107, 233]. The two loop action was calculated in [231, 232] with the worldline formalism. It is interesting to note that in the first paper on the worldline instanton formalism [127] higher order terms were considered. These terms are obtained by including in (2.5) the additional term $e^{-iS_{\rm int}}$, where

$$S_{\rm int}=-\frac{ie^2}{8\pi^2}\int\limits_0^T \mathrm{d}\tau\mathrm{d}\tau'\frac{\dot{x}(\tau)\dot{x}(\tau')}{(x(\tau)-x(\tau'))^2-i\epsilon} \;. \tag{8.2}$$

Including $e^{-iS_{\rm int}}$ gives the quenched approximation, which captures the corrections due to diagrams with an arbitrary number of photon lines starting and ending on the same (dressed) fermion loop, but neglects diagram with photon lines connecting two or more loops, see [234] for more on the quenched approximation. By substituting the worldline instanton solution into S_{int}, Affleck et al. [127] conjectured that for weak electric fields $E \to 0$ the imaginary part of the effective action is to all orders in $\alpha = e^2/4\pi$ given by

$$\text{Im}\,\Gamma \propto E^2 \exp\left(-\frac{\pi m^2}{E} + \alpha\pi\right), \tag{8.3}$$

where m is the physical renormalised mass. This conjecture (8.3) was independently obtained by Lebedev and Ritus [235] from the weak field limit of the exact two-loop effective action (for spinor QED). The 2D version of this conjecture has been studied in [237] with the aim of testing it at three-loop level [236]. However, it now seems that the conjecture fails at three-loop level for 2D QED [238], which casts doubt also on the 4D version (8.3).

A similar worldline integral was used in [211, 221] to study RR. The saddle point approximation used in [211, 221] to perform the worldline path integral can be compared with the calculation in [127] which lead Affleck et al. to the all-order conjecture (8.3). Since this conjecture seems to fail [238] (at least in 2D), it would be reassuring if one could confirm the RR results in [211, 221] with different methods.

To first order in e^2 we were able in Paper VII to rule out some of the classical equations, but to this order it is not possible to distinguish the two most common equations: ALD and LL. In order to do so one has to go to second order and still use finite times. Simply extending our method for plane waves to second order might not be the most efficient route to take, since it would require extremely lengthy calculations. However, although our method would allow us to treat the background field exactly also to second order, we actually only need to consider perturbative terms $\sim a_0^2$ to distinguish between ALD, LL and EFO (Paper VII). This is an interesting challenge for the future.

References

[1] G. V. Dunne, Eur. Phys. J. D **55** (2009) 327 [arXiv:0812.3163 [hep-th]].

[2] T. Heinzl and A. Ilderton, Eur. Phys. J. D **55** (2009) 359 [arXiv:0811.1960 [hep-ph]].

[3] A. Di Piazza, C. Muller, K. Z. Hatsagortsyan and C. H. Keitel, Rev. Mod. Phys. **84** (2012) 1177 [arXiv:1111.3886 [hep-ph]].

[4] T. Heinzl, Int. J. Mod. Phys. A **27** (2012) 1260010 [Int. J. Mod. Phys. Conf. Ser. **14** (2012) 127] [arXiv:1111.5192 [hep-ph]].

[5] F. Sauter, Z. Phys. **69**, 742 (1931).

[6] W. Heisenberg and H. Euler, Z. Phys. **98** (1936) 714

[7] J. S. Schwinger, Phys. Rev. **82**, 664 (1951).

[8] ELI-NP: http://www.eli-np.ro/

[9] ELI: http://www.eli-laser.eu/

[10] HBEF: http://www.hzdr.de/db/Cms?pOid=35325&pNid=3214

[11] European XFEL: http://www.xfel.eu/

[12] XCELS: http://www.xcels.iapras.ru/

[13] CLF: http://www.clf.stfc.ac.uk

[14] T. Heinzl, B. Liesfeld, K. -U. Amthor, H. Schwoerer, R. Sauerbrey and A. Wipf, Opt. Commun. **267** (2006) 318 [hep-ph/0601076].

[15] H.-P. Schlenvoigt, T. E. Cowan, T. Heinzl, R. Sauerbrey, U. Schramm, *to appear.*

[16] F. Karbstein, H. Gies, M. Reuter and M. Zepf, arXiv:1507.01084 [hep-ph].

[17] J. Jaeckel and A. Ringwald, Ann. Rev. Nucl. Part. Sci. **60** (2010) 405 [arXiv:1002.0329 [hep-ph]].

[18] R. Bähre *et al.*, JINST **8** (2013) T09001 [arXiv:1302.5647 [physics.ins-det]].

[19] H. Gies, Eur. Phys. J. D **55** (2009) 311 [arXiv:0812.0668 [hep-ph]].

[20] V. Skokov, A. Y. Illarionov and V. Toneev, Int. J. Mod. Phys. A **24** (2009) 5925 [arXiv:0907.1396 [nucl-th]].

[21] *Strongly Interacting Matter in Magnetic Fields* (2013) Lecture notes in physics, Springer-Verlag Berlin Heidelberg.

[22] M. N. Chernodub, Phys. Rev. D **82** (2010) 085011 [arXiv:1008.1055 [hep-ph]].

[23] A. Hartin, G. Moortgat-Pick and S. Porto, PoS ICHEP **2012** (2013) 480 [arXiv:1304.2632 [hep-ph]].

[24] S. Porto, A. Hartin and G. Moortgat-Pick, PoS Corfu **2012** (2013) 039 [arXiv:1304.4241 [hep-ph]].

[25] V. Yanovsky *et al.*, Opt. Exp. 16, 2109 (2008).

[26] S. S. Bulanov, N. B. Narozhny, V. D. Mur and V. S. Popov, Phys. Lett. A **330** (2004) 1 [hep-ph/0403163].

[27] A. M. Fedotov, Laser Physics **19** (2009) 214

[28] S. S. Bulanov, V. D. Mur, N. B. Narozhny, J. Nees and V. S. Popov, Phys. Rev. Lett. **104** (2010) 220404 [arXiv:1003.2623 [hep-ph]].

[29] G. V. Dunne, H. Gies and R. Schutzhold, Phys. Rev. D **80** (2009) 111301 [arXiv:0908.0948 [hep-ph]].

[30] A. Di Piazza, E. Lotstedt, A. I. Milstein and C. H. Keitel, Phys. Rev. Lett. **103** (2009) 170403 [arXiv:0906.0726 [hep-ph]].

[31] M. J. A. Jansen and C. Müler, Phys. Rev. A **88** (2013) 5, 052125 [arXiv:1309.1069 [hep-ph]].

[32] P. A. Sturrock, Astrophys. J. **164** (1971) 529.

[33] Y. Luo and P. Ji, Monthly Notices of the Royal Astronomical Society **420** (2012) 1673

[34] A. Stebbins and H. Yoo, arXiv:1505.06400 [astro-ph.HE].

[35] D. Allor, T. D. Cohen and D. A. McGady, Phys. Rev. D **78** (2008) 096009 [arXiv:0708.1471 [cond-mat.mes-hall]].

[36] F. Fillion-Gourdeau and S. MacLean, Phys. Rev. B **92** (2015) 3, 035401.

[37] M. F. Linder and R. Schutzhold, arXiv:1503.07108 [cond-mat.mes-hall].

[38] T. Oka and H. Aoki, Phys. Rev. Lett. **95** (2005) 137601

[39] N. Szpak and R. Schutzhold, Phys. Rev. A **84** (2011) 050101(R)

[40] N. Szpak and R. Schutzhold, New J. Phys. **14** (2012) 035001 [arXiv:1109.2426 [quant-ph]].

[41] F. Queisser, P. Navez, and R. Schutzhold, Phys. Rev. A **85** (2012) 033625.

[42] V. Kasper, F. Hebenstreit, M. Oberthaler and J. Berges, arXiv:1506.01238 [cond-mat.quant-gas].

[43] F. Dreisow, S. Longhi, S. Nolte, A. Tunnermann and A. Szameit, Phys. Rev. Lett. **109** (2012) 110401.

[44] V. S. Popov, Phys. Usp. **47** 855 (2004)

[45] R. Dabrowski and G. V. Dunne, Phys. Rev. D **90** (2014) 2, 025021 [arXiv:1405.0302 [hep-th]].

[46] S. P. Kim, JHEP **0711** (2007) 048 [arXiv:0710.0915 [hep-th]].

[47] A. Casher, H. Neuberger and S. Nussinov, Phys. Rev. D **20** (1979) 179.

[48] G. C. Nayak, Phys. Rev. D **72** (2005) 125010 [hep-ph/0510052].

[49] G. C. Nayak and P. van Nieuwenhuizen, Phys. Rev. D **71** (2005) 125001 [hep-ph/0504070].

[50] E. Keski-Vakkuri and P. Kraus, Phys. Rev. D **54** (1996) 7407 [hep-th/9604151].

[51] Y. Tanizaki and T. Koike, Annals Phys. **351** (2014) 250 [arXiv:1406.2386 [math-ph]].

[52] A. Alexandru, G. Basar and P. Bedaque, arXiv:1510.03258 [hep-lat].

[53] G. V. Dunne and M. Unsal, Phys. Rev. D **89** (2014) 4, 041701

[54] G. Basar, G. V. Dunne and M. Unsal, JHEP **1310** (2013) 041

[55] J.S. Toll, PhD thesis, Princeton, 1952 (unpublished).

[56] S. L. Adler, Annals Phys. **67** (1971) 599.

[57] W. y. Tsai and T. Erber, Phys. Rev. D **10** (1974) 492.

[58] W. y. Tsai and T. Erber, Phys. Rev. D **12** (1975) 1132.

[59] G. Zavattini, U. Gastaldi, R. Pengo, G. Ruoso, F. Della Valle and E. Milotti, Int. J. Mod. Phys. A **27** (2012) 1260017 [arXiv:1201.2309 [hep-ex]].

[60] B. Marx, K. S. Schulze, I. Uschmann, T. Kämpfer, R. Lötzsch, O. Wehrhan, W. Wagner, C. Detlefs, T. Roth, J. Härtwig, E. Förster, T. Stöhlker and G.G. Paulus, Phys. Rev. Lett. **110** 254801 (2013)

[61] W. Dittrich and H. Gies, Springer Tracts Mod. Phys. **166** (2000) 1.

[62] G. M. Shore, Nucl. Phys. B **778** (2007) 219 [hep-th/0701185].

[63] V. Dinu, T. Heinzl, A. Ilderton, M. Marklund and G. Torgrimsson, Phys. Rev. D **89** (2014) 12, 125003 [arXiv:1312.6419 [hep-ph]].

[64] V. Dinu, T. Heinzl, A. Ilderton, M. Marklund and G. Torgrimsson, Phys. Rev. D **90** (2014) 4, 045025 [arXiv:1405.7291 [hep-ph]].

[65] G. Torgrimsson, Few Body Syst. **56** (2015) 6-9, 615 [arXiv:1409.8069 [hep-ph]].

[66] H. Gies, F. Karbstein and N. Seegert, New J. Phys. **15** (2013) 083002 [arXiv:1305.2320 [hep-ph]].

[67] H. Gies, F. Karbstein and N. Seegert, New J. Phys. **17** (2015) 4, 043060 [arXiv:1412.0951 [hep-ph]].

[68] B. King, A. Di Piazza and C. H. Keitel, Nature Photon. **4** (2010) 92 [arXiv:1301.7038 [physics.optics]].

[69] H. Gies, F. Karbstein and R. Shaisultanov, Phys. Rev. D **90** (2014) 3, 033007 doi:10.1103/PhysRevD.90.033007 [arXiv:1406.2972 [hep-ph]].

[70] P. Böhl, B. King and H. Ruhl, arXiv:1503.05192 [physics.plasm-ph].

[71] E. Lundstrom, G. Brodin, J. Lundin, M. Marklund, R. Bingham, J. Collier, J. T. Mendonca and P. Norreys, Phys. Rev. Lett. **96** (2006) 083602 [hep-ph/0510076].

[72] S. L. Adler, J. N. Bahcall, C. G. Callan and M. N. Rosenbluth, Phys. Rev. Lett. **25** (1970) 1061.

[73] Z. Bialynicka-Birula and I. Bialynicki-Birula, Phys. Rev. D **2** (1970) 2341.

[74] S. L. Adler and C. Schubert, Phys. Rev. Lett. **77** (1996) 1695 [hep-th/9605035].

[75] A. Di Piazza, A. I. Milstein and C. H. Keitel, Phys. Rev. A **76** (2007) 032103 [arXiv:0704.0695 [hep-ph]].

[76] B. King and T. Heinzl, arXiv:1510.08456 [hep-ph].

[77] D. A. Burton and A. Noble, Contemp. Phys. **55** (2014) 110 [arXiv:1409.7707 [physics.plasm-ph]].

[78] V. Malka, J. Faure, Y. A. Gauduel, A. Rousse, K. T. Phuoc and E. Lefebvre, Nature Phys. **4** (2008) 447.

[79] A. Gonoskov *et al.*, Phys. Rev. Lett. **113** (2014) 014801 [arXiv:1306.5734 [physics.plasm-ph]].

[80] L. L. Ji, A. Pukhov, I. Yu. Kostyukov, B. F. Shen, K. Akli, Phys. Rev. Lett. **112** (2014) 145003

[81] A. M. Fedotov, N. V. Elkina, E. G. Gelfer, N. B. Narozhny, H. Ruhl, Phys. Rev. A **90** (2014) 053847

[82] D. G. Green and C. N. Harvey, Phys. Rev. Lett. **112** (2014) 164801 [arXiv:1307.8317 [hep-ph]].

[83] N. Neitz and A. Di Piazza, Phys. Rev. Lett. **111** (2013) 5, 054802.

[84] S. R. Yoffe, Y. Kravets, A. Noble, D. Jaroszynski, New J. Phys. **17** (2015) 053025

[85] A. G. R. Thomas, C. P. Ridgers, S. S. Bulanov, B. J. Griffin, and S. P. D. Mangles, Phys. Rev. X **2**, 041004 (2012)

[86] A. Di Piazza, K. Z. Hatsagortsyan and C. H. Keitel, Phys. Rev. Lett. **102** (2009) 254802 [arXiv:0810.1703 [physics.class-ph]].

[87] C. Harvey, T. Heinzl and M. Marklund, Phys. Rev. D **84** (2011) 116005 [arXiv:1110.0628 [physics.class-ph]].

[88] S. V. Bulanov *et al.*, Phys. Rev. E **84** (2011) 056605.

[89] W. P. Leemans, R. Duarte, E. Esarey, S. Fournier, C. G. R. Geddes, D. Lockhart, C. B. Schroeder, C. Toth, J. L. Vay, S. Zimmermann, AIP Conf. Proc. **1299** (2010) 3

[90] V. Dinu, C. Harvey, A. Ilderton, M. Marklund and G. Torgrimsson, arXiv:1512.04096 [hep-ph].

[91] D. L. Burke *et al.*, Phys. Rev. Lett. **79** (1997) 1626.

[92] C. Bamber, S. J. Boege, T. Koffas, T. Kotseroglou, A. C. Melissinos, D. D. Meyerhofer, D. A. Reis and W. Ragg *et al.*, Phys. Rev. D **60** (1999) 092004.

[93] T. Heinzl, D. Seipt and B. Kampfer, Phys. Rev. A **81** (2010) 022125 [arXiv:0911.1622 [hep-ph]].

[94] F. Mackenroth, A. Di Piazza and C. H. Keitel, Phys. Rev. Lett. **105** (2010) 063903 [arXiv:1001.3614 [physics.acc-ph]].

[95] A. Hartin and G. Moortgat-Pick, Eur. Phys. J. C **71**, 1729 (2011) [arXiv:1106.1671 [hep-th]].

[96] D. Seipt and B. Kampfer, Phys. Rev. A **88** (2013) 012127 [arXiv:1305.3837 [physics.optics]].

[97] V. Dinu, Phys. Rev. A **87** (2013) 052101 [arXiv:1302.1513 [hep-ph]].

[98] A. I. Titov, B. Kämpfer, T. Shibata, A. Hosaka and H. Takabe, Eur. Phys. J. D **68** (2014) 10, 299 [arXiv:1408.1040 [hep-ph]].

[99] T. Heinzl, A. Ilderton and M. Marklund, Phys. Lett. B **692** (2010) 250 [arXiv:1002.4018 [hep-ph]].

[100] A. I. Titov, H. Takabe, B. Kampfer and A. Hosaka, Phys. Rev. Lett. **108** (2012) 240406 [arXiv:1205.3880 [hep-ph]].

[101] T. Nousch, D. Seipt, B. Kämpfer and A. I. Titov, Phys. Lett. B **715** (2012) 246.

[102] A. I. Titov, B. Kämpfer, H. Takabe and A. Hosaka, Phys. Rev. A **87** (2013) 4, 042106 doi:10.1103/PhysRevA.87.042106 [arXiv:1303.6487 [hep-ph]].

[103] B. King and H. Ruhl, Phys. Rev. D **88** (2013) 1, 013005 doi:10.1103/PhysRevD.88.013005 [arXiv:1303.1356 [hep-ph]].

[104] E. Lotstedt and U. D. Jentschura, Phys. Rev. Lett. **103** (2009) 110404 doi:10.1103/PhysRevLett.103.110404 [arXiv:0909.4984 [quant-ph]].

[105] D. Seipt and B. Kampfer, Phys. Rev. D **85** (2012) 101701 doi:10.1103/PhysRevD.85.101701 [arXiv:1201.4045 [hep-ph]].

[106] T. Heinzl and A. Ilderton, Opt.Commun. **282** (2009) 1879

[107] G. V. Dunne, In *Shifman, M. (ed.) et al.: From fields to strings, vol. 1* 445-522 [hep-th/0406216].

[108] N. B. Narozhnyi and A. I. Nikishov, Yad. Fiz. **11** (1970) 1072, [Sov. J. Nucl. Phys. **11** (1970) 596].

[109] G. V. Dunne and T. Hall, Phys. Rev. D **58** (1998) 105022 [hep-th/9807031].

[110] A. I. Nikishov, Nucl. Phys. B **21** (1970) 346.

[111] G. V. Dunne and T. M. Hall, Phys. Lett. B **419** (1998) 322 [hep-th/9710062].

[112] H. Reiss, J. Math. Phys. **3**, 59 (1962).

[113] A. I. Nikishov and V. I. Ritus, Zh. Eksp. Teor. Fiz. **46** (1964) 776; Zh. Eksp. Teor. Fiz. **46** (1964) 1768.

[114] N. B. Narozhnyi, A. Nikishov, and V. Ritus, Zh. Eksp. Teor. Fiz. **47**, 930 (1964).

[115] L. S. Brown and T. W. B. Kibble, Phys. Rev. **133** (1964) A705.

[116] C. Harvey, T. Heinzl, A. Ilderton and M. Marklund, Phys. Rev. Lett. **109** (2012) 100402 [arXiv:1203.6077 [hep-ph]].

[117] R. Schützhold, H. Gies and G. Dunne, Phys. Rev. Lett. **101** (2008) 130404 [arXiv:0807.0754 [hep-th]].

[118] C. Schneider and R. Schützhold, arXiv:1407.3584 [hep-th].

[119] M. F. Linder, C. Schneider, J. Sicking, N. Szpak and R. Schützhold, arXiv:1505.05685 [hep-th].

[120] M. Orthaber, F. Hebenstreit and R. Alkofer, Phys. Lett. B **698** (2011) 80 [arXiv:1102.2182 [hep-ph]].

[121] A. Otto, D. Seipt, D. Blaschke, B. Kämpfer and S. A. Smolyansky, Phys. Lett. B **740** (2015) 335 [arXiv:1412.0890 [hep-ph]].

[122] A. Otto, D. Seipt, D. Blaschke, S. A. Smolyansky and B. Kämpfer, Phys. Rev. D **91** (2015) 10, 105018 [arXiv:1503.08675 [hep-ph]].

[123] F. Hebenstreit, R. Alkofer, G. V. Dunne and H. Gies, Phys. Rev. Lett. **102** (2009) 150404 [arXiv:0901.2631 [hep-ph]].

[124] C. K. Dumlu, Phys. Rev. D **82** (2010) 045007 [arXiv:1006.3882 [hep-th]].

[125] C. Kohlfurst, M. Mitter, G. von Winckel, F. Hebenstreit and R. Alkofer, Phys. Rev. D **88** (2013) 045028

[126] R. P. Feynman, Phys. Rev. **80** (1950) 440.

[127] I. K. Affleck, O. Alvarez and N. S. Manton, Nucl. Phys. B **197** (1982) 509.

[128] M. J. Strassler, Nucl. Phys. B **385** (1992) 145 [hep-ph/9205205].

[129] C. Schubert, Phys. Rept. **355** (2001) 73 [hep-th/0101036].

[130] G. V. Dunne and C. Schubert, Phys. Rev. D **72** (2005) 105004 [hep-th/0507174].

[131] G. V. Dunne, Q. h. Wang, H. Gies and C. Schubert, Phys. Rev. D **73** (2006) 065028 [hep-th/0602176].

[132] G. V. Dunne and Q. h. Wang, Phys. Rev. D **74** (2006) 065015 [hep-th/0608020].

[133] C. K. Dumlu and G. V. Dunne, Phys. Rev. D **84** (2011) 125023 [arXiv:1110.1657 [hep-th]].

[134] E. Strobel and S. S. Xue, Nucl. Phys. B **886** (2014) 1153 [arXiv:1312.3261 [hep-th]].

[135] A. Ilderton, G. Torgrimsson and J. Wårdh, Phys. Rev. D **92** (2015) 2, 025009 [arXiv:1503.08828 [hep-th]].

[136] A. Ilderton, G. Torgrimsson and J. Wårdh, Phys. Rev. D **92** (2015) 6, 065001 [arXiv:1506.09186 [hep-th]].

[137] C. K. Dumlu, arXiv:1507.07005 [hep-th].

[138] A. Ilderton, JHEP **1409** (2014) 166 [arXiv:1406.1513 [hep-th]].

[139] T. N. Tomaras, N. C. Tsamis and R. P. Woodard, Phys. Rev. D **62** (2000) 125005 [hep-ph/0007166].

[140] T. N. Tomaras, N. C. Tsamis and R. P. Woodard, JHEP **0111** (2001) 008 [hep-th/0108090].

[141] H. Gies and K. Langfeld, Nucl. Phys. B **613** (2001) 353 [hep-ph/0102185].

[142] H. Gies and K. Klingmuller, Phys. Rev. D **72** (2005) 065001 [hep-ph/0505099].

[143] H. Gies and L. Roessler, Phys. Rev. D **84** (2011) 065035 [arXiv:1107.0286 [hep-ph]].

[144] M. Schafer, I. Huet and H. Gies, arXiv:1509.03509 [hep-th].

[145] F. Hebenstreit, arXiv:1106.5965 [hep-ph].

[146] F. Hebenstreit, R. Alkofer and H. Gies, Phys. Rev. Lett. **107** (2011) 180403 [arXiv:1106.6175 [hep-ph]].

[147] D. Berenyi, S. Varro, V. V. Skokov and P. Levai, Phys. Lett. B **749** (2015) 210 arXiv:1401.0039 [hep-ph].

[148] C. Kohlfürst and R. Alkofer, arXiv:1512.06668 [hep-ph].

[149] D. M. Volkov, Z. Phys. **94** (1935) 250.

[150] W. H. Furry, Phys. Rev. **81** (1951) 115.

[151] P. A. M. Dirac, Rev. Mod. Phys. **21** (1949) 392.

[152] T. Heinzl, hep-th/9812190.

[153] S. J. Brodsky, H. -C. Pauli and S. S. Pinsky, Phys. Rept. **301** (1998) 299 [hep-ph/9705477].

[154] R. A. Neville and F. Rohrlich, Phys. Rev. D **3** (1971) 1692.

[155] A. Ilderton and G. Torgrimsson, Phys. Rev. D **88** (2013) 025021 [arXiv:1304.6842 [hep-th]].

[156] Y. Kluger, J. M. Eisenberg, B. Svetitsky, F. Cooper and E. Mottola, Phys. Rev. D **45** (1992) 4659.

[157] Y. Kluger, E. Mottola and J. M. Eisenberg, Phys. Rev. D **58** (1998) 125015 [hep-ph/9803372].

[158] J. C. R. Bloch, V. A. Mizerny, A. V. Prozorkevich, C. D. Roberts, S. M. Schmidt, S. A. Smolyansky and D. V. Vinnik, Phys. Rev. D **60** (1999) 116011 [nucl-th/9907027].

[159] F. Hebenstreit, J. Berges and D. Gelfand, Phys. Rev. D **87** (2013) 10, 105006 [arXiv:1302.5537 [hep-ph]].

[160] F. Gelis and N. Tanji, Phys. Rev. D **87** (2013) 12, 125035 [arXiv:1303.4633 [hep-ph]].

[161] A. R. Bell and J. G. Kirk, Phys. Rev. Lett. **101** (2008) 200403.

[162] N. V. Elkina, A. M. Fedotov, I. Y. Kostyukov, M. V. Legkov, N. B. Narozhny, E. N. Nerush and H. Ruhl, Phys. Rev. ST Accel. Beams **14** (2011) 054401 [arXiv:1010.4528 [hep-ph]].

[163] E. N. Nerush, I. Y. Kostyukov, A. M. Fedotov, N. B. Narozhny, N. V. Elkina and H. Ruhl, Phys. Rev. Lett. **106** (2011) 035001 [Phys. Rev. Lett. **106** (2011) 109902] [arXiv:1011.0958 [physics.plasm-ph]].

[164] A. A. Mironov, N. B. Narozhny and A. M. Fedotov, Phys. Lett. A **378** (2014) 3254 [arXiv:1407.6760 [physics.plasm-ph]].

[165] E. G. Gelfer, A. A. Mironov, A. M. Fedotov, V. F. Bashmakov, E. N. Nerush, I. Y. Kostyukov and N. B. Narozhny, Phys. Rev. A **92** (2015) 2, 022113.

[166] A. M. Fedotov, N. B. Narozhny, G. Mourou and G. Korn, Phys. Rev. Lett. **105** (2010) 080402 [arXiv:1004.5398 [hep-ph]].

[167] A. Gonoskov, I. Gonoskov, C. Harvey, A. Ilderton, A. Kim, M. Marklund, G. Mourou and A. M. Sergeev, Phys. Rev. Lett. **111** (2013) 060404 [arXiv:1302.4653 [hep-ph]].

[168] A. Ilderton and G. Torgrimsson, Phys. Lett. B **725** (2013) 481 [arXiv:1301.6499 [hep-th]].

[169] H. Gies and G. Torgrimsson, arXiv:1507.07802 [hep-ph].

[170] S. Weinberg, *The Quantum Theory of Fields I*, 1995, Cambridge University Press.

[171] C. Schubert, Nucl. Phys. B **585** (2000) 407 [hep-ph/0001288].

[172] K. Daikouji, M. Shino and Y. Sumino, Phys. Rev. D **53** (1996) 4598 [hep-ph/9508377].

[173] N. Ahmadiniaz, A. Bashir and C. Schubert, arXiv:1511.05087 [hep-ph].

[174] K. Hornbostel, Phys. Rev. D **45** (1992) 3781.

[175] C. R. Ji and C. Mitchell, Phys. Rev. D **64** (2001) 085013 [hep-ph/0105193].

[176] C. R. Ji and A. T. Suzuki, Phys. Rev. D **87** (2013) 6, 065015 [arXiv:1212.2265 [hep-th]].

[177] D. D. Dietrich and G. V. Dunne, J. Phys. A **40** (2007) F825 doi:10.1088/1751-8113/40/34/F01 [arXiv:0706.4006 [hep-th]].

[178] S. P. Kim and D. N. Page, Phys. Rev. D **75** (2007) 045013 doi:10.1103/PhysRevD.75.045013 [hep-th/0701047].

[179] H. Gies and G. Torgrimsson, *To appear.*

[180] A. Zee, Quantum Field Theory in a Nutshell, Second Edition, Princeton University Press (2010)

[181] C. Itzykson and J. B. Zuber, New York, Usa: Mcgraw-hill (1980) 705 P.(International Series In Pure and Applied Physics)

[182] M. Henneaux and C. Teitelboim, *Quantization of gauge systems*, Princeton University Press (1992)

[183] P. J. Steinhardt, Annals Phys. **128** (1980) 425.

[184] T. Heinzl, S. Krusche and E. Werner, Phys. Lett. B **275** (1992) 410.

[185] Y. Nakawaki and G. McCartor, Prog. Theor. Phys. **103** (2000) 161 [hep-th/9903017].

[186] C. Harvey, T. Heinzl and A. Ilderton, Phys. Rev. A **79** (2009) 063407 [arXiv:0903.4151 [hep-ph]].

[187] L. Mandel and E. Wolf, *Optical Coherence and Quantum Optics*, Cambridge University Press (1995)

[188] M. Forger and H. Romer, Annals Phys. **309** (2004) 306 [hep-th/0307199].

[189] X. Zhao, A. Ilderton, P. Maris and J. P. Vary, Phys. Rev. D **88** (2013) 065014 [arXiv:1303.3273 [nucl-th]].

[190] N. B. Narozhnyi, Zh. Eksp. Teor. Fiz. **55** 714 (1968) [Sov. Phys. JETP **28** (1969)].

[191] I. A. Batalin and A. E. Shabad, Sov. Phys. JETP **33** 483 (1971).

[192] V. I. Ritus, Annals Phys. **69** (1972) 555.

[193] L. F. Urrutia, Phys. Rev. D **17** (1978) 1977.

[194] G. K. Artimovich, Sov. Phys. JETP **70** 787 (1990).

[195] S. Meuren, C. H. Keitel and A. Di Piazza, Phys. Rev. D **88** (2013) 1, 013007 [arXiv:1304.7672 [hep-ph]].

[196] F. Karbstein, Phys. Rev. D **88** (2013) 8, 085033 [arXiv:1308.6184 [hep-th]].

[197] S. Meuren, K. Z. Hatsagortsyan, C. H. Keitel and A. Di Piazza, Phys. Rev. Lett. **114** (2015) 14, 143201 [arXiv:1407.0188 [hep-ph]].

[198] F. Karbstein and R. Shaisultanov, Phys. Rev. D **91** (2015) 8, 085027 [arXiv:1503.00532 [hep-ph]].

[199] M. Abraham, *Theorie der Elektrizität* (1905) Teubner, Leipzig.

[200] H. A. Lorentz, *The Theory of Electrons* (1909) Teubner, Leipzig.

[201] P. A. M. Dirac, Proc. Roy. Soc. London A **167** (1938) 148.

[202] L. D. Landau, E. M. Lifshitz, *The classical theory of fields*, 1975, Elsevier, Oxford.

[203] C. J. Eliezer, Proc. R. Soc. London, A **194** (1948) 543.

[204] G. W. Ford and R. F. O'Connell, Phys. Lett. A **157** (1991) 217.

[205] T. C. Mo and C. H. Papas, Phys. Rev. D **4** (1971) 3566.

[206] J. C. Herrera, Phys. Rev. D **15** (1977) 453.

[207] I. V. Sokolov, JETP **109** (2009) 207.

[208] S. Coleman, in *Electromagnetism: Paths to Research,* Vol. I (1982) Plenum, New York.

[209] C. W. Nakhleh, Am. J. Phys. **81** (2013) 180 [arXiv:1207.1745 [physics.class-ph]].

[210] R. F. O'Connell, Phys. Lett. A **313** (2003) 491;

[211] P. R. Johnson and B. L. Hu, Phys. Rev. D **65** (2002) 065015 [quant-ph/0101001].

[212] S. Zhang, arXiv:1303.7120 [hep-th].

[213] Y. Kravets, A. Noble, and D. Jaroszynski, Phys. Rev. E **88**, 011201(R) (2013)

[214] K. A. Olive *et al.* [Particle Data Group Collaboration], Chin. Phys. C **38** (2014) 090001.

[215] V. S. Krivitsky and V. N. Tsytovich, Sov. Phys. Usp. **34** (1991) 250 [Usp. Fiz. Nauk **161** (1991) 125].

[216] H. Reeh and S. Schlieder, Nuovo Cimento **22** (1961) 1051.

[217] D. Newton and E. P. Wigner, Rev. Mod. Phys. **21** (1949) 400.

[218] A. Duncan, *The conceptual framework of quantum field theory* (2012) Oxford University Press, USA.

[219] E. Bagan, M. Lavelle and D. McMullan, Annals Phys. **282** (2000) 471

[220] E. J. Moniz and D. H. Sharp, Phys. Rev. D **15** (1977) 2850.

[221] P. R. Johnson and B. L. Hu, quant-ph/0012135.

[222] A. Higuchi and G. D. R. Martin, Phys. Rev. D **73** (2006) 025019 [quant-ph/0510043].

[223] NIST Digital Library of Mathematical Functions, http://dlmf.nist.gov/.

[224] V. Dinu, T. Heinzl and A. Ilderton, Phys. Rev. D **86** (2012) 085037 [arXiv:1206.3957 [hep-ph]].

[225] F. Bloch and A. Nordsieck, Phys. Rev. **52** (1937) 54.

[226] D. R. Yennie, S. C. Frautschi and H. Suura, Annals Phys. **13** (1961) 379.

[227] A. Ilderton and G. Torgrimsson, Phys. Rev. D **87** (2013) 085040 [arXiv:1210.6840 [hep-th]].

[228] T. D. Lee and M. Nauenberg, Phys. Rev. **133** (1964) B1549.

[229] M. Lavelle and D. McMullan, JHEP **0603** (2006) 026 [hep-ph/0511314].

[230] V. I. Ritus, Zh. Eksp. Teor. Fiz **69** (1975) 1517 [Sov. Phys. JETP **42** (1975) 774].

[231] D. Fliegner, M. Reuter, M. G. Schmidt and C. Schubert, Theor. Math. Phys. **113** (1997) 1442 [Teor. Mat. Fiz. **113** (1997) 289] [hep-th/9704194].

[232] B. Kors and M. G. Schmidt, Eur. Phys. J. C **6** (1999) 175 [hep-th/9803144].

[233] M. Krasnansky, Int. J. Mod. Phys. A **23** (2008) 5201 [hep-th/0607230].

[234] H. Gies, J. Sanchez-Guillen and R. A. Vazquez, JHEP **0508** (2005) 067 doi:10.1088/1126-6708/2005/08/067 [hep-th/0505275].

[235] S. L. Lebedev and V. I. Ritus, Sov. Phys. JETP **59** (1984) 237 [Zh. Eksp. Teor. Fiz. **86** (1984) 408].

[236] I. Huet, M. Rausch de Traubenberg and C. Schubert, Int. J. Mod. Phys. Conf. Ser. **14** (2012) 383 [arXiv:1112.1049 [hep-th]].

[237] I. Huet, D. G. C. McKeon and C. Schubert, JHEP **1012** (2010) 036 [arXiv:1010.5315 [hep-th]].

[238] Presentation by C. Schubert at EXHILP conference in Heidelberg July 2015, available at: http://www.exhilp-heidelberg.de/presentations/

[239] D. Binosi, L. Theussl, Comput. Phys. Commun. **161** (2004) 76-86.

[240] D. Binosi, J. Collins, C. Kaufhold, L. Theussl, Comput. Phys. Commun. **180** (2009) 1709-1715.